SAPIENZA
UNIVERSITÀ DI ROMA

PhD in Cell Science and Morphogenesis

XXV° CYCLE

Functional role of Nuclear Factors-I in hematopoietic ontogenesis

PhD student: Rotilio Valentina

Tutor: Prof.ssa Clara Nervi

Coordinator: Prof. Sergio Adamo

Table of contents

Acknowledgements

I would like to first acknowledge my supervisor Prof. Clara Nervi for giving me the opportunity to complete a Ph.D. within her lab and for her constant guidance and dedication over the past four years. I also give special thanks to Dr. Linda M. Starnes and Dr. Lucia Spath, that taught me how to stay in lab and helped me at the beginnings of my Ph.D project. I would like to thank Dr. Emma Nora Di Capua, Dr. Laura Vian, Dr. Anna Busanello, Dr. Francesca Pagano, Dr. Francesca Fantasia, Dr. Cristina Rofani and all of the other Nervi lab members for their collaboration, big support and affection and for making my time in the lab enjoyable. I acknowledge my coordinator of the Ph.D. program Prof. Sergio Adamo. I would also like to thank Prof. Elisabetta Vivarelli and Prof. Luciana De Angelis, Prof. Claudio Di Cristofano and Dr. Jessica Cacciotti, that actively collaborates to this project.

Abstract

Nuclear Factor I (NFI) transcriptional factors constitute a family of four members, NFI-A, B, C and X, known for their positive and negative transcriptional regulatory roles in a cell type and promoter specific context. We previously identified NFI-A as a relevant target of the myeloid regulator microRNA-223, then we found that its levels play a key role in directing hematopoietic progenitors to the erythroid or granulocytic lineage. This prompted us to examine whether the expression of NFI-A and/or other NFIs factors could regulate primitive and definitive hematopoiesis *in vivo*. To this end we initially studied the expression pattern of NFIs factors in different tissues and stages of embryo development of CD1 mice. Our preliminary results indicate that NFI-A presents the most interesting expression pattern among NFIs factors, being express in hematopoietic tissues earlier and at the highest level during embryo development. In addition, performing colony-forming progenitor assays, we found NFI-A expression in primitive erythroid progenitor and during definitive hematopoietic colonies production, implicating it in having a possible role in primitive and definitive hematopoiesis. To elucidate the role of NFI-A in hematopoiesis we used two different strains of NFI-A-/- mice: B6N31 and B6hyb129mice. Histological examinations of hematopoietic tissues of NFI-A-/- mice showed that *Nfi-A* disruption results in hypocellularity of hematopoietic compartment together with a marked decrease of M/E ratio. Genes expression analysis performed on B6N31 hematopoietic tissues indicates that NFI-A -/- mice have a delay in the repression of embryonic β-globins and a perinatal decrease in adult globins expression, suggesting an involvement for NFI-A in the control of β-globins switching. In addiction NFI-A -/- hematopoietic tissues presents an up-regulation of NFI-B expression, indicating its possible action as compensator of NFI-A.

To investigate about the role of NFI-A in adult hematopoiesis, we performed complete blood counts of peripheral blood from adults B6N31 NFI-A +/- and we observed a decreased MCV, an increased RDW and a decreased MCH compared with adult NFI-A +/+ B6N31 mice, demonstrating an haploinsufficiency of NFI-A factor and an altered hemoglobin synthesis. These data indicates that NFI-A could be

involved in the pathogenesis of hematological diseases, further underlying its importance in hematopoietic development.

1. Introduction

1.1. Hematopoiesis

Adult mammalian blood contains different types of cells with specific biologic function, ranging from the transport of oxygen to the production of antibodies. Blood cells have limited life spans and they are produced throughout the whole life; all the processes involved in the production are collectively called **hematopoiesis** and they all originate in the bone marrow from a common stem cell: the **Hematopoietic Stem Cell** (**HSC**). The HSC is characterized by two main properties: self-renewal and multipotency. Self-renewal ensures maintenance of the pool of HSC, whereas multipotency allows generation of all types of differentiated blood cells. Initially, differentiation of HSCs generates two kinds of progeny, **Common Lymphocyte Progenitors** (**CLPs**) and **Common Myeloid Progenitors** (**CMPs**). CLPs have the potential to differentiate into different downstream progenitors, including the B, T and Natural Killer (NK) cell lineages. CMPs give rise to two progenitor cells: **Granulocyte/Macrophage Progenitors** (**GMPs**), which differentiate further to produce granulocytes and monocyte/macrophages; and **Megakaryocyte/Erythrocyte progenitors** (**MEPs**), producing megakaryocytes and red blood cells (Figure 1.1) (Orkin and Zon 2008). During normal steady state conditions, HSCs reside mainly in the marrow cavity, but under certain stress conditions they migrate and colonize other organs such as liver and spleen in a process termed **extramedullary hematopoiesis** (Greer, Foerster et al. 2008).

The HSCs arise during embryonic development. Within the mammalian embryo the hematopoietic system is one of the first complex tissues to be formed during ontogeny, derived from the mesodermal germ layer, with the allocation and specification of distinct blood cells in sequential overlapping sites. Hematopoiesis begins early during embryogenesis and undergoes many changes during fetal and neonatal development. The initial hematopoiesis is termed **primitive hematopoiesis**, while the second phase takes the name of **definitive hematopoiesis** (Greer, Foerster et al. 2008).

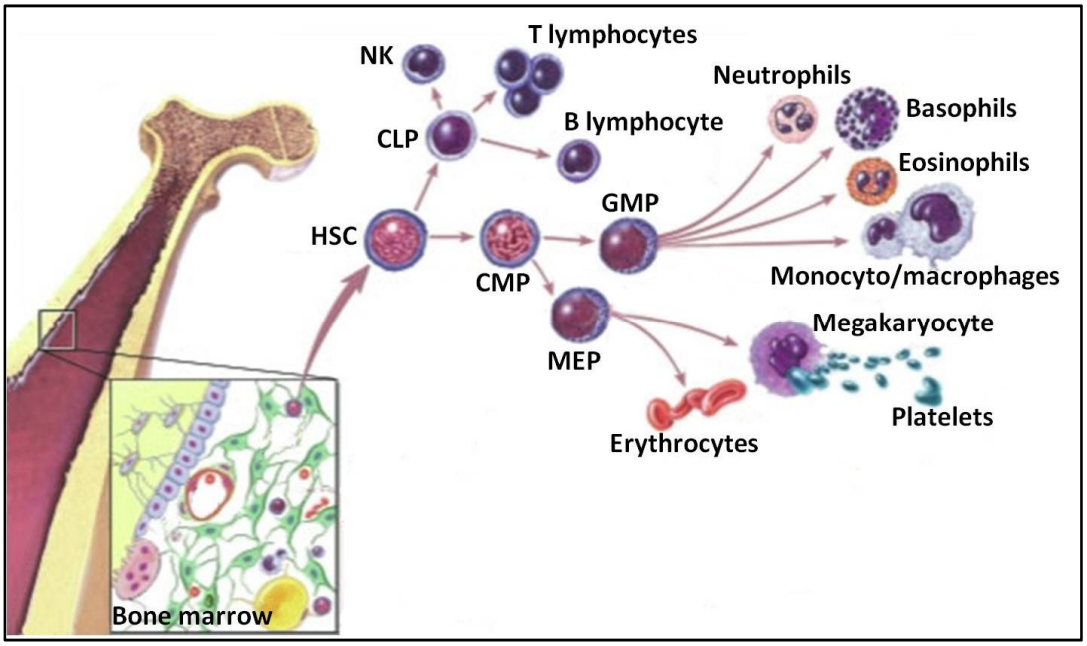

Figure 1.1: **Schematic representation of the main lineage commitment steps in adult mammalian hematopoiesis**. The hematopoietic stem cell (HSC) resides mainly in the bone marrow and gives rise to the common lymphoid progenitor (CLP) and the common myeloid progenitor (CMP). CLPs give rise to Natural Killer (NK), B and T cells, while CMPs give rise to Megakaryocyte-Erythrocyte Progenitors (MEP) and Granulocyte-Monocyte Progenitors (GMPs). Erythrocytes and megakaryocytes origin from MEPs, while GMPs give rise to neutrophils, basophils and eosinophils granulocytes and to monocyte/macrophage cells. (adapted from: © 2001 Terese Winslow, Lydia Kibiuk)

1.2. Primitive hematopoiesis

Hematopoiesis is one of the first processes established following implantation of the blastocyst. The initial wave of blood production take place in the mammalian yolk sac and is termed **‘‘primitive’’**. The development of primitive erythroblasts in the yolk sac is critical for the survival of the mammalian embryo. Indeed, the primary function of primitive hematopoiesis is to produce red blood cells facilitating tissue oxygenation as the embryo undergoes rapid growth (Orkin and Zon 2008). In mouse targeted disruption of genes involved in yolk sac’s primitive erythropoiesis, including SCL (TALl), LM02 (RBTN2), and GATA-1, leads to early embryonic death (Palis and Segel 1998). Primitive hematopoiesis results above all in the production of erythroid cells, but is not limited to this lineage. Klimchenko and colleagues defined a **bi-potential hematopoietic progenitor (MEP-P)** that gives rise to both primitive erythrocytes and **primitive megakaryocytes** (Klimchenko, Mori et al. 2009). Moreover careful analysis of staged embryos indicated the presence of **macrophage progenitors** associated temporally and spatially with primitive erythroid progenitors at E7.25 (Palis, Robertson et al. 1999). Their early development has led to the hypothesis that they also represent a “primitive” population: they mature rapidly, possibly bypassing the monocyte stage of development, and they express lower levels of certain genes than later stage macrophages, suggesting that they could represent a unique population (Keller, Lacaud et al. 1999). Therefore the term “primitive hematopoiesis” should be used to describe cellular lineages arising temporally and spatially with the primitive erythroid lineage in the presomitic yolk sac (McGrath and Palis 2005).

In this chapter we will focus our attention to primitive erythropoiesis, that results in the production of primitive erythroblasts earning the name of **megaloblasts**. These cells have several characteristics distinguishing them from their later definitive counterparts: first of all they differentiate within the vascular network, they are characterized by more rapid differentiation, by an increased sensitivity to erythropoietin, by a larger volume, with an estimated MCV of 250 fl/cell, and they express embryonic hemoglobin (Palis and Segel 1998).

1.2.1. Primitive erythroid cells emergence: the blood island and the hemangioblast

The first morphological evidence of hematopoiesis in mammalian embryos, including mouse and human, is the appearance of pools of immature primitive erythroid cells, termed **blood islands**, within the mesoderm layer of the yolk sac. These blood islands emerges between E7.0 and E7.5 of mouse development and at about 16 days of development in humans and consist of immature primitive erythroid cells that rapidly become enveloped by endothelial cells (Palis, Malik et al.; Ferkowicz and Yoder 2005). The developing vascular plexus of the visceral yolk sac, a honeycomb-like series of vessels, separates the distal embryo proper and the proximal blood island region. Between E7.0 and E7.5 of mouse development, local proliferations of the extra-embryonic mesodermal sheet produce thickened regions called **mesodermal masses** (Silver and Palis 1997; Ferkowicz and Yoder 2005). Cells of mesodermal masses rapidly divide and form, by the late neural plate stage (E7.75), **angioblastic cords**, that eventually differentiate into recognizable **Maximow-type blood islands**, consisting of isolated clusters of blood cells enclosed by sinuous visceral endoderm and mesothelium (Figure 1.2).

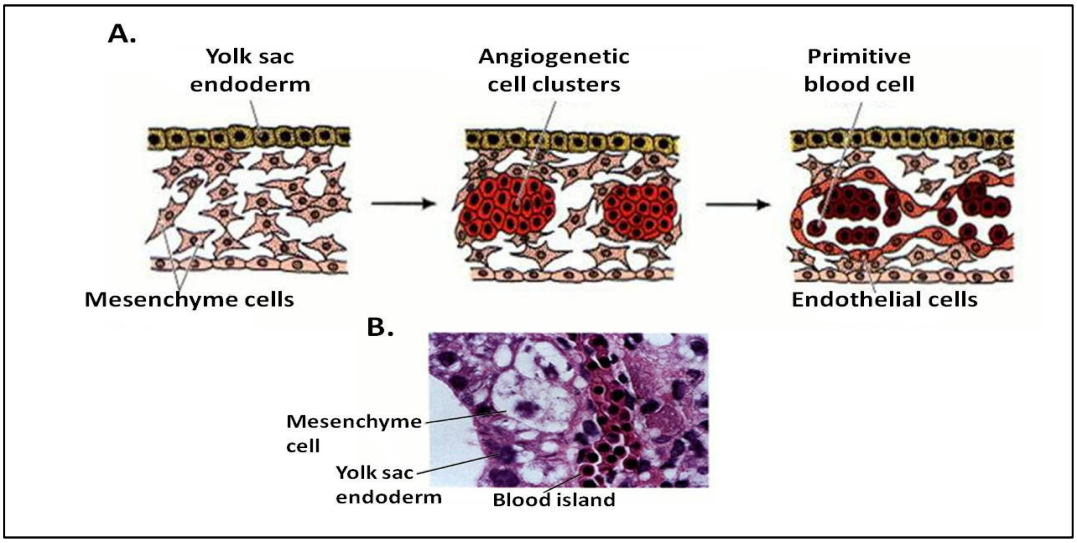

Figure 1.2: **Blood islands morphogenesis. A)** in the wall of the yolk sac undifferentiated mesenchyme condenses to form angiogenetic cell clusters. The centers of these clusters form the blood cells, and the outsides of the clusters develop into blood vessel endothelial cells. **B)** Photograph of a human blood island in the mesoderm surrounding the yolk sac (adapted from Gilbert 2005).

Primitive erythropoiesis defines the onset of hematopoiesis in the yolk sac of the early embryo and is initiated by the emergence of progenitors assayed as colony-forming cells (**EryP-CFCs**) (Wong, Chung et al. 1986). These primitive progenitors form *in vitro* compact colonies of large primitive erythroid cells (Palis, Robertson et al. 1999). EryP-CFC emerge within the developing yolk sac at the late primitive streak stage (approximately E7.0 of mouse development), after the onset of gastrulation but before morphological evidence of blood island formation (Palis, Robertson et al. 1999). The close spatial and temporal appearance of blood cells and endothelial cells in the yolk sac suggested that they originate from a common precursor, called **hemangioblast** (Keller, Lacaud et al. 1999; Palis, Malik et al. 2010), which require yolk sac visceral endoderm-derived factors for blood island formation. Dissection of gastrulating embryos into distal embryo proper and proximal yolk sac portions reveals that EryP-CFCs are found in both the prospective blood island region and distally, near the primitive streak of the embryo proper (Palis, Robertson et al. 1999). This finding is consistent with the proposal that early extra-embryonic mesoderm or hemangioblasts commit the primitive erythroid lineage soon after its emergence from the primitive streak and that the primitive erythroid and endothelial lineages diverge before reaching the region of the yolk sac blood islands (Moore and Owen 1967; Ottersbach, Smith et al. 2009; Costa, Kouskoff et al. 2012).

1.2.2. Primitive erythroid cells mature in the blood stream

The transient appearance of EryP-CFCs leads to the generation of a wave of synchronously maturing erythroid precursors. Immature primitive erythroblasts begin to enter the bloodstream with the onset of cardiac contractions, by E8.5 of mouse development (Ji, Phoon et al. 2003; McGrath, Koniski et al. 2003). Over the next 8 days, the EryPs mature in the circulation and undergo morphological changes classically associated with definitive erythroid precursor maturation in the adult marrow, including decrease in erythroblast cell size, nuclear condensation with loss of euchromatin, and hemoglobin accumulation (Figure 1.3) (Kingsley, Malik et al. 2004; Fraser, Isern et al. 2007; Palis, Malik et al. 2010). The latter, in association with decreased RNA levels, results in loss of cytoplasmic basophilia observed by

Wright-Giemsa staining. Like definitive erythropoiesis, the maturation of primitive erythroid precursors is associated with several cell divisions. Primitive erythroblast numbers expand 100-fold between E8.5 and E10.5 of mouse gestation. The presence of mitotic cells in the bloodstream (Bethlenfalvay and Block 1970), studied by thymidine incorporation experiments (De la Chapelle, Fantoni et al. 1969), and cell cycle analysis (Sangiorgi, Woods et al. 1990), indicate that circulating murine primitive erythroblasts stop dividing by E13.5. Primitive erythroblasts rapidly accumulate hemoglobin, ultimately achieving steady state levels of **80-100 pg/cell** (Fantoni, De la Chapelle et al. 1969; Palis, Malik et al. 2010).

The presence of nucleated primitive erythroid cells in mammalian embryos has raised the possibility that this lineage shares many features with their non-mammalian counterparts. However, in the early 1970's, enucleated **"megalocytes"** having the same size and hemoglobin content as nucleated yolk sac erythroblasts were detected at later times of mouse gestation (Bethlenfalvay and Block 1970). These cells are 3-fold larger than the fetal liver-derived **"macrocytes"** that enter the bloodstream beginning at E12.5, and were postulated to be primitive erythroblasts that had undergone enucleation (Palis 2008). While nucleated yolk sac-derived erythroid cells are no longer present in the bloodstream after E16.5, megalocytes were found in the bloodstream until E18.5 (Bethlenfalvay and Block 1970). Using antibodies specific for embryonic globins to identify primitive erythroid cells, it was determined that primitive erythroblasts in the mouse fetus enucleate between E12.5-E16.5 of gestation (Kingsley, Malik et al. 2004). Enucleated primitive erythrocytes have been identified in the bloodstream of mice even several days after birth (Kingsley, Malik et al. 2004). Enucleation of erythroid cells in the marrow results in the formation of two daughter cells. The first is the **enucleated reticulocyte** that completes its maturation by removing internal organelles and reorganizing its cytoskeleton. The second consists of the condensed nucleus surrounded by a thin rim of cytoplasm and an intact cell membrane. This second cell, recently termed **"pyrenocyte"**, is rapidly ingested by macrophages (McGrath, Kingsley et al. 2008). Primitive pyrenocytes have been detected in the bloodstream of mouse embryos between E12.5-E16.5 of gestation, during the time when primitive erythroid cells enucleate (McGrath, Kingsley et al. 2008). These observations suggest that terminal differentiation of mammalian primitive erythroid cells results in erythrocytes, which

are more similar to the enucleated red cells of mammals rather than the nucleated red cells of birds, fish and amphibians (Palis, Malik et al. 2010).

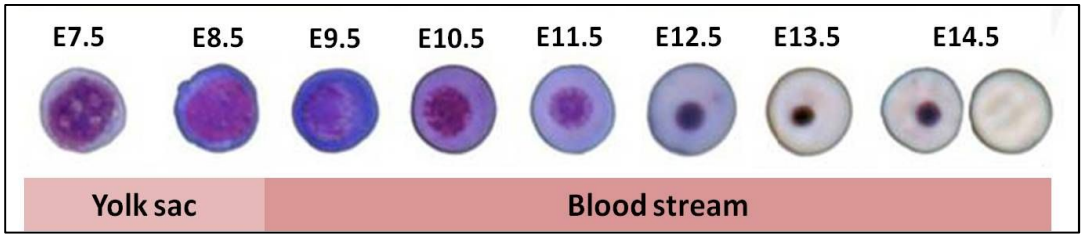

Figure 1.3: **Stages of primitive hematopoiesis**: summary of different phases of EryP development, from progenitor to terminal maturation and enucleation. The images of EryP at different stages were cropped from photographs of Giemsa stained cells (adapted from Baron, Isern et al. 2012)

1.2.3. *Hemoglobin "switching*

Over the ontogenesis, both the **α- and β-like polypeptide subunits of hemoglobin** varies, leading to the assembly of hemoglobin molecules with different physiological properties. Embryonic (ε) and fetal (Gγ-Aγ) hemoglobins have a higher affinity for oxygen than adult (δ-β) ones. This facilitate oxygen exchange across the placenta.

The human and mouse β-globin loci are the most intensively studied mammalian globin loci, they are positioned respectively on the chromosome 11 and 7 and contain several globin genes, a large upstream regulatory element, named Locus Control Region (LCR), and a number of additional regulatory elements (Figure 1.4A). During development, the expression of globins changes in a process called **hemoglobin switching** and the genes are positioned on the chromosome in the same order of their expression during ontogenesis (Grosveld, Dillon et al. 1993; Dillon, Trimborn et al. 1997; Noordermeer and de Laat 2008; Palis, Malik et al. 2010). Since this switch in globin expression coincided temporally with the transition from primitive to definitive erythropoiesis, it was initially thought that primitive and definitive erythroid cells exclusively express embryonic and adult globins, respectively. However, this hypothesis did not explain the complexity of globin gene expression in the mouse or in the human.

The human β-globin locus contains 5 functional genes that are expressed in the order of their arrangement within the locus (ε-Gγ-Aγ-δ-β). These genes undergo two major transitions in expression during ontogeny, the first from embryonic (ε) to fetal (Gγ-Aγ) globins and the second from fetal to adult (δ-β) globins.

In the mouse, there are four functional β -globin genes (*Hbb-y, Hbb-bh1, Hbb-b1, Hbb-b2*) (Figure 1.4A). The mouse *Hbb-bh1* and human *γ-globin* genes are thought to have evolved from a common ancestral γ-globin gene However the mouse Hbb-bh1-globin has not been modified to be expressed in definitive fetal red cells as seen in humans, but represents a second embryonic β-globin together with *Hbb-y* (Kingsley, Malik et al. 2006; Palis, Malik et al. 2010). Moreover, in murine embryonic tissue, the *Hbb-bh1* gene initially appears to be expressed at higher levels than *Hbb-y*, also if is positioned downstream this one. Thus, in the mouse, there is no fetal to adult hemoglobin switch and defined stages of development gene expression is not strictly correlated with their order on the chromosome 7 (Kingsley, Malik et al. 2006; Noordermeer and de Laat 2008).

At the α-globin locus a similar switch from an embryonic to an adult α-globin subunits occurs in both mice and humans (Figure 1.4B) (McGrath and Palis 2005; McGrath and Palis 2008). The functional genes of the α-globin cluster are organized with an embryonic ζ-globin gene, located at 5', and two adult α-globin genes, located at 3' (Leder, Swan et al. 1981). The embryonic ζ-globin gene is the first to be expressed at the onset of erythropoiesis in the yolk sac of the developing embryo. As the expression of the embryonic ζ-globin decreases, the adult α-globin genes are activated and expressed throughout the lifetime of the mouse (Figure 1.4B) (Leder, Daugherty et al. 1997). However, the α- like globins switch appears to occur earlier than the β-globins switching, within the primitive lineage (Peschle, Mavilio et al. 1985; Kingsley, Malik et al. 2006).

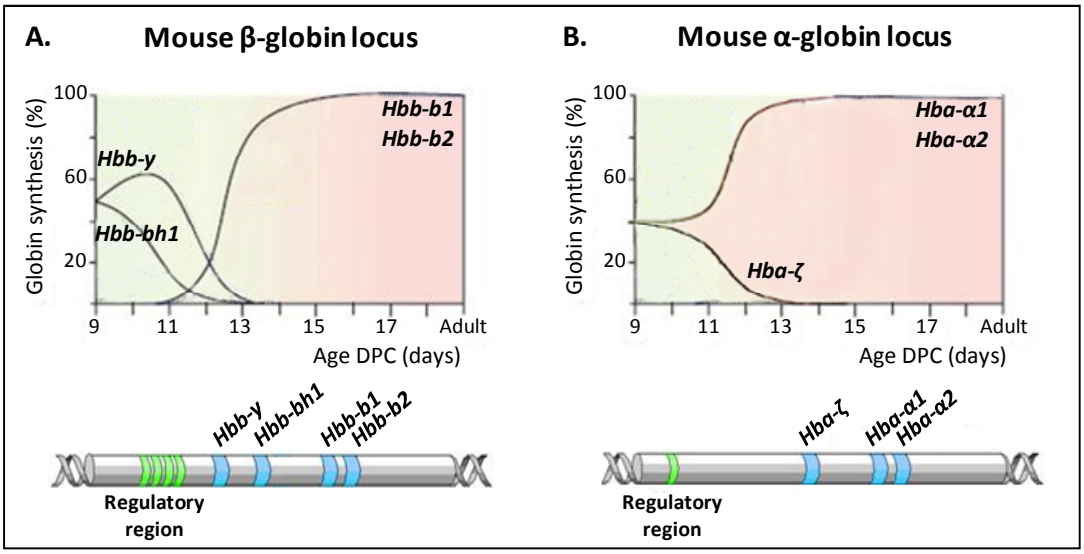

<u>Figure 1.4</u>: A diagram illustrating the developmental switching of the β-like globins (2 A) and the α-like globins (2 B) gene expression in mouse. Below each diagram is illustrated the organization of the correspondent locus (adapted from Sankaran, Xu et al. 2010)

1.3. Definitive hematopoiesis

During vertebrate ontogeny hematopoiesis takes place in several discrete anatomical niches that change rapidly, accompanying the highly dynamic processes characteristic of embryonic development (figure 1.5). Emergence of blood cells in new embryonic niches is usually characterized by a decline in the hematopoietic activity of the prior site (Cumano and Godin 2007; Costa, Kouskoff et al. 2012). Shifting the anatomical location of hematopoiesis during ontogeny may be an effective strategy to adapt blood production to the changing needs of the embryo. In fact, it may be easier to shift blood production to a new niche rather than having to remodel an existing niche; in particular some blood forming tissues, such as the yolk sac and placenta, are transient in nature. Moreover, temporal overlap of blood production in multiple sites creates a redundant system, which is able to safeguard against defects that can affect a single site (Ottersbach, Smith et al. 2009). In mammals, the very first blood cell emerge within the **yolk sac** before circulation is initiated. As organogenesis starts, hematopoietic cells are detected in the developing **Aorta Gonads Mesonephros** (AGM) region, **placenta, vitelline and umbilical arteries**. Later in gestation, the **fetal liver** becomes the main organ harboring hematopoietic activity. Just before birth, blood cell development is transferred to the **bone marrow**, the final and lifelong site of adult hematopoiesis (figure 1.5) (Costa, Kouskoff et al. 2012). Nevertheless, not all hematopoietic anatomical regions hold the capacity to generate blood cells de novo. The true hematopoietic stem cell (HSC) potential of the progenitors generated in each site and their relative contribution to the adult pool is not yet clear and has been the subject of long-standing debates (Costa, Kouskoff et al. 2012). This aspect will be described in more detail below.

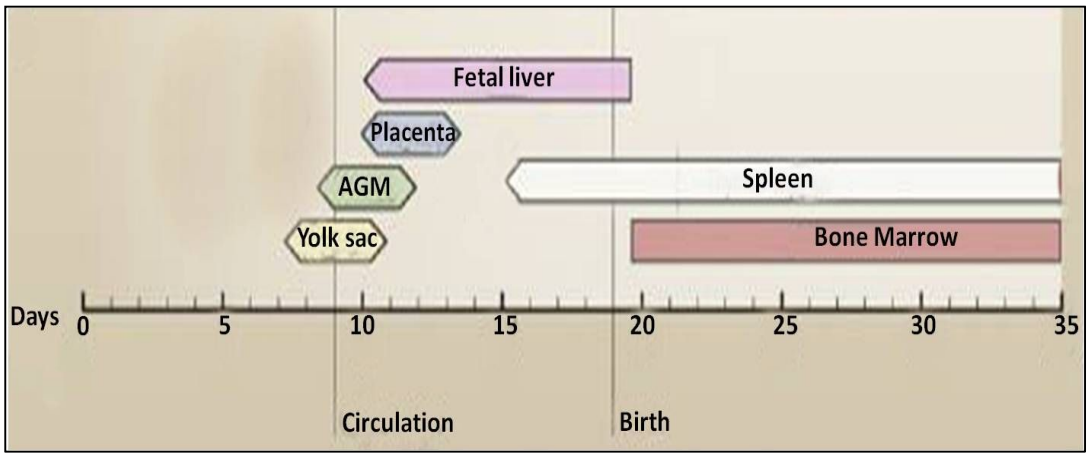

Figure 1.5: **Developmental time windows for shifting sites of hematopoiesis** (adapted from Orkin and Zon 2008).

1.3.1. Emergence of definitive HSCs

The yolk sac was originally believed to be the unique embryonic hematopoietic site with the potential to produce progenitors of all adult blood lineages (Moore and Owen 1965; Moore and Owen 1967). This idea was challenged in the 1970s by compelling evidence from experiments involving chicken-quail chimeric embryos. Quail donor embryos transplanted onto chicken recipient yolk sacs before circulation resulted in chimeras whose hematopoietic system was composed only of donor cells (Dieterlen-Lievre 1975). These experiments suggested that extra-embryonic hematopoiesis is transient. They also revealed the existence of an intra-embryonic hematopoietic source, later on shown to be the **mesoderm aortic region**. Concordant results were obtained in murine embryos extending this new paradigm to mammalian models (Costa, Kouskoff et al. 2012). The hematopoietic determination of mesodermal cells takes place in the caudal intra-embryonic region, beginning at the presomitic stage (E 7.5 of murine ontogenesis). As for the yolk sac, mesoderm is associated with endoderm in intra-embryonic hemogenic sites, a combination termed **Splanchnopleura (Sp)** (figure 1.6). After the 15-somite stage (E8.5–10.0 of murine development), the tissues derived from the Sp takes the name of **Para-aortic Sp** (P-Sp), and comprise the endoderm of the developing gut, the dorsal aorta, the omphalomesenteric artery, and the splanchnopleural lining of these tissues (figure 1.6) (Medvinsky and Dzierzak 1996). When fetal liver colonization by hematopoietic stem cells begins, the P-Sp develops comprising, besides the aorta, the developing

gonads and the mesonephros and is referred to as **AGM region** (10.0–11.5 murine embryos) (figure 1.6) (Muller, Medvinsky et al. 1994; Garcia-Porrero, Godin et al. 1995; North, Gu et al. 1999; de Bruijn, Speck et al. 2000).

Colony Forming Units-Spleen (CFU-S) arise in the mouse AGM of E9.0 embryos, in consistently higher numbers than in the yolk sac (Medvinsky, Samoylina et al. 1993; Medvinsky and Dzierzak 1996; Medvinsky, Rybtsov et al. 2011). Moreover, cells from the AGM compartment of E10.0 embryos successfully exhibited HSC properties with and without previous expansion in vitro, restoring the hematopoietic system of recipient irradiated adult mice whereas yolk sac-derived cells failed to do so (Muller, Medvinsky et al. 1994; Medvinsky and Dzierzak 1996). This ability is due to the presence of **long-term repopulating hematopoietic stem cells** (**LTR-HSCs**), the adult-type definitive stem cells, able to produce all hematopoietic lineages over the entire lifespan of an animal. LTR-HSCs first appear in the AGM, they emerge in very small number only one day after in the yolk sac and two days later they are also found in the liver. Yolk sac derived hematopoiesis becomes unnecessary at this point and disappears. Eventually, LTR-HSCs migrate from the fetal liver to the bone marrow in the circulation, and the bone marrow becomes the primary site of hematopoiesis. A very small reserve of stem cells remaining in the liver. Once definitive hematopoiesis begins, erythrocytes, lymphocytes, monocytes, granulocytes, and platelets are formed (Greer, Foerster et al. 2008).

Definitive hematopoietic hierarchy in the mouse has been deduced by the culture of hematopoietic progenitors in semisolid media. In murine bone marrow the most undifferentiated erythroid progenitors is the **Burst Forming Unit-Erythroid cell** (BFU-E), the name of which derive from the ability to give rise to big erythroid colonies after 7-10 days in methylcellulose culture. A more mature erythroid progenitor is represented by **Colony Forming Unit-Erythroid cells** (CFU-E), that form erythroid colonies smaller than BFU-E ones after 2-3 days in culture. Within the murine yolk sac BFU-Es become detectable at E8.25, just before the beginning of blood circulation, and expand in this site during the following 24 hours. definitive erythroid progenitors are found in increasing numbers in the bloodstream between E9.5 and E10.5; they expand exponentially and differentiate into the liver soon after it emerges as a hematopoietic organ, at E10.0 (Wong, Chung et al. 1986; Palis and Yoder 2001). CFU-Es are detectable from E9.5 during murine development in yolk

sac, blood stream and intra-embryonic tissues. In the yolk sac BFU-E and CFU-E number starts to decreases between E10.5 and E11.5, while increases esponentially in the developing liver, consistently with the maturation of definitive erythroblasts (Palis and Yoder 2001). While the generation of erythroid and myeloid precursors in this tissue has been clearly described (Palis, Robertson et al. 1999), the lymphoid cell development is only now being understood. Recent studies have demonstrated that the murine yolk sac contains precursor cells of the first innate B lymphocytes at E9.0 that originate independently from the equivalent progenitors generated in intra-embryonic sites (Yoshimoto, Montecino-Rodriguez et al. 2011).

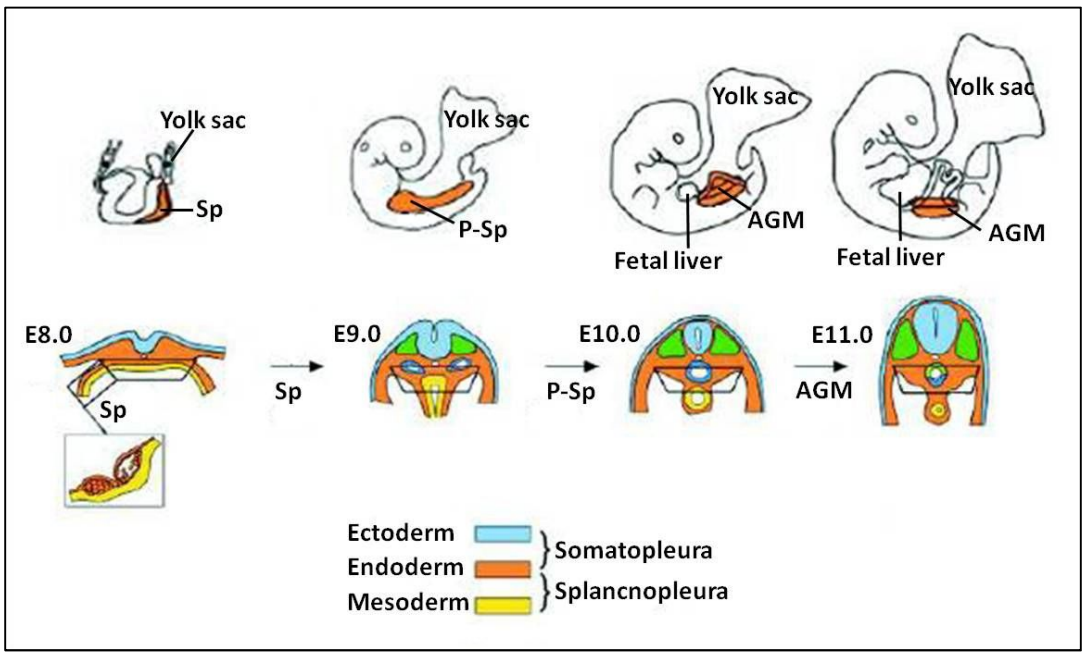

Figure 1.6: **Localization and evolution of the intra-embryonic hemogenic site in the mouse embryo (adapted from Cumano and Godin 2007).**

1.3.2. *Intra-embryonic vs extra-embryonic HSCs origin*

Whether the yolk sac is capable of autonomously generating precursors with HSC potential has been a matter of great controversy. Blood precursors in the yolk sac seem to be primed to restricted hematopoietic lineages, and thus are intrinsically distinct from the consensual multilineage properties of HSCs (Costa, Kouskoff et al. 2012). Yolk sac was shown to harbor in vitro clonogenic myeloid progenitors, called **Colony Forming Units-Culture** (**CFU-Cs**) and **Colony Forming Units-Splenic** (**CFU-S**). CFU-Cs are progenitors that can be stimulated in vitro to generate a colony of hematopoietic cells, which cannot self-renew although some can be re-plated a limited number of times. CFU-Cs are classified according to the composition of the colonies they generate. CFU-S is an immature progenitor cells that can form morphologically distinguishable colonies of myeloid cells in spleens of irradiated animals following transplantation. However, a more stringent assay in which irradiated recipient mice were used to prevent the regeneration of endogenous splenic colonies showed that the yolk sac lacks CFU-S prior to E9.5 (Medvinsky, Samoylina et al. 1993) and subsequent studies showed lack of definitive HSCs prior to E11.5 (Muller, Medvinsky et al. 1994; Medvinsky and Dzierzak 1996). Nevertheless, a non-invasive strategy designed at labeling precursors during the early stages of extra-embryonic hematopoiesis suggested that the yolk sac contains progenitors that constitute the ancestry of adult blood cells, including the HSC pool (Samokhvalov, Samokhvalova et al. 2007). Although such observations remain controversial, as the level of labeled cells found in the adult hematopoietic system was relatively low, this study reopened the debate on the embryonic sites of HSC emergence (Costa, Kouskoff et al. 2012). Cultured pre-circulatory yolk sac's cells were tested for their ability to reconstitute adult irradiated immunodeficient mice ($Rag2^{-/-}\gamma c^{-/-}$) (Colucci, Soudais et al. 1999; Cumano, Ferraz et al. 2001) and could only provide short-term myeloid reconstitution (Boisset and Robin 2012). Thus, paradoxically, yolk sac hematopoiesis occurs in the absence of definitive HSCs (Medvinsky, Rybtsov et al. 2011). On the other hand, the P-Sp/AGM intra-embryonic tissue, as already said, is the first tissue to harbor LTR-HSCs (figure 1.7). These findings suggested that adult mammalian hematopoiesis has an intra-embryonic origin, but they did not fully exclude the possibility that the yolk sac contributes to the adult hematopoietic system as embryonic ancestors of definitive HSCs, not detectable owing to the lack of

appropriate assays. In fact the specific assay used to determine stem cell activity for one population of cells (such as immune reconstitution following irradiation of adult animals) may not be appropriate for a different stem cell population. Distinct host requirements may be necessary, such as the use of neonatal recipients for cells of the yolk sac. Some of the intrinsic differences between cell populations, such as developmental stage, ease of access, the local niche, and whether they are dividing, may preclude a host transplant assay from detecting engraftment and multilineage reconstitution (Orkin and Zon 2008). Data in support of these hypothesis come from studies on murine yolk sac explants from pre-circulation embryos co-cultured with E10.5 AGM stromal cells, that have been shown to produce progenitors with HSC potential. These observations suggest that the AGM produces factors able to create a microenvironment suitable to support the generation of adult type HSCs (figure1.7) (Matsuoka, Tsuji et al. 2001). It doesn't exclude that cells originated in the yolk sac could express their full HSC potential only when exposed to the intra-embryonic environment.

During mammalian ontogeny the dorsal aorta is connected to the yolk sac and to the placenta through the vitelline and umbilical arteries, respectively. The identification of hematopoietic cells in these arteries suggested that they also harbor HSCs (Garcia-Porrero, Godin et al. 1995). This was later confirmed by the detection of cell populations with HSC properties emerging around the same stage and with frequencies similar to those found in the AGM (Corbel, Salaun et al. 2007; Costa, Kouskoff et al. 2012). This raises the possibility that HSCs have an extra-embryonic origin and then they colonize AGM and other hematopoietic embryonic tissues through the blood flow (figure 1.7). In support of this hypothesis it was reported that in mutant embryos lacking a heartbeat and therefore blood flow, intra-embryonic haematopoietic cells are absent, demonstrating that definitive haematopoiesis in the AGM must originate from the yolk sac, as the latter was found to retain some progenitors (Lux, Yoshimoto et al. 2008). However the fact that HSC emergence within the aorta is evolutionarily conserved and starts only after the beginning of circulation, has induced to investigate whether the sheer stress experienced by AGM exposed to the vigorous blood flow within the aorta is required for HSC formation (Adamo, Naveiras et al. 2009; North, Goessling et al. 2009). Through a screen of chemical compounds, Leonard Zon's group discovered that increased blood flow is

associated with enhanced phenotypic HSC numbers in zebrafish embryos (North, Goessling et al. 2009). Using mutant embryos these authors showed that the heartbeat is necessary for arterial identity and HSC formation and that the downstream effector is nitric oxide, the production of which is induced by circulation-associated sheer stress. They also confirmed the role of nitric oxide in HSC formation in mouse embryos. Another group quantified the sheer stress to which the aorta is exposed and recreated it *in vitro*, obtaining an enhancement of definitive blood cell production from cultured embryonic stem (ES) and AGM cells (Adamo, Naveiras et al. 2009). Altogether these studies suggests a scenario in which cells on the ventral side of the aorta are induced by the action of nitric oxide, transcription factors (such as AML1) and additional environmental features, to produce HSCs and release them into the circulation from where they colonize the fetal liver. The subsequent gradual replacement of the ventral endothelium and smooth muscle layer by somite-derived precursors then causes HSC production to cease. It will be of interest to determine if a similar process takes place in the placenta and the yolk sac, and whether these tissues can also independently generate HSCs (Ottersbach, Smith et al. 2009).

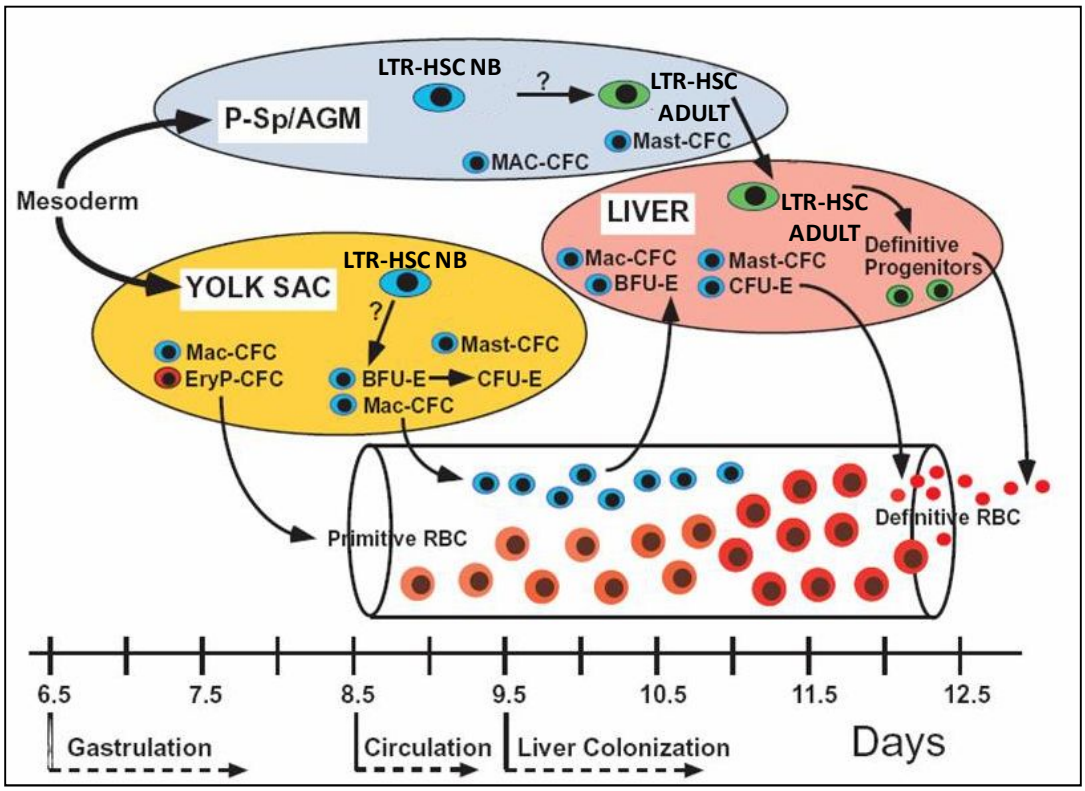

Figure 1.7: **Model of early hematopoietic ontogeny in the mouse embryo.** P-Sp/AGM, para-aortic splanchnopleura/aorta-gonad-mesonephros region; RBC, red blood cells; EryPCFC, primitive erythroid progenitors; Mac-CFC, macrophage progenitors; BFU-E, burst forming unit erythroid; CFU-E, colony-forming unit erythroid; Mast-CFC, mast cell progenitors; LTR-HSC NB: long term newborn-repopulating stem cells; LTR-HSC ADULT: long-term adult-repopulating stem cells (Adapted from Palis, Robertson et al. 1999).

1.3.3. Sites of definitive hematopoiesis

During murine ontogenesis, definitive erythropoiesis is established in the liver beginning at 28-32 somite pairs (E9.5) (Palis, Robertson et al. 1999; Lux, Yoshimoto et al. 2008), probably with an initial colonization of committed progenitors originated within the yolk sac. From E11.5 onwards, HSCs from the AGM region seed the fetal liver, which subsequently becomes the major center for hematopoiesis until around the time of birth (Ottersbach, Smith et al. 2009). Subsequently, around E14.0, HSCs migrate from the liver into the spleen and into the bone marrow around E17.0. Thereafter, HSCs reside in both spleen and BM throughout the life of a mouse (figure 1.5) (Morita, Iseki et al. 2011).

The hematopoietic tissues usually consist of a three-dimensional organization of vascular endothelial cells, stroma and blood cells that provides the microenvironment for haematopoiesis (Tada, Widayati et al. 2006). **Stroma** is the term used to refer to the various cells and the extracellular macromolecules that occupy the hematopoietic tissue along with the hematopoietic cells. The stromal cells include specialized fibroblasts, adipocytes, macrophages, and lymphocytes, as well as the endothelial cells of capillaries and sinuses. The stroma thus constitutes the microenvironment in which the hematopoietic progenitor cells grow and differentiate, and there is strong evidence that various stromal cells as well as extracellular matrix molecules play critical and diverse roles in hematopoiesis (Greer, Foerster et al. 2008).

Unlike yolk sac erythropoiesis, maturation and enucleation of definitive erythrocytes takes place within well-defined anatomical units referred to as erythroblast islands (Chasis and Mohandas 2008). Each such island contains one or two macrophages that give rise to a series of long cytoplasmic projections. Interspersed between these projections are clusters of up to 30 erythroblasts at varying stages of differentiation. In general, the more differentiated progenitors lie at the periphery of the erythroblast island and, as they enucleate, they enter a blood sinusoid, leaving behind their nucleus, which is phagocytosed by the macrophage (Figure 1.8). The importance of macrophages to normal erythroblast development is demonstrated by impairment of erythropoiesis following disruption of normal macrophage function both *in vitro* and *in vivo* (Iavarone, King et al. 2004; Liu, Li et al. 2007). Erythroblasts are situated in close proximity to other erythroblasts within the erythroblast islands and regulatory interactions are also believed to occur between adjacent erythroblasts. Early erythroblasts express a number of receptors mediating signals to activate the extrinsic

apoptosis pathway. The corresponding ligands for these receptors are expressed by late erythroblasts, and activation of the receptors on early erythroblasts leads to inhibition of differentiation and to apoptosis (De Maria, Zeuner et al. 1999). This pathway is believed to act as a negative feedback loop to regulate erythropoiesis, a large numbers of mature erythroblasts shut off the supply of further mature erythroblasts by inhibiting differentiation and inducing apoptosis in the early erythroblast population. This negative feedback loop is inhibited by erythropoietin. Thus, erythroid development, just like other aspects of hematopoiesis, is regulated by a complex interplay of signals, through direct interactions and the secretion of cytokines, emanating from the stroma and other hematopoietic cells (Ottersbach, Smith et al. 2009).

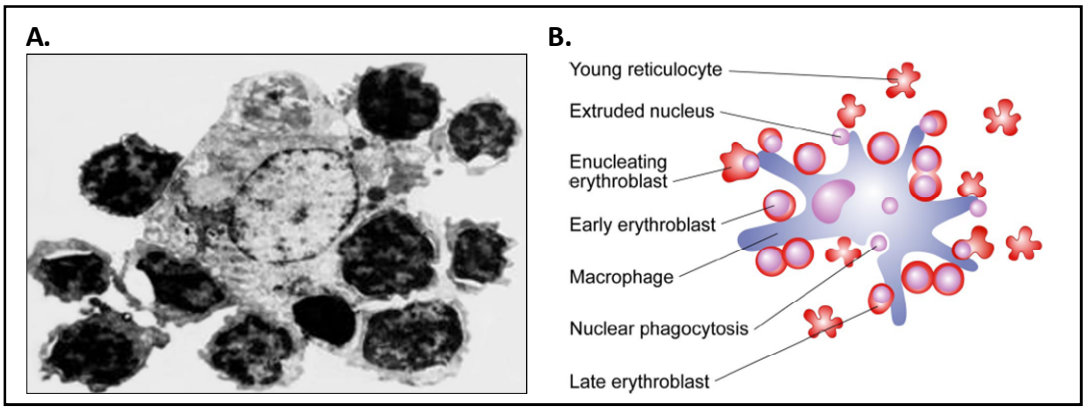

Figure 1.8: **Erythroblastic Island. A)** Transmission electron micrograph of an erythroblastic island isolated from rat bone marrow. **B)** Proliferation and differentiation processes occurring within the erythroid niche. Early-stage erythroblasts are larger cells with centrally located nuclei; more differentiated erythroblasts are smaller cells containing nuclei located adjacent to plasma membranes. Expelled nuclei undergo phagocytosis by central macrophage. Young multilobulated reticulocytes are initially attached to the macrophage surface and later detach.

The Liver is the major site of hematopoiesis in the foetus. Beginning at E12.5 of mouse embryo development, many erythroblasts are present in the liver parenchyma. They form erythroblastic islands along the sinusoids from E12.5 to D0, that decrease gradually from D2 onward. Moreover E12.5 fetal liver contains also megakaryocytes, that are constantly present until D10, neutrophils, that increase slightly in number at E14.5 and then decrease, and lymphocytes (Tada, Widayati et al. 2006).

In mouse splenic tissue can first be identified at gestation day 12.5, a reticular mesh is formed at E14.5 and the first hematopoietic cells can be seen at gestation day 15.5 (Seymour et al., 2006). Precursors of the erythroid lineage in the spleen are activated between E14.5 and E16.5. After E16.5, erythropoiesis, granulopoiesis and lymphopoiesis began. Erythropoiesis and granulopoiesis still occurred in the marginal zone and red pulp at day four of post-natal life (Cesta 2006; Tada, Widayati et al. 2006). In rodents, spleen remains an extra-medullary hematopoietic organ for all adult life and also if extra-medullary hematopoiesis tends to be decreased in adult animals, it can become more intense when there is increased demand for blood cells, as in cases of anemia, inflammation, decreased production by the bone marrow, or in cases of neoplasia (Cesta 2006; Greer, Foerster et al. 2008).

In the late stages of mammalian fetal development, the bone marrow becomes the main site of hematopoiesis and in humans it is the exclusive site of postnatal hematopoiesis under normal circumstances. The venous structure of the marrow cavity is a complex maze of sinuses that eventually drains into central veins. Hematopoietic progenitors differentiate outside the sinuses that are formed by a continuous layer of endothelial cells partially covered , on the extra-luminal side, by a discontinuous layer of adventitial reticular cells: myofibroblast cells that have processes forming a network throughout the extra-luminal space of the marrow cavity. Mature cells pass through the cytoplasm of the endothelial cells and enter in the blood flow (Greer, Foerster et al. 2008).

In the mouse, bone marrow starts to be recognizable at E14.5, erythroblasts are visible near the blood vessel from E18.5 and many erythroblasts forming islets appear suddenly from D0 to D2 after birth. In the bone marrow there are few CFUs until D4, then their number increase remarkably from D7 onwards and the area of the hematopoietic compartment in the femur enlarge (Wolber, Leonard et al. 2002; Tada, Widayati et al. 2006).

1.4. Hematopoiesis and transcription factors

Many leukemias are characterized by recurrent chromosome translocations resulting in either dysregulated (ectopic) expression or the generation of fusion proteins with aberrant functionality. With the advent of modern molecular biology, molecular analysis of translocation breakpoints demonstrated that a large proportion of the genes involved in these translocations, encode DNA-binding transcription factors (e.g. Tal1/Scl, AML1, Etv6/Tel), (Rabbitts 1994; Rosenbauer and Tenen 2007), subsequently demonstrated to be involved in essential functions during normal hematopoiesis. In addition to those factors identified through their involvement in chromosomal abnormalities, many additional transcription factors have been discovered to be important in normal hematopoiesis using biochemical, cell biological, genetic and phylogenetic approaches. Functional analysis has resulted in a transcription factor map that illustrates those factors that are required for individual progenitor and/or differentiated lineages (figure 1.9) (Cantor and Orkin 2001; Ottersbach, Smith et al. 2009; Palis, Malik et al. 2010). The emerging picture within hematopoiesis is that transcription factor combinations are critical for specific lineage commitment. Hematopoietic genes have regulatory elements specifically active in lineage-specific manner, containing combinations of the binding sites for those specific factors. Recurring motif combinations present in multiple elements thus constitute regulatory codes that provide the link between the cell type-specific transcription factor environment and control of gene expression (Ottersbach, Smith et al. 2009).

In the same way the emergence of hematopoietic cells in two distinct and separate anatomical sites, the yolk sac and embryo body, along with the emergence of functionally different embryonic and adult hematopoietic cells within the embryo, is reflected in the genetic program. Targeted mutagenesis in mice demonstrated differential requirements for some genes (e.g. AML1, GATA-2, GATA-3, c-kit) in fetal liver hematopoiesis as compared to primitive yolk sac hematopoiesis. In contrast, the mutation of other genes (e.g. Flk-1, TAL-l/SCL) results in the impairment of both yolk sac and fetal liver hematopoiesis. Thus, the genetic programs of embryonic and adult hematopoietic cells appear to be initially overlapping during stages determining hematopoietic fate, but become unique and

more complex in cells destined to become part of the adult hematopoietic system (Durand and Dzierzak 2005; Costa, Kouskoff et al. 2012).

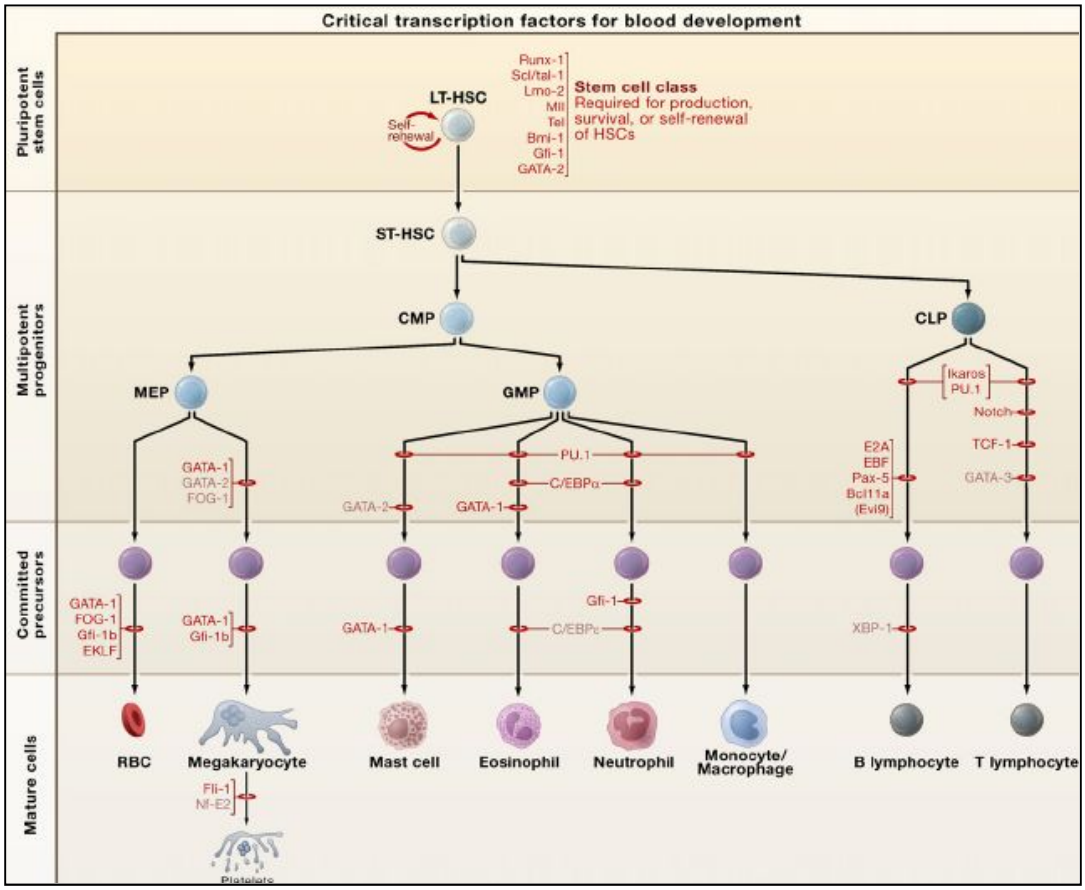

Figure 1.9: **Requirements of Transcription Factors in Hematopoiesis.** The stages at which hematopoietic development is blocked in the absence of a given transcription factor, as determined through conventional gene knockouts, are indicated by red bars. The factors depicted in black have been associated with oncogenesis. Those factors in light font have not yet been found translocated or mutated in human/mouse hematologic malignancies. Abbreviations: LT-HSC, long-term hematopoietic stem cell; ST-HSC, short-term hematopoietic stem cell; CMP, common myeloid rogenitor; CLP, common lymphoid progenitor; MEP, megakaryocyte/erythroid progenitor; GMP, granulocyte/macrophage progenitor; RBCs, red blood cells (Orkin and Zon 2008).

Among the genes most frequently deregulated in human acute myeloid leukemia there is AML1, also known as Cbfa2 and Runx1, that belongs to the family of runt domain-containing transcription factors (Roumier et al., 2003). AML1 is a crucial regulator of hematopoietic development and the absence of AML1 results in severe embryonic hemorrhaging, that eventually culminates in lethality around E12.5, and in profound fetal liver anemia (Costa, Kouskoff et al. 2012). Although these embryos

contain primitive erythroid blood precursors, they fail to undergo definitive hematopoiesis and show a complete absence of functional adult repopulating HSC (Durand and Dzierzak 2005; Rybtsov, Sobiesiak et al. 2011; Costa, Kouskoff et al. 2012) . Experiments on mice with conditional knockout of AML1 showed that, during adult definitive hematopoiesis, AML1 is necessary for the proper maturation of lymphocytes and megakaryocytes, but dispensable for other myeloid lineage cells. In absence of AML1, moreover, there is an expansion of the most immature progenitor population in the BM, (Putz, Rosner et al. 2006) suggesting a role for AML1 in HSC generation, localization and/or maintenance.

Examples of lineage-specific transcription factors are GATA1 and KLF1, that play central roles in erythroid-specific transcription by forming complexes with multiple other proteins to upregulate the expression of erythroid-specific genes. GATA1 is the founding member of the GATA transcription factor family of dual zinc finger proteins that bind a WGATAR consensus motif present in essentially all erythroid-specific genes. Targeted disruption of GATA1 in the mouse leads to a block of primitive erythroid cell maturation at the proerythroblast stage of maturation resulting in embryonic death of severe anemia between E9.5-10.5, prior to the shift of hematopoiesis from the yolk sac to the fetal liver (Fujiwara, 1996). Thus, hematopoiesis including erythroid commitment appears to occur in the absence of GATA-1. The arrested proerythroblasts contain an elevated level of transcripts for the related transcription factor GATA-2, which we showed is essential in its own right for the proliferation or survival of hematopoietic progenitors (Tsai et al., 1994). Hence, it is likely that a failure to repress GATA-2 in absence of GATA-1 provides for partial erythroid differentiation due to overlapping functions of these related proteins. The arrested GATA-/- proerythroblasts undergo apoptosis, indicating that GATA-1 acts to prevent death of erythroid precursors in which it is expressed

KLF1 (EKLF) was the first of 17 KLFs to be identified in mouse and man and its expression is largely restricted to both primitive and definitive erythroid lineages, While it was initially thought that KLF1 primarily up-regulates the adult β-globin gene through interactions with its CACC motif, it is now recognized that KLF1 also regulates the expression of multiple erythroid-specific genes, including cytoskeletal proteins and alpha hemoglobin stabilizing protein (Hodge, Coghill et al. 2006). *Klf1*-/- mice develop fatal anemia associated with a marked deficit in β-globin expression

during definitive fetal liver erythropoiesis, due to a defect in the maturation of red blood cells, and die by E16.0 (Drissen, 2005; Basu, 2007). The time of death coincides with the stage of development in which the fetuses become dependent on definitive, fetal liver-derived, erythroid cells that take over the oxygen transport from the primitive, yolk sac-derived cells It was initially reported that KLF1 does not affect embryonic and fetal globin gene expression, however, KLF 1 is expressed in these cells and also plays an essential role in hemoglobin metabolism and membrane stability in primitive erythroid cells, so KLF1 protein is functionally present in both primitive and definitive erythroid populations (Palis, Malik et al. 2010)

1.5. Nuclear factor I: a family of transcription factors

Nuclear Factor I (NFI) transcriptional factors constitute a family of site-specific DNA-binding proteins that play wide roles in animal physiology, biochemistry and pathology. While first described as being required for the replication of Adenovirus DNA, this family of transcription/replication proteins has been implicated in the replication of several other viruses and has been shown to regulate the transcription of a large variety of cellular and viral genes (Gronostajski, Adhya et al. 1985). In addition, NFI proteins have been associated with changes in cell growth and with a number of oncogenic processes and disease states. It was demonstrated that NFI-binding sites function in both DNA replication and gene expression (Jones, Kadonaga et al. 1987). Subsequent studies have identified NFI-binding sites in the promoter, enhancer and silencer regions of more than 100 cellular and viral genes, and mutation analyses indicate that these sites are important for the expression of most or all of these genes (Gronostajski, Adhya et al. 1985). NFI proteins bind as dimers or heterodimers (see below) to the dyad symmetric consensus sequence TTGGC(N5)GCCAA on duplex DNA. Sequences flanking the consensus and present in the degenerate 5 nucleotides spacer region appear to modulate the NFI-binding affinity (Gronostajski 1986; Gronostajski 1987). Quantitative analysis of binding showed that while NFIs factors bind very tightly to a dyad symmetric site, they can also bind specifically to individual half sites (TTGGC or GCCAA) with a reduced affinity (Meisterernst, Gander et al. 1988).

Several different nomenclatures arose for the NFI genes, leading to confusion regarding the number of NFI genes in mammals. The most popular is based on the four NFI genes identified in the chicken and named NFI-A, NFI-B, NFI-C and NFI-X (Rupp, Kruse et al. 1990; Kruse, Qian et al. 1991). Homologs of these four NFI genes have been described in every vertebrate species examined from xenopus, to mouse and humans, and likely represent all of the NFI genes in vertebrates.

All NFI genes are composed by 11 exons and they show an high degree of structural homology. These observations demonstrate that little divergence of the genes has occurred since their generation prior to the establishment of the avian lineage, which contains all four genes. Transcripts of each of the four NFI genes are alternatively spliced generating multiple proteins from each gene. This complexity of protein and

mRNA isoforms can be simplified considering domains that are conserved in all of the isoforms and between the four vertebrate genes.

NFI proteins are composed of a N-terminal DNA-binding/dimerization domain and C-terminal transcriptional activation and/or repression domains. The N-terminal DNA-binding/dimerization domain is preceded by an highly conserved region of alternative exons encoding 8–47 aa domains of unknown function (Meisterernst, Rogge et al. 1989; Rupp, Kruse et al. 1990; Kruse, Qian et al. 1991; Kruse and Sippel 1994). NFI factors DNA-binding/dimerization domain is ~200 aa in length and is ~90% identical between the four chicken, mouse, and human NFI genes. This N-terminal domain is sufficient for DNA-activity, dimerization and the stimulation of adenovirus DNA replication (Mermod, O'Neill et al. 1989; Gounari, De Francesco et al. 1990). Point mutations made within this domain have shown that dimerization is essential for DNA-binding activity, which can be abolished independently with retention of dimerization activity (Armentero, Horwitz et al. 1994). Point mutations within this domain can abolish adenovirus DNA replication while retaining both DNA binding and dimerization. Moreover the specific interaction of the N-terminal DNA-binding/dimerization with the Adenovirus DNA polymerase appears to be essential for the recruitment of the polymerase into a replication complex and the stimulation of replication (Bosher, Robinson et al. 1990; Chen, Mermod et al. 1990; Mul, Verrijzer et al. 1990; Armentero, Horwitz et al. 1994). The NFI DNA-binding domain has no detectable sequence homology with other known DNA-binding sites and thus may be structurally distinct. Four cysteine residues are conserved between all NFI DNA-binding domains, and three of the four residues are required for DNA-binding activity (Bandyopadhyay and Gronostajski 1994; Bandyopadhyay, Starke et al. 1998). While not essential for DNA-binding activity, the fourth cysteine residue makes NFI proteins sensitive to oxidative inactivation (redox regulation), a feature shared by a number of transcription factors that may play a role in the cellular response to oxidative damage (Abate, Patel et al. 1990; Guehmann, Vorbrueggen et al. 1992; Matthews, Wakasugi et al. 1992; Bandyopadhyay, Starke et al. 1998). The minimum size of the NFI DNA-binding/dimerization domain may differ slightly between the four NFI genes, and different C-terminal regions of the proteins, obtained by alternative splicing, may influence DNA-binding affinity. The DNA-binding affinity is higher when the isoform is larger (Gronostajski 2000).

While the DNA-binding and replication activities of NFI proteins reside in the N-terminal domain, C-terminal domains have been implicated in most, though not all, regulation of gene expression by NFI factors. As described above, alternative splicing generates many variants of the C-terminal domains of NFI proteins, a fraction of which have been tested for functional activity (Gronostajski 2000).

Unusual features of NFI transcripts are their large 5' and/or 3' untranslated regions and the presence of short (2–33 aa) putative open reading frames (ORFs) upstream of the predicted initiation codons. Analysis of the 5' regions of NFI cDNAs present in GenBank shows the presence of such ORFs from 8 to 98 residues upstream of the predicted initiation codons of all four NFI genes from a number of vertebrates (Gronostajski 2000). Together with the observation that the major NFI transcripts are very large, the presence of these short ORFs raises the possibility of translational regulation of NFI protein expression. Another possible function for the large untranslated regions of NFI mRNAs may be in the regulation of mRNA stability (Gronostajski 2000).

Since NFI proteins bind to DNA as dimers, several studies have examined whether heterodimers can form between the products of the different NFI genes. Efficient formation of DNA-binding heterodimers has been shown between products of all four chicken NFI genes, with few or no differences being seen in DNA-binding affinity, specificity, or stability of the dimers (Kruse and Sippel 1994). As was seen previously with homodimer formation of human and porcine NFI-C and rat NFI-A (Meisterernst, Rogge et al. 1989; Mermod, O'Neill et al. 1989), the different chicken NFI proteins needed to be co-translated in order to form heterodimers. Mixing of preformed homodimers yielded no heterodimers. Moreover heterodimers between NFI gene products may have different characteristics depending on the components of the heterodimer (Liu, Bernard et al. 1997).

NFI proteins affect transcription through multiple mechanisms. The best studied mechanism used by NFI proteins to activate transcription is through direct interaction with basal transcription factors. A second mechanism proposed for activation of target genes by NFI proteins is a epigenetic one: a number of studies suggest that histone H1 can bind weakly to consensus NFI-binding sites, and that NFI may activate transcription by direct displacement of histone binding at such sites

(Ristiniemi and Oikarinen 1989; Gao, Jiang et al. 1996). It is also likely that specific interactions between NFI proteins and various co-activator proteins play a role in transcriptional activation; NFI proteins, in fact, may interact with a variety of co-activators in vivo, and the relative importance of any given co-activator may be cell-type or promoter-specific (Gronostajski 2000). NFI proteins can repress transcription in cell-type and promoter-specific way. One mechanism postulated for repression by NFI proteins is through direct competition with more potent transactivators for binding at adjacent sites; such competition may play a role in cell-specific activation/repression by NFI proteins, where the balance between activation and repression may be dependent on the specific isoforms of NFI expressed in a given cell type (Gronostajski 2000). NFI-binding sites have also been seen to promote repression under conditions where competition between binding sites is unlikely (Macleod and Plumb 1991; Adams, Choate et al. 1995; Szabo, Moitra et al. 1995; Osada, Daimon et al. 1997; Crawford, Leahy et al. 1998; Rajas, Delhase et al. 1998; Cooke and Lane 1999; Leahy, Crawford et al. 1999). In these instances specific C-terminal regions of NFI proteins can function as repressors when attached to heterologous DNA-binding domains, supporting the hypothesis that direct repression by NFI proteins occurs in vivo. It is unknown how these repression domains of NFI function, but they may be related to known active processes such as the recruitment of corepressor proteins by hormone receptors, or direct interaction with the basal transcription apparatus (Pazin and Kadonaga 1997).

1.5.1. *NFI family and embryo development*

Binding sites for NFI proteins have been characterized from genes expressed specifically in almost every organ system and tissue, including brain, lung, liver, kidney, muscle, blood, testes, oviduct, thyroid, adrenal medulla, mammary gland, pituitary, retina, olfactory epithelium, fibroblasts, epithelial cells, adipocytes, chondrocytes, neurons and glia. For most of these, the NFI-binding sites have been shown to be important for gene expression control (Gronostajski 2000). The finding that NFIs control a set of tissue specific and developmentally regulated genes suggest their role in cell differentiation and embryo development.

During embryonic development in the mouse, the four NFI genes are expressed in unique, but widely overlapping, patterns, supporting the hypothesis that differential

expression of the genes results in differential expression of gene-specific target proteins during development (Chaudhry, Lyons et al. 1997).

The most direct evidence for a role for NFI proteins in development comes from the disruption of the NFIs genes in mice. For instance, the homozygous deletion of the *Nfi-A* gene (das Neves, Duchala et al. 1999), leads in more than 95% of cases to death shortly after birth, and the few survivors develop severe hydrocephalus and tremors indicating a neurological defect. All homozygous animals lack a corpus callosum, the major fiber tract connecting the two hemispheres of the brain. However, other than agenesis of the corpus callosum, no major anatomical defects have detected. Since some strains of mice show relatively high frequencies of callosal agenesis (Ozaki and Wahlsten 1992; Livy and Wahlsten 1997; Magara, Muller et al. 1999), it is unclear whether the agenesis of the corpus callosum contributes directly to the perinatal lethality. Since severe hydrocephalus develops within 2 weeks after birth in the rare surviving homozygotes, it is possible that relatively subtle neuro-anatomical defects contribute to early lethality. In the randomly bred Swiss genetic background, there is also a significant loss of heterozygous *Nfi-A*-deficient mice, but only if the knockout allele is transmitted by the maternal parent. This unusual trait suggests either that heterozygous females show some haploinsufficiency that affects rearing of heterozygous pups or that imprinting or some other epigenetic process affects the expression of, or response to, the *Nfi-A* gene. Given the early expression of *Nfi-A* in mouse development (E9.0 in heart and brain, widespread expression by E11.5), it is somewhat surprising that clear anatomical defects have been detected only at E16.0–E18.0 where failure of development of the corpus callosum is seen. One possibility is that the four NFI genes may play partially redundant roles in various tissues, and defects are seen only where one gene product is most important.

Nfi-B$^{-/-}$ mutant mice die within 15 min postpartum due to respiratory distress, due to a delay in the development of lungs, arrested the late pseudoglandular stage. Besides the lung phenotype, the only obvious phenotypic defect of these mutants are open eyes without eyelids. Other organs known to express the *Nfi-B* gene appeared normal, suggesting that in them *Nfi-B* is redundant and that its loss is possibly compensated by the expression of other NFI genes. *Nfi-B*$^{+/-}$ littermates survive and are indistinguishable from their wild-type littermates. However, the histology of their

lungs at E18.5 or shortly after birth showed mild alveolar hypoplasia, an intermediate status between homozygous mutants and wild-type littermates; these observations suggest that the gene dosage of *Nfi-B* is critical for lung development (Grunder, Ebel et al. 2002).

Loss of *Nfi-C* causes major defects in postnatal murine tooth development, the most striking defect being loss of molar root formation. In addition, there are clear defects in mandibular and maxillary incisor formation and in alveolar bone formation in molar tooth sockets. These tooth and bone defects cause runting and lethality unless the *Nfi-C*$^{-/-}$ animals are reared on a soft-dough diet. Since *Nfi-C*$^{-/-}$ animals can survive and be fertile if maintained on nutrient dough, it appears that the tooth defects cause the lethal phenotype seen with loss of *Nfi-C*. Whether additional nonlethal developmental defects are present in the *Nfi-C*$^{-/-}$ animals awaits further analyses (Steele-Perkins, Butz et al. 2003).

Nfi-X$^{-/-}$ mice die between postnatal days 21 and 28, exhibiting brain malformations, defects in endochondral ossification and some pathological changes of the digestive tract. Brain malformations are partially similar to ones caused by the loss of *Nfi-A*; these animals shows in fact hydrocephalus a partial agenesis of the corpus callosum. Histological analysis of spines and femurs of *Nfi-X*$^{-/-}$ mice revealed a delay in endochondral ossification that lead to a significantly reduced trabecular bone formation and calcification (Driller, Pagenstecher et al. 2007). Moreover it has been shown that *Nfi-X* activates fetal and suppresses embryonic genes in embryonic muscle, acting as a transcriptional regulator of the switch from embryonic to fetal myogenesis (Messina, Biressi et al. 2010).

Of interest that during development, NFI-A and NFI-C transcripts are expressed in the mesenchyme surrounding the posterior cardinal and vitelline veins and the area surrounding the aortic arches respectively (Chaudhry, Lyons et al. 1997), which are areas where hematopoietic development occurs. NFI-X knockout mice had an altered appearance of the bone marrow (Driller, Pagenstecher et al. 2007).

2. Research aims

Among NFI transcription factors, NFI-A became subject of interest in our lab, because of its involvement in hematopoiesis. Fazi et al. demonstrated that NFI-A is a target of miR-223 activity during granulocytopoiesis (Fazi, Rosa et al. 2005). NFI-A can compete with the CCAAT enhancer protein α (C/EBPα) binding to the CCAAT element on the miR-223 promoter. In myeloid precursors, the activation of C/EBPα by retinoic acid treatment displace NFI-A from this binding site on miR-223 promoter, thus allowing miR-223 upregulation. MiR-223 acts by repressing NFI-A and subtracts it from the competition with C/EBPα on miR-223 promoter, maintaining sustained levels of miR-223 expression and allowing granulocytic differentiation.

A regulatory circuitry similar to the one involving NFI-A and miR-223 during granulocytopoiesis, has been identified during monocytic-macrophage differentiation. To progress into monocyte lineage, hematopoietic progenitors up-regulate the lineage-specific transcription factor PU.1. PU.1 is able to induce the expression of miR-424, that synergizes with PU.1 for the activation of terminal differentiation genes through the repression of NFI-A (Rosa, Ballarino et al. 2007).

Further studies indicated that NFI-A plays a major role in the control of the erythroid-granulocytic lineage decision at the HPCs level. In unilineage erythroid and granulocytic cultures of human HPCs, which recapitulate the *in vivo* differentiation/maturation of hematopoietic stem cells to these hematopoietic lineages, the expression of NFI-A, although low in early HPC differentiation, was either sharply up-regulated or fully suppressed in later stages of erythroid or granulocytic culture respectively. NFI-A accumulation during initial erythroid differentiation results in progressive activation of β-globin gene transcription, coupled with repression of G-CSFR, thus channeling HPCs and early precursors into the erythroid lineage and shutting off their granulocytic potential. Conversely, NFI-A suppression in early granulocytopoiesis activates G-CSFR transcription and impedes β-globin expression, thereby directing HPCs and early precursors into the granulocytic pathway (Starnes, Sorrentino et al. 2009). Moreover a recent study of

gene expression profiling and chromatin immunoprecipitation, performed using $CD34^+$ HPCs and leukemic K562 cells efficiently expressing exogenous NFI-A at high level, revealed that NFI-A is able to induce an erythroid transcriptional program and to act directly at the proximal promoter regions of two fundamental erythroid genes: SLC4A1, encoding the major anion exchanger of the red cell, and ALAS2, encoding the erythroid specific form of the ALAS enzyme, that catalyze the first step in the heme biosynthetic pathway (Starnes, Sorrentino et al. 2010).

All these evidences prompted us to investigate about the *in vivo* role of NFIs factors during embryonic and adult hematopoiesis, with a particular attention to NFI-A.

To this end we have analyzed the behavior of NFIs factor in hematopoietic tissues, during embryo development of CD1 mice. In a second time we started to use two different strains of NFI-A -/- mice: B6N31 and B6hyb129 mice.

Principal Aims of this Ph.D project were the following:

- To define a correlation between NFIs factors and the progress of hematopoiesis;
- To analyze the effects of the disruption of NFI-A on embryonic and adult hematopoietic tissues, characterizing both our NFI-A -/- mouse models through histological and molecular analysis and defining the role of NFI-A in hematopoiesis
- To identify hematopoietic disorders potentially related to NFIs functional defects

3. Materials and methods

3.1. Mice genotyping

Tails from B6N31 pups and skin from B6N31 embryos were lysed at 55°C o/n with a lysis buffer composed of: 100mM Tris-HCl (Sigma, St Louis, MO, USA), pH8.8; 5mM EDTA (Sigma, St Louis, MO, USA), pH8.0; 0.2% SDS (Sigma, St Louis, MO, USA); 200mM NaCl (Sigma, St Louis, MO, USA); 100 ug/mL Proteinase K (Invitrogen, Carlsbad, CA, USA). The DNA content of the lysate was quantified by spectrophotometer and 75ng were used to do a PCR using was analyzed by PCR in a total volume of 30 µl with the following mix: 1 U of Platinum® Taq DNA polymerase (Invitrogen, Carlsbad, CA, USA), a primer mix (0.2 pmol/ µl each) composed of NfiaI2b, NfiaI2cc, Neo57, Neo371R, Sry1 and Sry2 (PCR genotyping primer's sequences are listed in the table 3.1) 2 x 10^{-4} dNTPs (Invitrogen, Carlsbad, CA, USA) and $MgCl_2$ 1.5 x 10^{-3} (Invitrogen, Carlsbad, CA, USA). PCR conditions were as follows: 4 minutes at 94°C followed by 30 seconds at 94°C, 1 minute at 60°C and 1 minute at 72°C for 30 cycles and a final extension of 10 minutes at 72°C. PCR products were resolved on 2% agarose gels and visualized with ethidium bromide.

3.2. Embryonic tissues

Timed pregnant CD1 and B6N31 mice were killed by cervical dislocation and uteri were removed from the peritoneum and washed with several changes of phosphate-buffered saline (PBS) (Gibco-BRL, Grand Island, USA). Decidual tissues and Reichert's membrane was dissected free of the embryos in PBS (Gibco-BRL)
10% FBS (Gibco-BRL) solution. Presomite embryos (E7.0) were staged and grouped according to established morphological criteria (Downs and Davies 1993), and somite stage embryos (E8.0-E14.0) were grouped according to somite number. Individual embryos were either kept whole or dissected to remove the yolk sac and

amnion= yolk sac, AGM, dorsal Aorta, GM, liver, heart, heads, FLB, HLB, spleen and bone marrow for further processing.

3.3. Adult tissues

Adult CD1 and B6N31 mice were euthanized via CO_2 inhalation. Immediately after inhalation peripheral blood was collected by cardiac puncture of the heart using a 1mL syringe and 27G needle (Terumo, Leuven, Belgium). Blood was collected and placed in a collection tube containing ethylenediaminetetraacetic acid (EDTA) (Starsted, Nünbrecht, Germany) to prevent coagulation. Red blood cells (RBCs) were lysed using the Buffer EL erythrocyte lysis buffer (Qiagen, Hilden, Germany) according to the manufacturer's instructions. The resulting cell pellet was then used for either RNA extraction or lysed to obtain protein for western blotting. Livers of adult mice were dissected from euthanized mice and washed several times in cold PBS. To obtain liver cells, spleens were then mechanically dissociated in cold PBS (Gibco-BRL) and passed through a 70 µM filter (BD Biosciences, Franklin Lakes, NJ, USA). The resulting cells were pelleted by refrigerated centrifugation at 1200 rpm for 5 min at 4°C and the RBCs were lysed as described previously. The resulting pellet was then used for RNA extraction, or was lysed to obtain protein for western blotting. To obtain sections, livers were fixed in 4 % paraformaldehyde and embedded in paraffin. The spleens of adult mice were dissected from the euthanized mice and washed several times in cold PBS. To obtain spleen cells, spleens were then mechanically dissociated in cold PBS (Gibco-BRL) and passed through a 70 µM filter (BD Biosciences, Franklin Lakes, NJ, USA). The resulting cells were pelleted by refrigerated centrifugation at 1200 rpm for 5 min at 4°C and the RBCs were lysed as described previously. The resulting pellet was then used for RNA extraction, or was lysed to obtain protein for western blotting. To obtain sections, spleens were fixed in 4 % paraformaldehyde and embedded in paraffin. For collection of bone marrow cells, whole legs were dissected free from the hip of a euthanized mouse, and muscle tissue was cleaned away from the femora and tibiae. To obtain cells, the head of the femur or tibia was cut and a 5mL syringe with 26G

needle containing cold IMDM medium (Gibco-BRL) and 10% FBS (Gibco-BRL) was used to flush bone cavities to collect bone marrow. The cells were centrifuged at 1200 RPM for 5 min at 4°C and the RBCs were lysed from the resulting pellet as above. Cell pellets were then used for RNA extraction or lysed to obtain protein for western blot.

3.4. Decalcification of bones

B6N31 and B6hyb 129bones were fixed in 4 % paraformaldehyde and placed in a volume of 14% EDTA (Sigma, St Louis, MO, USA) pH 7.3 equal to 20X the volume of the tissue. The samples are placed at +4°C and the solution changed every week until the decalcification was completed. Once decalcified the bones were embedded in paraffin.

3.5. RNA extraction and analysis

Total RNA was isolated using the Trizol® reagent (Invitrogen, Carlsbad, CA, USA) following the manufacturer's instructions for AML cell lines, unilineage and bilineage culture of human HPCs, and mouse whole tissues (yolk sac, AGM, spleen, liver, peripheral blood). For extraction of RNA from samples containing few cells (embryonic colonies), RNA was extracted using the RNeasy Plus Micro kit® (Qiagen). First-strand cDNA of all samples was synthesized with the SuperScript® II (Invitrogen) reverse transcriptase enzyme using equivalent amounts of total RNA for each sample and oligo (dT) (Invitrogen) primers. mRNA quantification of samples was performed in triplicate by real-time PCR using the **ABI PRISM 7700** Sequence Detection System (Applied Biosystems, Foster City, CA, USA) and SYBR Green® PCR reaction mix (Applied Biosystems) with ΔCt values normalized using endogenous GAPDH or HPRT1 as control. Primers used for SYBR Green® real-time PCR are listed in Table 3.1. Semiquantitative PCR was performed on 1 μl of

cDNA using the primers listed in Table 3.1, with the following mix: 1X PCR buffer (Invitrogen), Primer mix (0.2 pmol/ µl each), 2 x 10-4 dNTPs (Invitrogen), MgCl2 1.5 x 10-3 (Invitrogen), and 2.5 U Platinum® Taq DNA polymerase (Invitrogen).

Primer use	**Primer name and sequence**
Mice genotyping	Nfi-a I2B 5'-TGCTGTGTTCTGGTCAGTCAAG-3' Nfi-a I2CC 5'- CAAAGCAAATCTCCATGCTCGG-3'
Mice genotyping	Sry1 5'-AACAACTGGGCTTTGCACATTG-3' Sry2 5'-GTTTATCAGGGTTTCTCTCTAGC-3'
Mice genotyping	Neo57 5'- GGAGAGGCTATTCGGCTATGAC -3' Neo371R 5'- CGCATTGCATCAGCCATGATGG -3'
Quantitative and semiquantitative PCR	Gapdh for 5' - ATCAGCAATGCCTCCTGCAC - 3' Gapdh rev 5' - TGGCATGGACTGTGGTCATG - 3'
Quantitative and semiquantitative PCR	mNFIA for 5' - TGGCATACTTTGTACATGCAGC -3' mNFIA rev 5' - ACCTGATGTGACAAAGCTGTCC - 3'
Quantitative and semiquantitative PCR	mNFIB for 5' - GTTTTTGGCATACTACGTGCAGG - 3' mNFIB rev 5' - CTCTGATACATTGAAGACTCCG - 3'
Quantitative and semiquantitative PCR	mNFIC for 5' - GACCTGTACCTGGTCTACTTTG - 3' mNFIC rev 5' - CACACCTGACGTGACAAAGCTC - 3'
Quantitative and semiquantitative PCR	mNFIX for 5' - CTGGCTTACTTTGTCCACACTC - 3' mNFIX rev 5' - CCAGCTCTGTCACATTCCAGAC - 3'
Quantitative and semiquantitative PCR	mHprt1 for 5' - TCCTCCTCAGACCGCTTTT – 3' mHprt1 rev: 5' – CCTGGTTCATCATCGCTAATC – 3'
Semiquantitative PCR	Aml1 for 5' - GGCACTCTGGTCACCGTCAT - 3' Aml1 rev 5' - CGTTGAATCTCGCTACCTGGTT - 3'
Semiquantitative PCR	mHbb-bh1 for 5' - CCTGATTGTTTACCCATGGAC - 3' mHbb-bh1 rev 5' - CAATCACCAACATGTTGCCCAG - 3'
Semiquantitative PCR	mHbb-b for 5' - GGTGCACCTGACTGATG - 3' mHbb-b rev 5' - AGTGGTACTTGTGAGCC - 3'
Semiquantitative PCR	Gata-1 se 5' - GGAGCCCTCTCAGCTCAGC - 3' Gata-1 as 5' - GCCACCAGCTGGTCCTTCAG - 3'

Semiquantitative PCR	c-fms for 5’ - CTGAGTCAGAAGCCCTTCGACAAAG -3' c-fms rev 5’ -CTTTGCCCAGACCAAAGGCTGTAGC -3’
Semiquantitative PCR	mKLF1 for 5’ - GAGACTGTCTTACCCTCCAT - 3’ mKLF1 rev 5’ - CCACGAAGGGTTCAGGGGCT - 3’
Quantitative and semiquantitative PCR	mHba-α for 5′-CCTGGGGGAAGATTGGTG-3′ mHba-α rev 5′-GCCGTGGCTTACATCAAAGT-3’
Quantitative PCR	mHbb-bh1 for 5’ – AGTTTGGAAACCTCTCTTCTGCCCTG -3’ mHbb-bh1 rev: 5’ – TGTTCTTAACCCCCAAGCCCAAG - 3’
Quantitative PCR	mHbb-b for 5′-ATGGCCTGAATCACTTGGAC-3′ mHbb-b rev 5′-ACGATCATATTGCCCAGGAG-3″
Quantitative PCR	mHbb-γ for 5’ -TGGCCTGTGGAGTAAGGTCAA-3’ mHbb-γ rev 5’-GAAGCAGAGGACAAGTTCCCA-3’

Table 3.1: **Primer name and sequence for primers employed during mice genotyping, semiquantitative PCR, and qRT-PCR**

3.6. Immunoblotting

Total protein was extracted using CelLytic M Lysis® Reagent (Sigma, St Louis, MO, USA) following the manufacturer’s protocol, supplemented with Protease Inhibitor Cocktail (Sigma, St Louis, MO, USA). Protein concentration was determined by the Lowry Protein Assay (Lowry, Rosebrough et al. 1951). Total cell extracts were fractionated under denaturating conditions by electrophoresis on NuPAGE® 10% Bis-Tris gels (Invitrogen) using NuPAGE® MOPS SDS running buffer (Invitrogen) followed by electroblotting onto a nitrocellulose membrane (Whatman PROTRAN® Dassel, Germany). Blots were probed with the following primary antibodies: polyclonal anti-NFI-A (Abcam, Cambridge, UK), monoclonal anti-β-actin (Calbiochem, San Diego, CA, USA), polyclonal anti-AML1/RHD (Calbiochem, San Diego, CA, USA), polyclonal GATA-1 (Santa Cruz CA USA). Secondary antibodies used were as follows: anti-mouse IgG peroxidase conjugate and anti-rabbit IgG peroxidase conjugate (Pierce, Rockford, IL, USA). Immunoreactivity was measured using the ECL method (GE Healthcare, UK).

3.7. Primitive erythroid progenitor (EryP-CFC) assay

Yolk sacs of E8.0 CD1 embryos were dissected, as written below, pooled together and placed in Dulbecco's modified eagle medium (DMEM) (Gibco-BRL) with 10% FBS. Yolk Sacs were pelleted by brief centrifugation and resuspended in 200 µl PBS and 0.25% collagenase (Sigma, St Louis, MO, USA) and placed at 37°C for 30 min-1h after which single cells were obtained by vigorous pipetting. Excess cold PBS with 10% FBS was then added to the cells to stop the collagenase reaction followed by centrifugation at 1200 rpm for 5 min at 4°C. Cells were resuspended in IMDM 2% FBS (Gibco-BRL), and counted using Trypan Blue staining (Sigma, St Louis, MO, USA). Cells were plated in triplicate at 1 x 10^5 cells/mL in 0.9% methylcellulose-based media MethoCult® M3134 (StemCell Technologies, Vancouver BC, Canada) including IMDM, 2mM glutamine (Gibco-BRL), 1% penicillin/streptomycin (Gibco-BRL), 5% protein-free hybridoma medium II (PFHM-II; Gibco-BRL), 50 µg/mL ascorbic acid (Sigma, St Louis, MO, USA), 450 µM monothioglycerol (MTG; Sigma, St Louis, MO, USA), 200 µg/mL iron-saturated holo-transferrin (Sigma, St Louis, MO, USA), 15% plasma-derived serum (Sera Laboratories International LTD, West Sussex, UK) and 4 U/mL rhEPO (PBL Biomedical Laboratories, New Brunswick, NJ, USA). Primitive colony numbers were scored after 7 days of culture in a fully humidified incubator at 37°C with 5% CO_2 in air.

3.8. Embryonic definitive colony assay

Tissues from individual embryos of CD1 mice of yolk sac E9.0, AGM E11.0-12.0, and Liver E11.0 and E14.0 were isolated from individual embryos and then pooled together as described below. Individual tissues were then placed in DMEM (Gibco-BRL) with 10% FBS (Gibco-BRL). Tissues were pelleted by brief centrifugation and resuspended in 200-400 µl PBS and 0.25% collagenase (Sigma, St Louis, MO, USA) and placed at 37°C for 30 min-1h after which single cells were obtained by vigorous

pipetting. Excess cold PBS with 10% FBS was then added to the cells to stop the collagenase reaction followed by centrifugation at 1200 rpm for 5 min at 4°C. Cells were resuspended in IMDM 2% FBS, and counted using Trypan Blue staining (Sigma, St Louis, MO, USA). Yolk Sac E9.0 cells were plated in triplicate at 12 x 10^3 cells/mL in methylcellulose based media MethoCult GF 3434 (StemCell Technologies). AGM cells from E11.0 and E12.0 were plated in triplicate at a concentration of 20 x 10^3 cells/mL and Liver E14.0 cells were plated in triplicate at a concentration of 30 x 10^3 cells/mL in MethoCult® GF 3434. Embryonic definitive hematopoietic colonies (BFU-E, CFU-GM, CFU-G, CFU-M and CFU-GEMM) were scored after 7 days of culture in a fully humidified incubator at 37°C with 5% CO_2 in air.

3.9. Cellular morphologic analysis

For morphology of embryonic primitive colonies several EryP colonies were pooled, for definitive colony morphology individual colonies were picked. Collected types of cells were pelleted, washed 1X with cold PBS 1% BSA (Sigma, St Louis, MO, USA), and were spotted onto glass slides by centrifugation using the Shandon Cytospin 4 (Thermo electron©, Waltham, MA, USA). Slides were stained with standard May-Grünwald-Giemsa (Sigma, St Louis, MO, USA), and observed by conventional light field microscopy.

3.10. Indirect Immunofluorescence

Slides containing EryPs were fixed in 4% paraformaldehyde (Sigma, St Louis, MO, USA) at 4°C for 10 min and permeabilized using 1% BSA, 0.2% Triton X-100 (Sigma, St Louis, MO, USA) in PBS (PBST). Slides were incubated with 10% goat serum (Abcam, Cambridge, UK) in PBS for 1 h to block nonspecific binding, then incubated with primary polyclonal anti-NFIA antibody (Abcam, Cambridge, UK)

diluted 1:200 in PBS, 1% goat serum. Cells were washed with PBS and incubated with a Cy-2 conjugated secondary IgG anti-rabbit antibody (Jackson Immunoresearch Laboratories Inc, Suffolk, UK) diluted 1:250 in PBS 1% goat serum for 1h at room temperature. Slides were washed with PBST and then stained with 4,6-diamidino-2- phenylindole (DAPI; Sigma, St Louis, MO, USA) diluted 1:5000 in PBS for 10 min at room temperature, followed by washes with PBS and were mounted using Vectashield® Mounting Medium (Vector Laboratories Inc, Burlington, CA, USA). Cells were examined with epifluorescence on a Nikon Eclipse TE-2000-E microscope.

3.11. Myeloperoxidase activity staining

Spleens sections (4- to 5-µm thick) were cut from formalin fixed, paraffin-embedded tissues. Slides were incubated for 30 seconds at room temperature in a mixture composed of: 100 ml of 30% ethanol (Sigma, St Louis, MO, USA), 0.3g of benzidine dihydrocloride, 1ml of 0.132M $ZnSO_4$: $7H_2O$ (Sigma, St Louis, MO, USA), 1g CH_3COONa : $3H_2O$ (Sigma, St Louis, MO, USA), 0.7ml of H_2O_2 (Sigma, St Louis, MO, USA), 1.5ml of 1N NaOH (Sigma, St Louis, MO, USA), 0.2g of safranin. After staining, the slides were briefly washed under tap water, air dried and examined.

3.12. Immunohistochemistry

Tissue sections (4- to 5-µm thick) were cut from formalin fixed, paraffin-embedded tissues. Sections were deparaffinized and rehydrated by passage through a graded series of 100% xylene (Sigma, St Louis, MO, USA), 100% and 95% ethanol (Sigma, St Louis, MO, USA) and distilled water. The antigen was retrieved by heating the slides in a microwave oven in Na-citrate buffer pH 6.0 for 15 minutes.

To eliminate the endogenouse peroxidase activity, sections were incubated at room temperature with Peroxide Block for Image Analysis (ADA) (ScyTek, Logan, UT,

USA) for 12 minutes, then washed three times in PBS and incubated with Super Block (AAA) (ScyTek, Logan, UT, USA), for 5 minutes at room temperature to block nonspecific background staining. Sections were incubated at 4°C o/n with rabbit polyclonal antibody to mouse/rat/human

Myeloperoxidase (Novus Biologicals, Cambridge, UK) and with rat monoclonal antibody to mouse TER-119 (BioLegend, San Diego, CA ,USA) 1: 250, then were rinsed 3 times in PBS. CRF™ Anti-Polyvalent HRP Polymer was applied to the sections that, after an incubation of 30 minutes at room temperature, were rinsed 3 times with PBS. Immunostaining was performed using a DAB Chromogen Concentrate (ScyTek, Logan, UT, USA)/ DAB Substrate High Contrast (ScyTek, Logan, UT, USA) mixture. Slides were counterstained in hematoxylin (Sigma, St Louis, MO, USA), dehydrated by a passage through a graded series of 95% and 100% ethanol and 100% xylene and mounted in xylene-based mounting medium (Sigma, St Louis, MO, USA) before application of coverslips.

3.13. Complete blood counts

For complete blood counts, 250 µL blood was collected form retroorbital plexus into tubes containing potassium EDTA and blood count performed by Appialab. 11 B6N31 NFI-A +/+ and 12 B6N31 NFI-A +/- mice were analyzed.

3.14. Statistical analysis

All results are presented as mean ± SE. Levels of significance were determined using student's *t* test. p-values legend: * $p < 0.05$, ** $p < 0.01$

4. Results

4.1. Expression levels of NFIs factors during hematopoietic ontogeny

The presence and expression levels of NFIs factors during hematopoietic ontogeny was investigated in hematopoietic tissues obtained at different stages of development from adult CD1 mice and from CD1 embryos.

The mRNA expression levels of *Nfi-A, Nfi-B, Nfi-C* and *Nfi-X* were examined by semiquantitative PCR in adult peripheral blood, bone marrow and spleen, and in total embryo, Yolk Sac (YS), Aorta-Gonad-Mesonephros (AGM), aorta, Gonad-Mesonephros (GM) and fetal liver. With respect to the other NFI family members, at E7.0 to E9.0, *Nfi-A* shows the highest level of expression within the total embryo, YS and AGM. By E10.0 to E13.0 *Nfi-A* is detectable in all hematopoietic tissues and shows higher levels than the other *Nfi* factors in the AGM, aorta, and in GM tissues. *Nfi-B* is detectable in the AGM, Aorta, liver and GM. *Nfi-C* and *Nfi-X* are barely detectable or at low expression levels within the hematopoietic tissues, except for their high level in AGM and aorta (figure 4.1A). Within the peripheral blood, *Nfi-A* shows low expression, *Nfi-B* and *Nfi-C* are absent and *Nfi-X* is expressed at the highest levels.

NFI factors mRNA expression was also analyzed by qRT-PCR (Figure 4.1B-E). This analysis confirmed the time dependent increase of *Nfi-A* expression from E7.0 to E9.0 in CD1 total embryos and YS and in E9.0 to E12.0 AGM and livers. However, *Nfi-A* expression appears higher in definitive hematopoietic tissues (e.g. AGM and liver) with respect to the primitive ones (e.g. E8.0 YS) (Figure 4.1B). The other NFI factors present expression profiles similar to that of *Nfi-A*. *Nfi-B* expression increases in yolk sac, from E8.0 to E9.0, and in AGM from E9.0 to E12.0, as *Nfi-C* expression does (Figure 4.1C,D). *Nfi-X* mRNA levels are barely detectable from E7.0 to E10.0, while increase after E11.0 (Figure 4.1E).

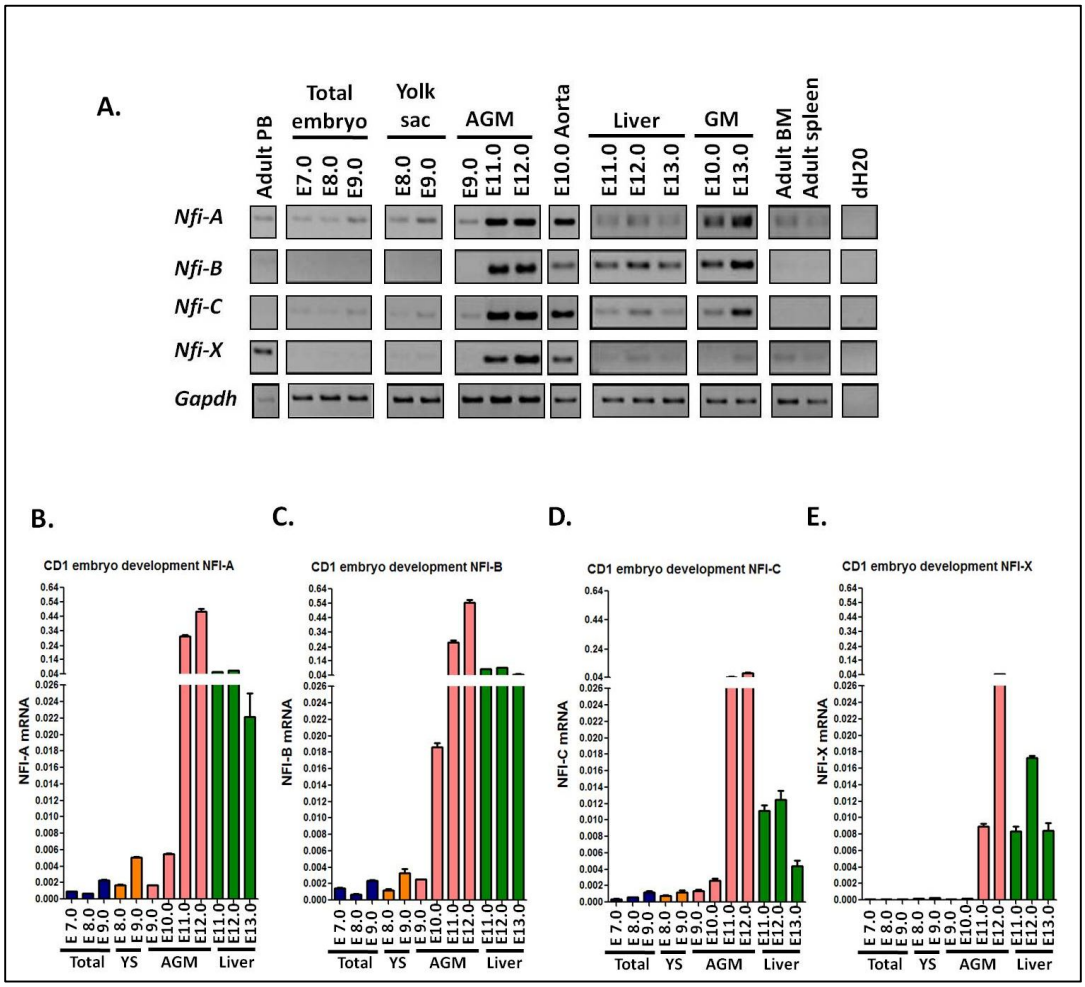

Figure 4.1: A**nalysis of NFI factors mRNA expression in CD1 mice in hematopoietic tissues. (A)** Semiquantitative PCR of NFI factors in embryonic and hematopoietic tissues and adult peripheral blood (PB), bone marrow (BM), and spleen. GAPDH was used as control.**(B-D)** qRT-PCR of Nfi-A **(B),** Nfi-B **(C)**, Nfi-C **(D)** and Nfi-X **(E)** mRNA expression in CD1 total embryos, Yolk Sacs (YS), AGM and liver**.**

The NFI factors mRNA expression levels were analyzed also in non hematopoietic tissues (Figure 4.2). In this case, the expression patterns of the four NFI genes are more similar among them. All NFIs factors are expressed at high levels by E10.0 to E13.0 heart. In particular *Nfi-A* is more expressed in E9.0 heart than *Nfi-B* and *Nfi-C*, while *Nfi-X* is absent. NFI factors are expressed in the head of E11.0 and, at higher levels, of E12.0 embryos. NFIs expression is low in somites and neural tube of E9.0, while is high in E12.0 Forelimb Buds (FLB) and Hindlimb Buds (HLB). All NFIs, except *Nfi-A,* are absent from E9.0 somite and neural tube (Som + NT) (figure 4.2).

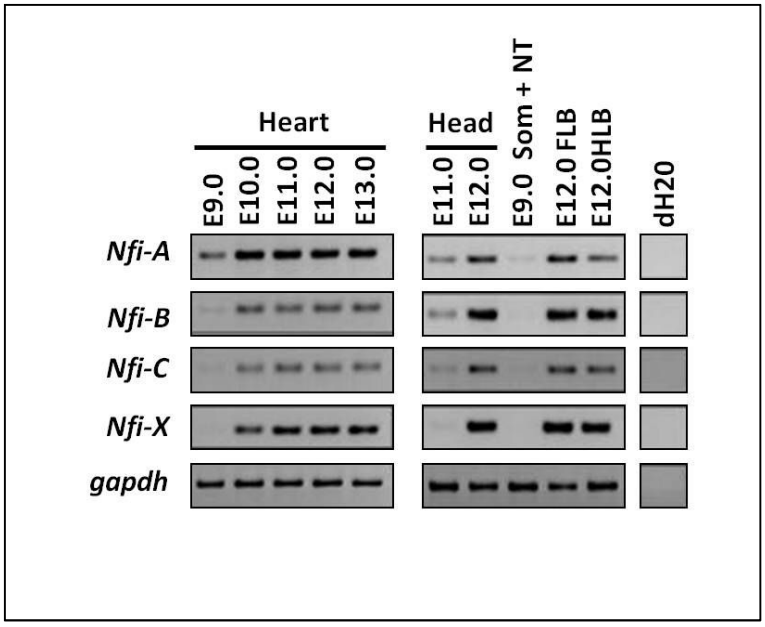

Figure 4.2: **Semiquantitative PCR of NFI factors in CD1 mice non hematopoietic embryonic tissues.** GAPDH was used as control.

To further investigate a correlation between NFI-A expression and hematopoietic development, *Nfi-A* mRNA expression levels were examined by semiquantitative PCR along with other lineage specific genes (Figure 4.3), including: *Hbb-bh1*, which encodes the embryonic β-globin, *Hbb-b*, encoding adult β-globin chains, *Klf1* and *Gata-1* encoding key transcription factors acting during primitive and definitive erythropoiesis, *c-fms*, encoding for the Colony-Stimulating Factor-1 Receptor (CSF-1R). The latter regulates the survival, growth, and differentiation of monocytes, and was used as a marker for the monocytic/macrophagic lineage. Interestingly, *Nfi-A* mRNA expression follow the same pattern of *Hbb-b* mRNA, with a time dependent increase of expression level in total embryos and YS from E7.0 to E9.0 and in AGM from E9.0 to E12.0. These results are in line with the action of NFI-A as an activator

of *Hbb-b* expression (Starnes, Sorrentino et al. 2009). *Hbb-bh1* mRNA also shows a similar expression patter of *Nfi-A* in E8.0 and E9.0 total embryos and YS, as well as in fetal liver and GM. However, unlike *Nfi-A* and *Hbb-b*, *Hbb-bh1* expression levels decreased by E9.0 to E12.0 in the AGM. Among hematopoiesis-related transcription factors, *Aml1* mRNA expression pattern is the best fitting with *Nfi-A* mRNA expression pattern in YS, AGM, liver and adult hematopoietic tissues (Figure 4.3). *Gata-1* and *Klf1* are expressed at high levels in yolk sac and liver. *c-fms* shows the highest expression within the peripheral blood fraction, its levels are low within the E9.0 yolk sac where myeloid progenitors have been noted to occur, and is expressed in E11.0-12.0 AGM. *Gata-1* and *Klf1* are expressed at high levels in yolk sac and liver. *c-fms* shows the highest expression within the peripheral blood fraction, its levels are low within the E9.0 yolk sac where myeloid progenitors have been noted to occur, and is expressed in E11.0-12.0 AGM (Figure 4.3).

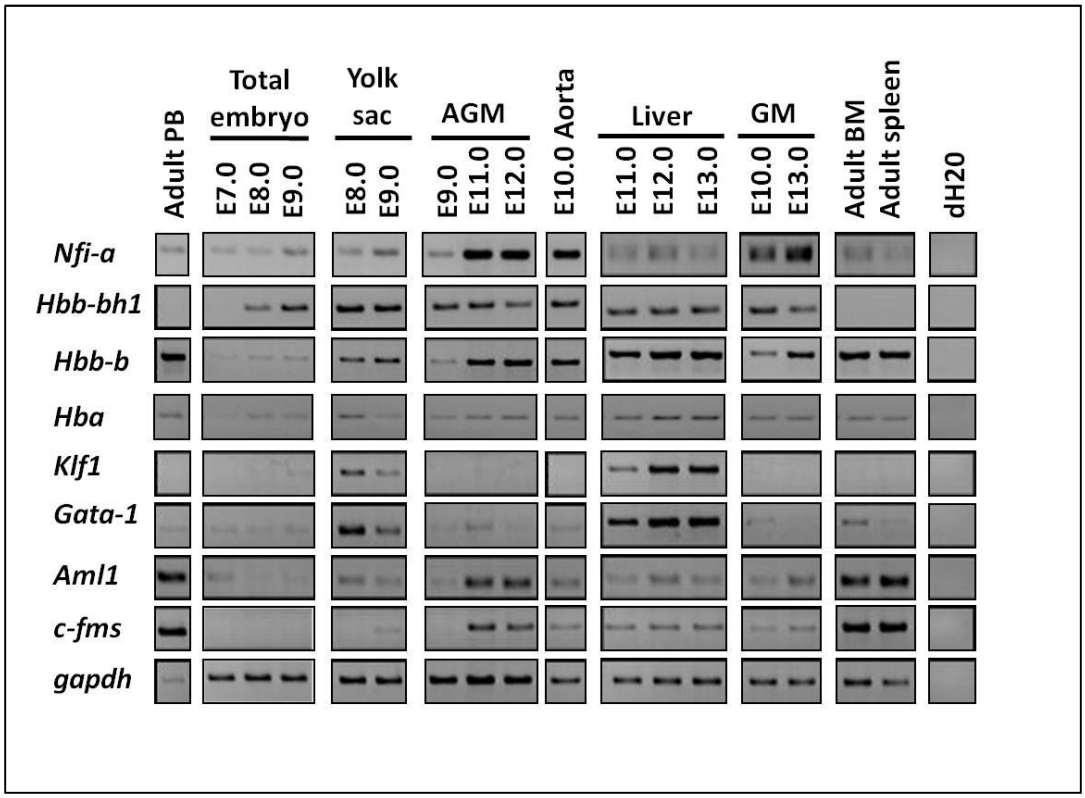

Figure 4.3: **Semiquantitative PCR of *Nfi-A* mRNA levels and other erythroid and myeloid associated genes in CD1 embryonic hematopoietic tissues and adult peripheral blood (PB), bone marrow (BM), and spleen. GAPDH was used as control.**

Based on these results, indicating a potential role of *Nfi-A* in hematopoietic ontogenesis we addressed its expression within the AGM region and yolk sac at the protein level using a specific antibody. K562 ectopically expressing NFI-A and wild type (WT) cells were used as controls (Figure 4.4). As seen in figure 4.4, in whole YS samples taken from E8.0-E11.0 embryos, NFI-A is slightly expressed at E8.0 and shows a time dependent up-regulation with the highest expression at E11.0. NFI-A is barely detectable in aorta at E10.0, but is rapidly up-regulated in the same tissue at E11.0-E12.0. NFI-A is also highly expressed in the GM region and in the liver at E11.0-12.0. Thus NFI-A appears to be expressed when primitive erythropoiesis starts and primitive erythroblasts are prominent in the yolk sac and circulation, suggesting a role for NFI-A in primitive hematopoiesis. Moreover NFI-A is expressed at high levels also in definitive hematopoietic tissues, such ad YS of E9.0-E.11.0, aorta E10.0-E12.0 and liver E11.0-E12.0, indicating a potential role also in the onset of definitive hematopoiesis.

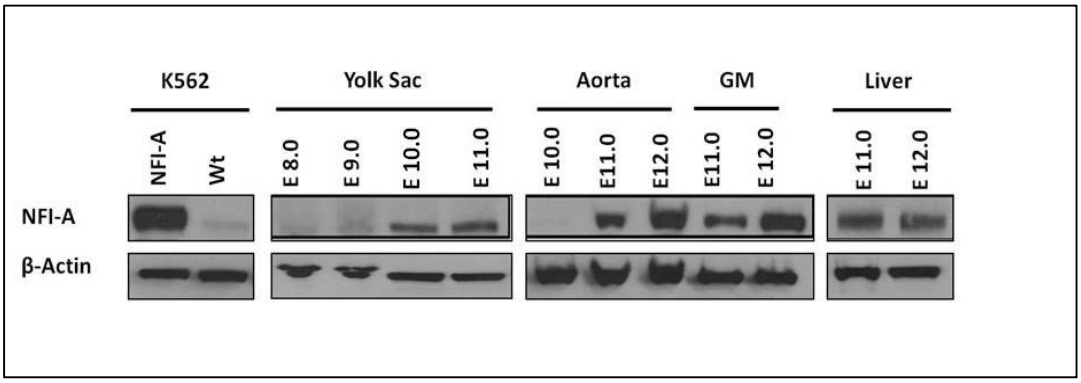

Figure 4.4: Western blot of NFI-A expression in K562 and embryonic samples. Expression analysis in whole yolk sac samples from E8.0-E11.0, Aorta and gonad-mesonephros (GM) samples from E10.0-E12.0. K562 wild-type (Wt) and NFI-A overexpressing samples were loaded as comparisons and control for NFI-A expression level. β-actin was used as a loading control.

4.2. NFI-A is expressed during primitive erythropoiesis

To further investigate the possible role of NFI-A in primitive hematopoiesis, a cell culture system specific for the development of colonies from primitive hematopoietic progenitors was established. This primitive colony assay was performed using cells suspensions obtained from E8.0 and E9.0 yolk sacs from CD1 mice, and placed in pre-made clonogenic media for the detection of primitive hematopoietic colonies (figure 4.5). After one week of culture, we obtained small bright red compact primitive erythroid colonies (EryP-CFC), macrophagic colonies (Mac-CFC) and definitive erythroid colonies (BFU-E) (Figure 4.5A). E8.0 yolk sac cells gave rise almost only to EryP-CFC, being the 96.63% of colonies obtained, with Mac-CFC comprising only 0.44% of the total CFCs, and BFU-E representing less than 1% of the total colonies (Figure 4.5B). In E9.0 yolk sac EryP-CFC decrease to the 14.35%, while Mac-CFC and BFU-E represent the 45% and 40.75% respectively (figure 4.5C). This is in line with the emergence of definitive hematopoietic progenitors in

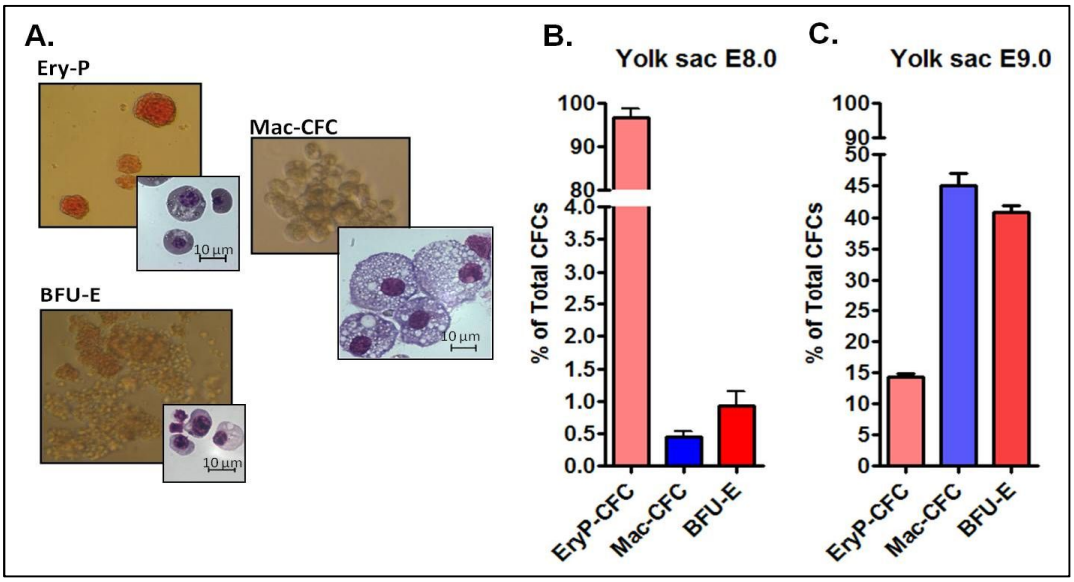

Figure 4.5: Yolk Sac primitive colony assay. 1 x 10^5 yolk sac cells were plated in triplicate in primitive EryP-CFC methylcellulose media and colonies were scored after 7 days. **(A)** Representative Ery-P, Mac-CFC and BFU-E colony and cellular morphology (original magnification X 1000) **(B)** Yolk sac E8.0 percentage of primitive erythroblasts (EryP-CFC), primitive macrophage (Mac-CFC), and definitive erythroid (BFU-E) colonies out of the total colony forming cells (CFCs) present (Mean +/- SD values from three independent experiments). **(C)** Yolk sac E9.0 percentage of primitive erythroblasts (EryP-CFC), primitive macrophage (Mac-CFC), and definitive erythroid (BFU-E) colonies out of the total colony forming cells (CFCs) present (Mean +/- SD values from two independent experiments).

murine yolk sac at around E8.25 and their expansion in this site during the following 24 hours (Wong, Chung et al. 1986; Palis and Yoder 2001).

To analyze NFI-A expression within primitive erythroid cells, individual EryP-CFC colonies obtained from E8.0 yolk sac were cytospun onto glass slides and indirect immunofluorescence using an antibody specific to NFI-A was performed. It was found that EryP-CFCs express NFI-A (Figure 4.6A). To confirm the results of indirect immunofluorescence, RNA was also extracted from E8.0 yolk sac EryP-CFCs colonies and analyzed by semiquantitative PCR (Figure 4.6B). EryP-CFCs colonies derived from two independent experiments of primitive colony assay were compared to results obtained from CD1 total embryo from E7.0-9.0, and yolk sacs from E8.0-9.0. As already seen, *Nfi-A* mRNA is expressed at a higher level in Ery-P CFCs than total E9.0 yolk sac. The embryonic globin *Hbb-bh1* is expressed starting at E8.0 in the total embryo and is present at E9.0 and throughout the yolk sac and EryP-CFCs colonies (Figure 4.6B). Western blot analysis on proteins isolated from pooled primitive colonies plates, shows the time dependent increase of NFI-A within the yolk sac from E9.0-11.0; however, most striking is the large expression of NFI-A protein within the pooled colonies sample, not fully appreciable by the western blot in figure 4.6C, due to its lower protein content. GATA-1 expression is found in the yolk sac E9.0-11.0, and is highly expressed in the pooled colonies (Figure 4.6C).
Therefore based on these expression studies we can conclude that NFI-A is highly expressed at the mRNA and protein level during primitive hematopoiesis, most likely within the EryP-CFCs, as seen by indirect immunofluorescence, RNA analysis, and western blot analysis (Figure 4.6).

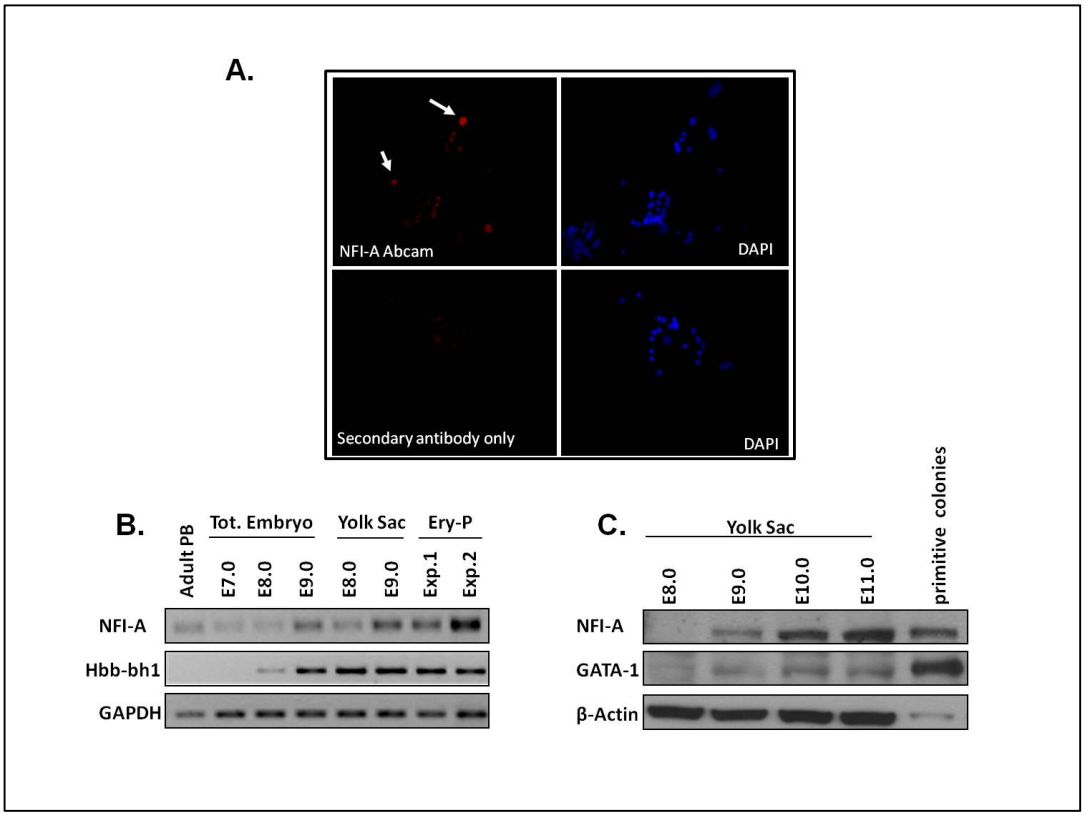

Figure 4.6: NFI-A detection in primitive erythroblasts. (A) Indirect immunofluorescence: EryP colonies were picked and pooled together followed by cytospin onto glass slides. The upper left panel shows several bright red cells staining for nuclear localized NFI-A as detected by a NFI-A specific antibody. Nuclear localization is indicated by DAPI staining in the upper right panel, and the lower left panel contains staining by secondary antibody only as a control. The lower right panel shows the nuclear localization of the secondary only staining cells. **(B)** Semiquantitative mRNA expression analysis of Hbb-bh1 and NFI-A with GAPDH used as a loading control in peripheral blood (PB) from adult mice, total (Tot.) embryo E7.0-9.0, yolk sac E8.0-9.0, and two separate experiments picking and pooling together individual EryP colonies. **(C)** Western blot for NFI-A and GATA-1 expression with β-actin used as a loading control in yolk sac E8.0-11.0 and in colonies pooled from the primitive colony assay.

4.3. NFI-A is expressed during definitive hematopoiesis

Semiquantitative PCR and western blot analysis showed the correlation between NFI-A expression and the progression of hematopoietic development (figure 4.1, 4.3, 4.4). NFI-A is expressed at high level and with a pattern similar to adult β-globin and AML1 in the YS at E9.0, in the AGM and liver at E11.0-E13.0 and in adult hematopoietic tissues. To study the role of NFI-A in definitive hematopoiesis, we used a cell culture system similar to that used for primitive hematopoiesis, but specific for the growth of colonies from definitive hematopoietic progenitors.

This analysis was performed on cell suspensions obtained from E9.0 yolk sacs (figure 4.7B), AGM of E11.0 and E12.0 (figure 4.7C-D) and livers from E11.0 and E12.0 (figure 4.7E-F) of CD1 mice.

Single suspension cells were placed in pre-made clonogenic media for the detection of definitive hematopoietic colonies; BFU-E, Colony-Forming Unit-Granulocyte Macrophage (CFU-GM), CFU-Macrophage (CFU-M). Each colony is derived from individual progenitors of the erythroid, granulocyte-macrophage, and macrophage lineages respectively. This media also allows the detection of CFU-Granulocyte,-Erythroid-Macrophage-Megakaryocyte (CFU-GEMM) which is derived from a multipotent progenitor, and therefore cells within this colony can consist of the granulocyte, erythroid, macrophage and Megakaryocyte lineages. Figure 4.7A shows colony and cellular morphology of individually picked colonies. As seen in Figure 4.7B 52.1% of the cells from YS E9.0 are BFU-E, 10% are CFU-M, 11.2% are CFU-GM, and 17.8% are CFU-GEMM. These data further confirm that the yolk sac at E9.0 contains many definitive progenitors, with the majority of them being definitive erythroid progenitors in line with previous findings (Palis, Robertson et al. 1999). Within the E11.0 AGM there is a prevalence of CFU-GEMM (36.9%) as well as CFU-GM (39.9%), the percentage of BFU-E is 10.2% and CFU-M are 14.6%; there is also a small percentage of CFU-Granulocyte (CFU-G) (0.4%) (Figure 4.7C). In E12.0 AGM CFU-GM and CFU-G percentages increased to 53.1% and 18% respectively, while CFU-GEMM progenitors decreased to 5%. In addiction we obtained a 5.9% of BFU-E and a 16.5% of CFU-M (Figure 4.7D). Within the liver at E11.0 the majority of progenitors are BFU-E (66.5%), followed by CFU-GM

(17.2%), CFU-M (8.6%), CFU-GEMM (3.6%) and CFU-G (1%) (Figure 4.7E). E12.0 liver's progenitors gave rise to a 10.5% of CFU-GEMM, a 46.3% of CFU-

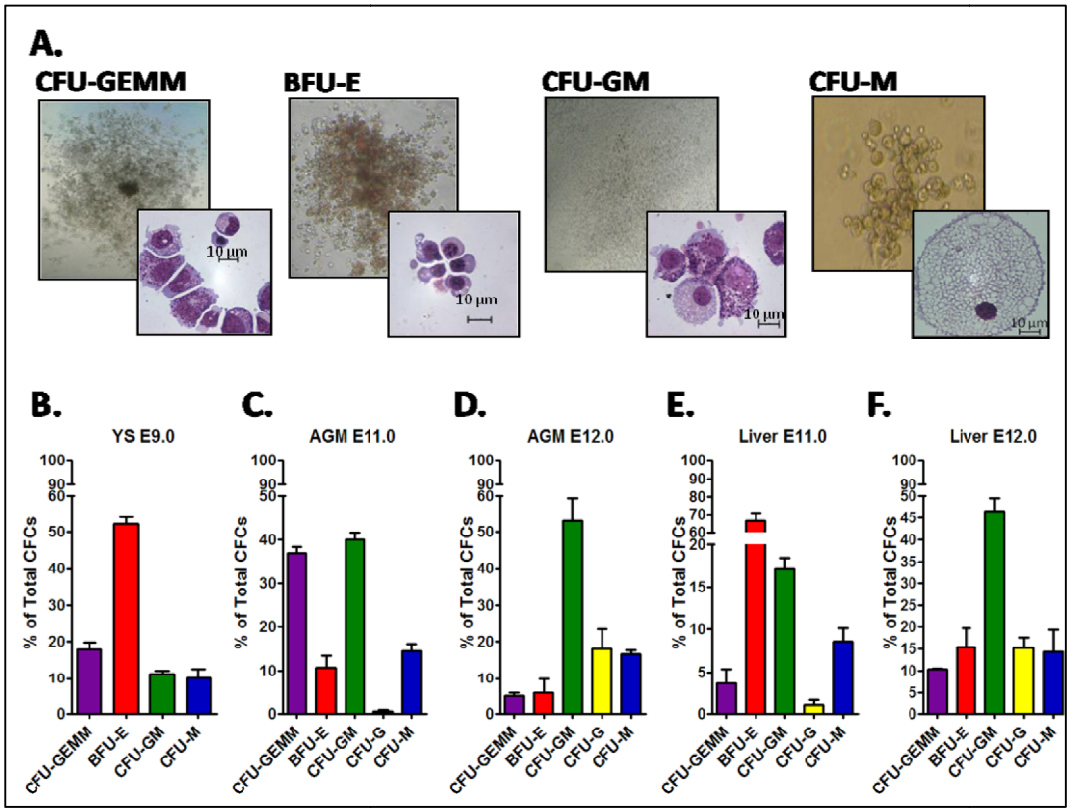

Figure 4.7: Definitive colony distribution in YS E9.0, AGM E11.0-12.0 and Liver E11.0-E12.0 of CD1 mice. A) Representative colony morphology and cellular morphology of individual picked colonies (original magnification 1000X). **B)** 12 x 10^3 cells from dissociated YS E9.0 were plated in triplicate in definitive colony clonogenic media, and colonies were scored after 7 days. Percentage of CFU-granulocyte erythroid macrophage megakaryocyte (CFU-GEMM), burst-forming unit-erythroid (BFU-E), CFU-granulocyte macrophage (CFU-GM), CFU-granulocyte (CFU-G) and colony-forming units macrophage (CFU-M), out of total colony forming cells (CFCs) (Mean +/- SD values from two independent experiments) **C)** 20 x 10^3 AGM E11.0 dissociated cells were plated in triplicate in definitive clonogenic media and colonies were scored after 7 days (Mean +/- SD values from two independent experiments). **D)** 20 x 10^3 AGM E12.0 dissociated cells were plated in triplicate in definitive clonogenic media and colonies were scored after 7 days (Mean +/- SD values from triplicate platings). **E)** 12 x 10^3 liver E11.0 dissociated cells were plated in triplicate within definitive clonogenic media and colonies were scored after 7 days (Mean +/- SD values from triplicate platings). **F)** 20 x 10^3 liver E12.0 dissociated cells were plated in triplicate within definitive clonogenic media and colonies were scored after 7 days (Mean +/- SD values from triplicate platings).

GM, a 15.3% of CFU-G, a 14.7% of CFU-M and only to a 8% of BFU-E (Figure 4.7F). These results are also in line with previous findings (Mikkola and Orkin 2006), and allow us to establish CFCs distribution profiles for CD1 mice.

The same data obtained from E9.0 YS, E12.0 AGM and E11.0 and E12.0 liver definitive colony assays were analyzed for the relative frequency of definitive colonies obtained from each of these tissues (figure 4.8A). From this analysis the similarity of hematopoietic progenitors composition is clear between E9.0 YS and E11.0 liver and between E12.0 AGM and E12.0 Liver, compatible with the colonization of fetal liver by a first wave of yolk sac's progenitor and a second of HSCs originated in the AGM (Mikkola and Orkin 2006). In order to correlate the different stages of definitive hematopoiesis with NFI-A expression, we analyzed by qRT-PCR NFI-A mRNA levels in colonies pooled from E9.0 yolk sac, E12.0 AGM, E11.0-12.0 liver definitive colony assays (figure 4.8B). The results shows that NFI-A expression increases in line with the acquisition of multipotency of the progenitors' population, following a pattern similar to the one observed in the whole tissues (figure 4.1A). From the above data we can deduce that NFI-A expression is localized in the hematopoietic compartment of these tissues.

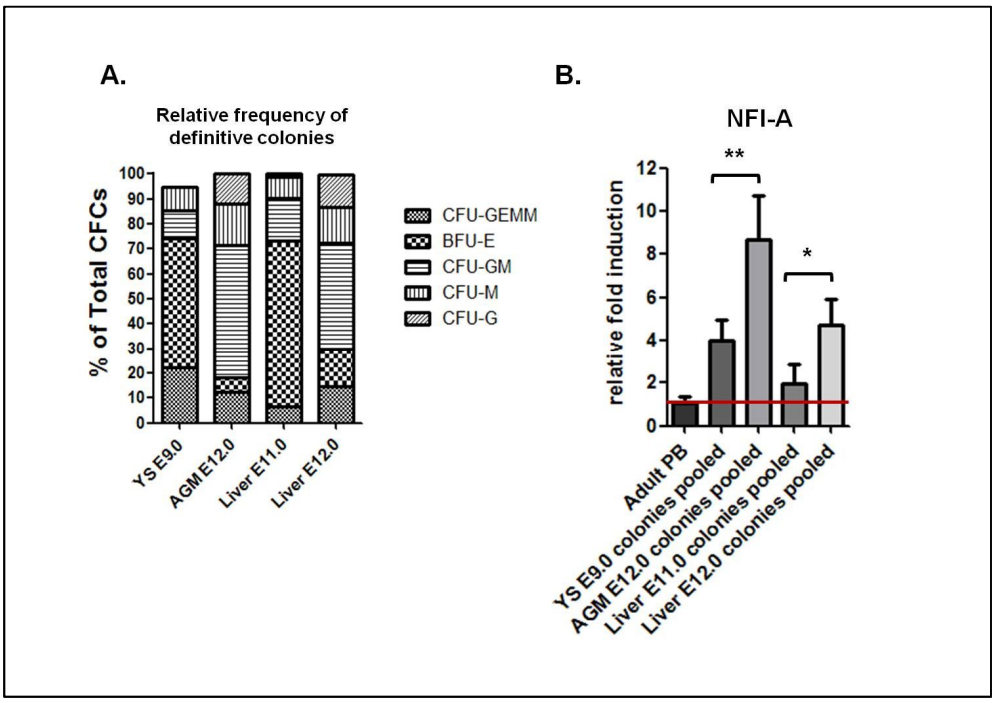

<u>Figure 4.8</u>: (A) Definitive colony assay relative frequency of definitive colonies in YS E9.0, AGM E12.0 and Liver E11.0-E12.0 of CD1 mice. (B) qRT-PCR analysis of Nfi-a mRNA levels in definitive colonies obtained from YS E9.0, AGM E12.0 and Liver E11.0-E12.0 of CD1 mice.

4.4. B6N31 NFI-A -/- mice

We addressed the role of NFI-A on definitive hematopoiesis *in vivo*, in NFI-A depleted (NFI-A -/-) mouse models. The first strain we used, B6N31, has a C57BL/6 genetic background and showed a high perinatal mortality rate associated to NFI-A disruption (das Neves, Duchala et al. 1999). We studied hematopoiesis in these mice by immunohistochemistry, in which, by the use of antibodies against a myeloid and an erythroid marker, is possible to estabilish the cellularity of the bone marrow, such as the ratio of hematopoietic cells to the adipose tissue, and the myeloid to erythroid ratio (M/E) of hematopoietic tissue, doing a comparison of relative proportions of granulocytic and erythroid cells. As myeloid marker we used myeloperoxidase (MPO) and as erythroid marker we used Ter119, an erythroid specific protein of membrane. In addiction we evaluated the possible existence of compensatory actions on hematopoiesis for NFI-A absence carried out by the other members of NFI family and we investigated about the expression of embryonic and adult globin genes in the course of development. Eventually we looked at adult definitive hematopoiesis performing complete blood counts of adult mice peripheral blood.

4.4.1 *During liver definitive hematopoiesis B6N31 NFI-A -/- mice show a delay in the downregulation of embryonic ß-globins*

Livers, spleens and posterior legs' bone marrow from E13.0, E19.0 and D1 mice were excised, fixed and sectioned for examination to further characterize the hematopoietic defects of NFI-A -/- B6N31 mice. An immunohistochemical analysis was performed on sections of B6N31 organs, using antibodies against MPO and Ter119, to detect cells of myeloid and erythroid lineage respectively. At E13.0 the main hematopoietic tissue is the liver, while the spleen and the bone marrow are still not recognizable; therefore, these tissues were examined starting from E19.0. E13.0 NFI-A -/- livers don't show significantly appreciable differences from their wild type counterparts, except for a mild increase in myeloid to erythroid ratio (M/E) (figure 4.9A).

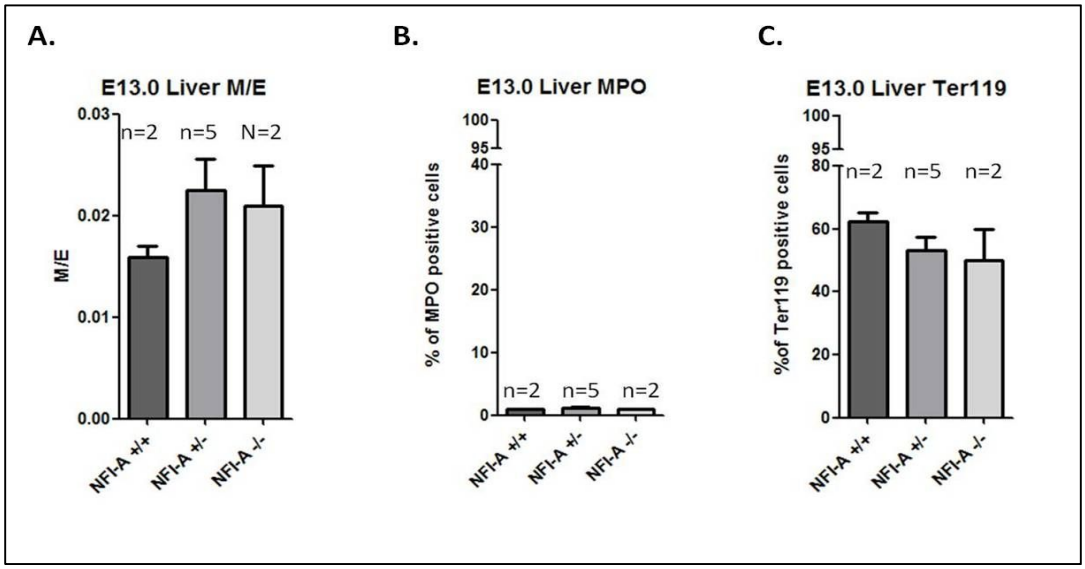

Figure 4.9: Immunohistochemical analysis of B6N31 E13.0 livers. (A) M/E, **(B)** percentage of MPO positive cells and **(C)** percentage of Ter119 positive cells of E13.0 livers of B6N31NFI-A +/+ (n=2), NFI-A +/- (n=5) and NFI-A -/-

To explore the effects of NFI-A disruption on the behavior of the other members of NFI family, we analyzed NFI-B, NFI-C and NFI-X expression in E12.0 livers by qRT-PCR (figure 4.10A). In B6N31 NFI-A -/- E12.0 livers, there aren't appreciable differences in NFI-B, NFI-C and NFI-X mRNA expression, with respect to B6N31 NFI-A +/+ E12.0 livers.

We also analyzed E12.0 livers of B6N31 mice for mRNA expression of embryonic and adult globins. This is the embryonic stage in which the switching of β-globin locus occurs. The expression of embryonic Hbb-Y and Hbb-bh1 globins show respectively a 3.3 and a 3.4 fold increase in the E12.0 fetal livers of NFI-A -/- mice compared to NFI-A +/+ littermates (Figure 4.10 B). E12.0 fetal livers of NFI-A +/- mice present a 2.6 fold increase of Hbb-Y and a 2.7 fold increase of Hbb-bh1 respect to NFI-A +/+ mice (Figure 4.10B), suggesting a haploinsufficiency of NFI-A factor. Adult Hbb-b and Hba-α globins mRNA level doesn't change with the disruption of NFI-A gene (Figure 4.10 C). These data show a correct activation of adult globins genes expression, but a delay in the repression of embryonic globins, suggesting a role of NFI-A in controlling β-globin switching.

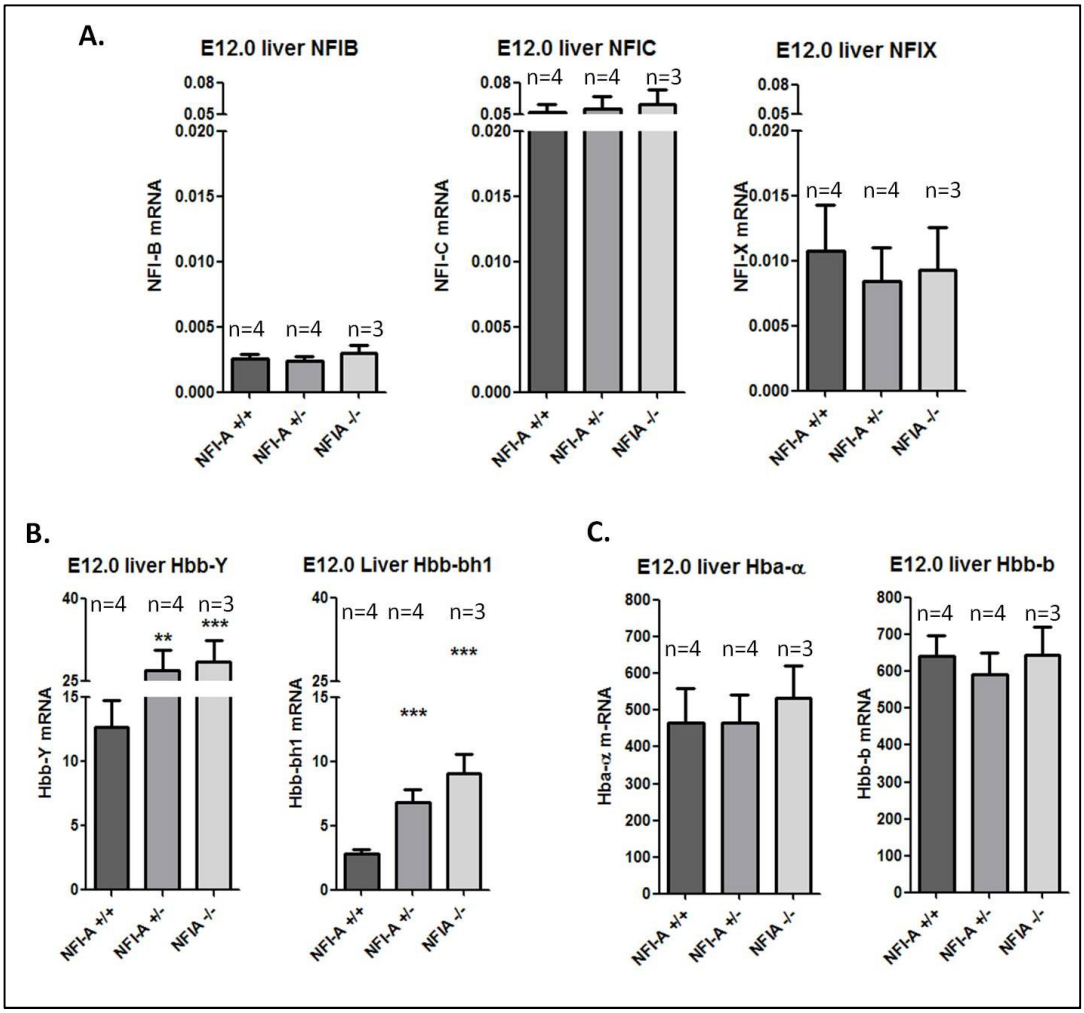

<u>Figure 4.10</u>: qRT-PCR analysis of (A) NFIs factors, (B) embryonic Hbb-y and Hbb-bh1 and (C) adult Hbb-b and Hba-α in B6N31 E12.0 NFI-A +/+, NFI-A+/- and NFI-A -/- livers.

4.4.2 *Spleen hematopoiesis around the time of birth shows a reduced M/E ratio*

We next looked at definitive hematopoietic tissues around the time of birth of B6N31 NFI-A +/+, NFI-A +/- and NFI-A -/- mice. Just before birth, at 19 days of embryo development, M/E ratio of NFI-A -/- livers appears to be lower than in NFI-A +/+ livers, due to the increased Ter119 positive component (figure 4.11A left and right).

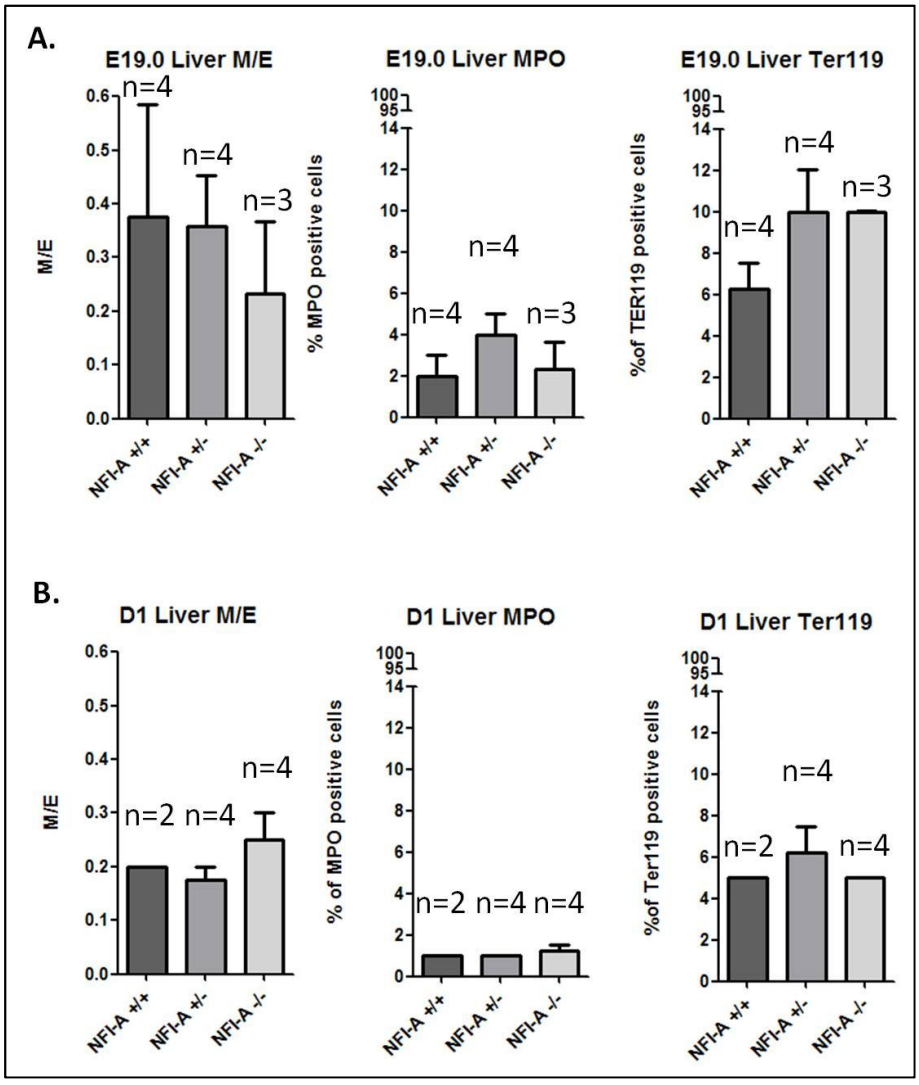

Figure 4.11: Immunohistochemical analysis of livers of B6N31 mice. (A) M/E, percentage of MPO positive cells and of Ter119 positive cells of E19.0 livers of B6N31 NFI-A +/+ (n=4), NFI-A +/- (n=4) and NFI-A -/- (n=3) mice. **(B)** M/E, percentage of MPO positive cells and of Ter119 positive cells of livers of D1 B6N31 NFI-A +/+ (n=2), NFI-A +/- (n=5) and NFI-A -/- (n=4) mice.

These differences become undetectable soon after birth in D1 livers (figure 4.11B).

In the spleen of E19.0 NFI-A -/- mice we could observe a reduced M/E ratio compared with NFI-A +/+ spleens, that is to attribute to a decreased MPO positive myeloid component (Figure 4.12A left, middle). Ter119 positive erythroid component also resulted to be reduced in E19.0 NFI-A -/- spleen respect to NFI-A +/+ spleens, but not as much as MPO positive population. This phenotype

becomes stronger in D1 NFI-A -/- spleens, where the MPO positive component is ¼ of D1 NFI-A +/+ spleens MPO positive component and the M/E ratio is less than ½ of that of D1 NFI-A +/+ spleens. Also in D1 NFI-A -/- spleens erythroid Ter119 positive component resulted to be lower than in D1 NFI-A +/+ spleens, but not enough to compensate the decrease of myeloid MPO positive component in the M/E ratio (Figure 4.12B). These data in the main hematopoietic tissue of newborn mice suggest that the disruption of NFI-A causes a decrease of the myeloid to erythroid ratio.

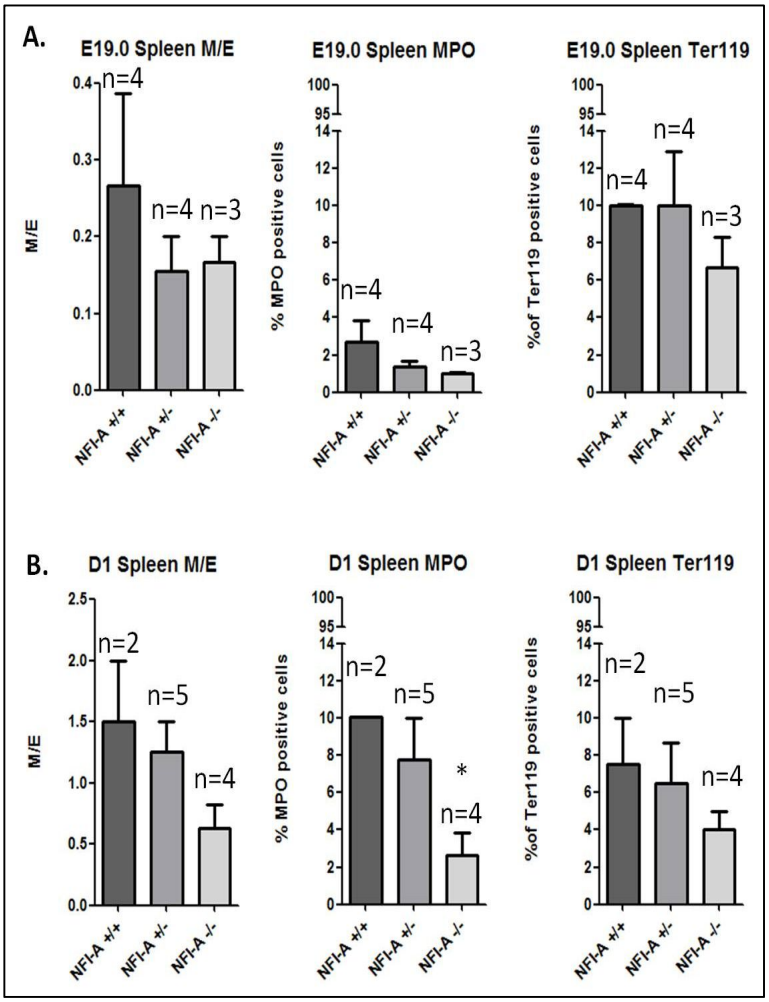

Figure 4.12: Immunohistochemical analysis of spleens of B6N31 mice. (A) M/E, percentage of MPO positive cells and of Ter119 positive cells of E19.0 spleens of B6N31 NFI-A +/+ (n=4), NFI-A +/- (n=4) and NFI-A -/- (n=3) mice. **(B)** M/E, percentage of MPO positive cells and of Ter119 positive cells of spleens of D1 B6N31 mice NFI-A +/+ (n=2), NFI-A +/- (n=5) and NFI-A -/- (n=4) mice.

E19.0 and D1 bone marrows were also examined. At E19.0 there aren't appreciable differences between bone marrows of NFI-A -/- and NFI-A +/+ mice, except for a mild increase in M/E ratio, due to a little expansion of myeloid MPO positive component (Figure 4.13A).

At D1, NFI-A -/- bone marrows show a slight reduction of cellularity compared to wild type littermate controls (Figure 4.13B left). M/E ratio resulted to be higher in D1 NFI-A -/- bone marrows than in D1 NFI-A +/+ bone marrows, because of a reduction of erythroid Ter119 positive component (Figure 4.13B). Erythroblasts first appear in bone marrow's hematopoietic compartment at E18.5, but erythroblastic islets appear after birth, from D0 to D2 (Tada, Widayati et al. 2006). The data obtained from immunohistochemistry analysis on B6N31 bone marrows samples indicate a probable delay in bone marrow erythroid lineage progenitors maturation with respect to myeloid lineage progenitors in NFI-A -/- mice.

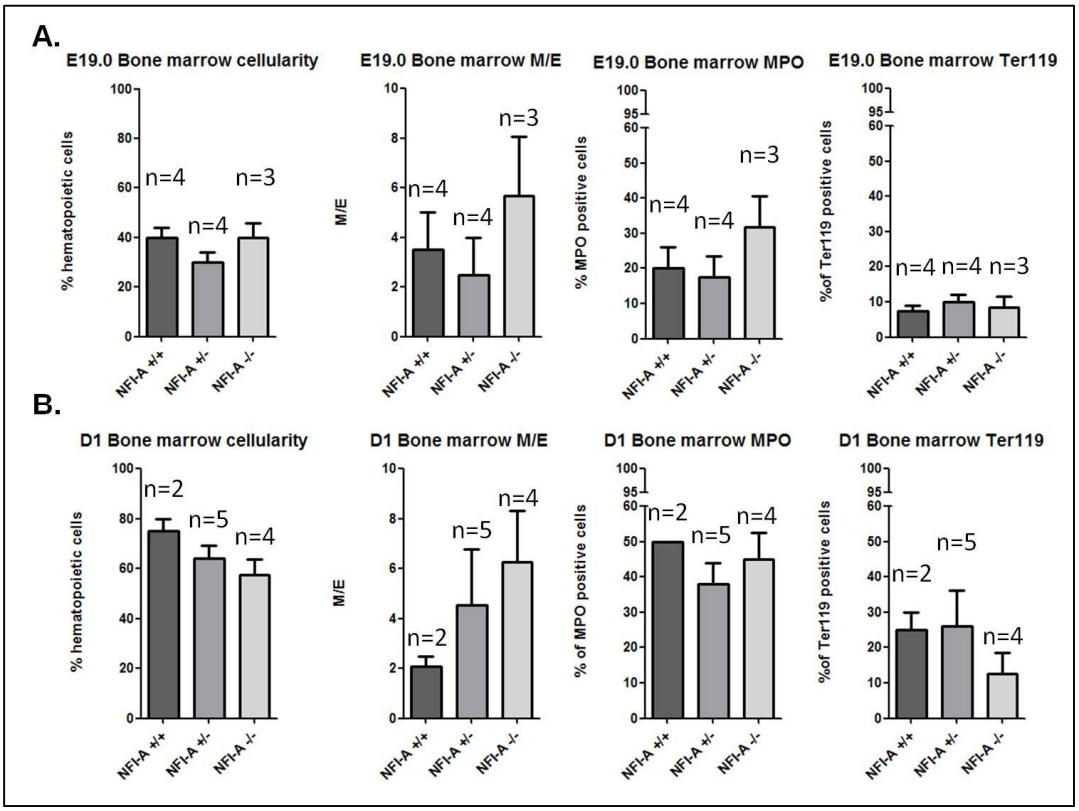

Figure 4.13: Immunohistochemical analysis of bone marrows of B6N31 mice. (A) Cellularity of hematopoietic compartment, M/E, percentage of MPO positive cells and percentage of Ter119 positive cells of E19.0 livers of B6N31 NFI-A +/+ (n=4), NFI-A +/- (n=4) and NFI-A -/- (n=3) mice. **(B)** Cellularity of hematopoietic compartment, M/E, percentage of MPO positive cells and percentage of Ter119 positive cells of bone marrows of D1 B6N31 NFI-A +/+

4.4.3 Spleen hematopoiesis around the time of birth shows an increased expression of NFI-B and a downregulation of adult globins expression

As already done for E12.0 livers, definitive hematopoietic tissues of newborn mice were analyzed for NFI-B, NFI-C, NFI-X and globins expression by qRT-PCR. In D1 livers of NFI-A -/- mice there aren't very appreciable differences in NFI-B, NFI-C and NFI-X mRNA expression respect to D1 livers of NFI-A +/+ mice, confirming the phenotype already observed in E12.0 livers of NFI-A -/- mice (figure 4.14A, B, C).

In D1 spleens of NFI-A -/- mice there is a 2.6 fold induction of NFI-B compared to D1 spleens of NFI-A +/+ mice (figure 4.14A). Spleen is the main hematopoietic organ in mice until the full activation of bone marrow, that takes place at around 10 days after birth (Tada, Widayati et al. 2006). After bone marrow full activation, spleen remains active as extramedullary hematopoietic organ (Cesta 2006). The increase in NFI-B expression during the stage maximum hematopoietic activity of the spleen, suggests an action of its compensation to the absence of NFI-A. Indeed, NFI-C and NFI-X mRNA expression result slightly decreased in D1 NFI-A -/- spleens compared to D1 NFI-A +/+ spleens (Figure 4.14B, C).

D1 bone marrows of NFI-A -/- mice also show a slightly increased NFI-B expression (figure 4.14 A) and decreased expression of NFI-C and NFI-X (figure 4.14 B,C) with respect to D1 bone marrows of NFI-A +/+ mice. Bone marrow is still not fully active as hematopoietic organ, so the mild alterations of NFIs expression in the bone marrow of NFI-A -/- mice could be an indication of the development of hematopoiesis in this tissue.

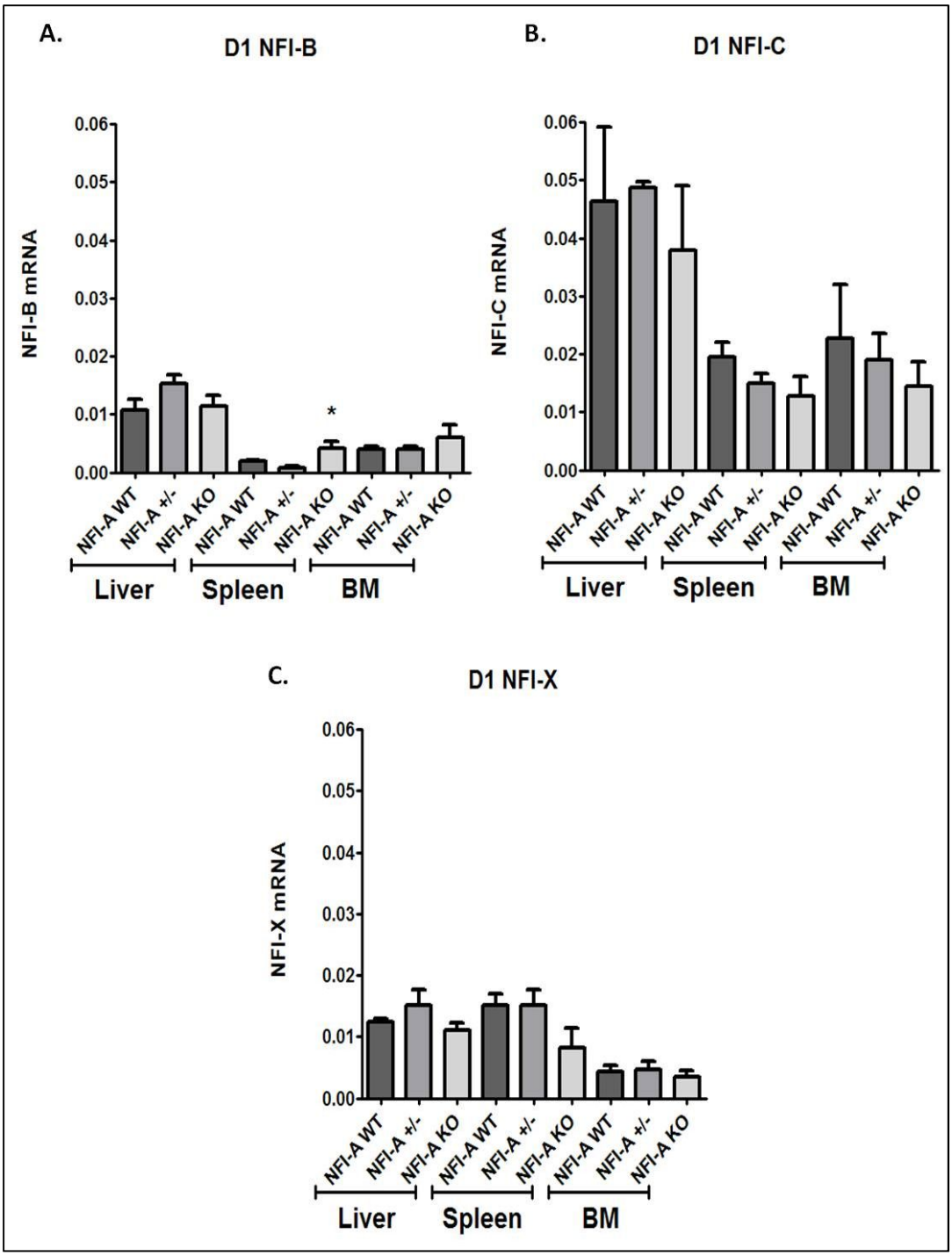

<u>Figure 4.14</u>: qRT-PCR analysis of NFI-B (A), NFI-C (B) and NFI-X (C) expression in livers, spleens and bone marrows of D1 NFI-A +/+, NFI-A +/- and NFI-A -/- B6N31 mice.

To assess whether NFI-A has a role in hematopoietic development after the switching of β-globin locus, we looked also at *Hba-α* and embryonic and adult β-globins mRNA levels in hematopoietic tissues of D1 NFI-A +/+, NFI-A +- and NFI-A -/- mice (Figures 4.15). Interestingly there is a reduced fold induction of adult *Hbb-b* and *Hba-α* globins in D1 NFI-A -/- spleen compared with NFI-A+/+ (figure 4.15 A, B), confirming the delay on β-locus switching found on E12.0 NFI-A -/- livers and highlighting NFI-A as a key factor for the correct production of adult hemoglobin.

In D1 NFI-A -/- and NFI-A +/+ livers adult *Hbb-b* globins and *Hba-α* globin resulted to be decreased respect to D1 NFI-A +/+ livers, while there are not noticeable differences in adult globins expression between D1 NFI-A -/-, NFI-A +/- and NFI-A +/+ bone marrows (figure 4.15). Embryonic beta globins expression levels in D1 hematopoietic tissues were also analyzed but the levels were in almost undetectable so a difference between NFI-A +/+, NFI-A +/- and NFI-A -/- mice was not valuable (data not shown).

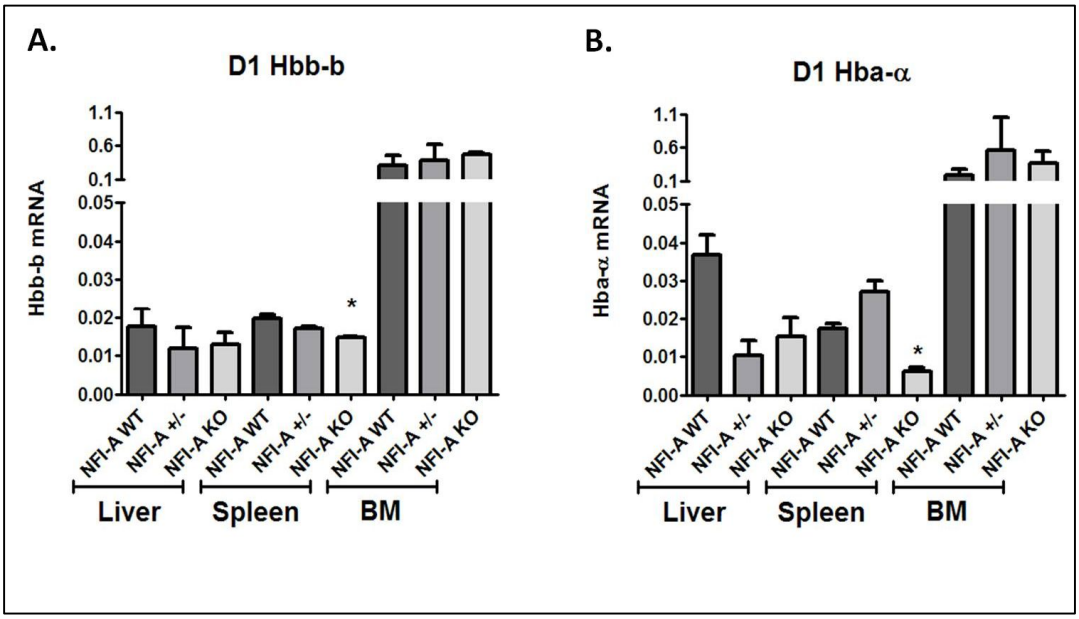

Figure 4.15: qRT-PCR analysis of adult (A) Hbb-b and (B) Hba-α globins expression in livers, spleens and bone marrows of D1 B6N31 NFI-A +/+, NFI-A +/- and NFI-A -/- mice.

4.4.4 *NFI-A -/- hematopoiesic tissues after birth shows ipocellularity of the hematopoietic compartment*

Due to the high perinatal mortality of NFI-A -/- B6N31 mice, we could obtain the posterior legs' bone marrow from only one 3 days old (D3) pup, which was analyzed by immunohistochemistry, as already done for E19.0 and D1 bone marrows. As showed in figure 4.16A the cellularity of hematopoietic compartment of the D3 NFI-A -/- bone marrow resulted to be dramatically reduced in respect to D3 NFI-A +/+ bone marrows. Moreover both myeloid MPO positive and erythroid Ter119 positive components appear to be decreased in D3 NFI-A -/- pup compared to D3 NFI-A +/+ (figure 4.16 C,D), but the reduction of the myeloid compartment is stronger leading to a resulting M/E ratio in D3 NFI-A -/- bone marrow that is ½ of D3 NFI-A +/+ bone marrow (figure 4.16 B).

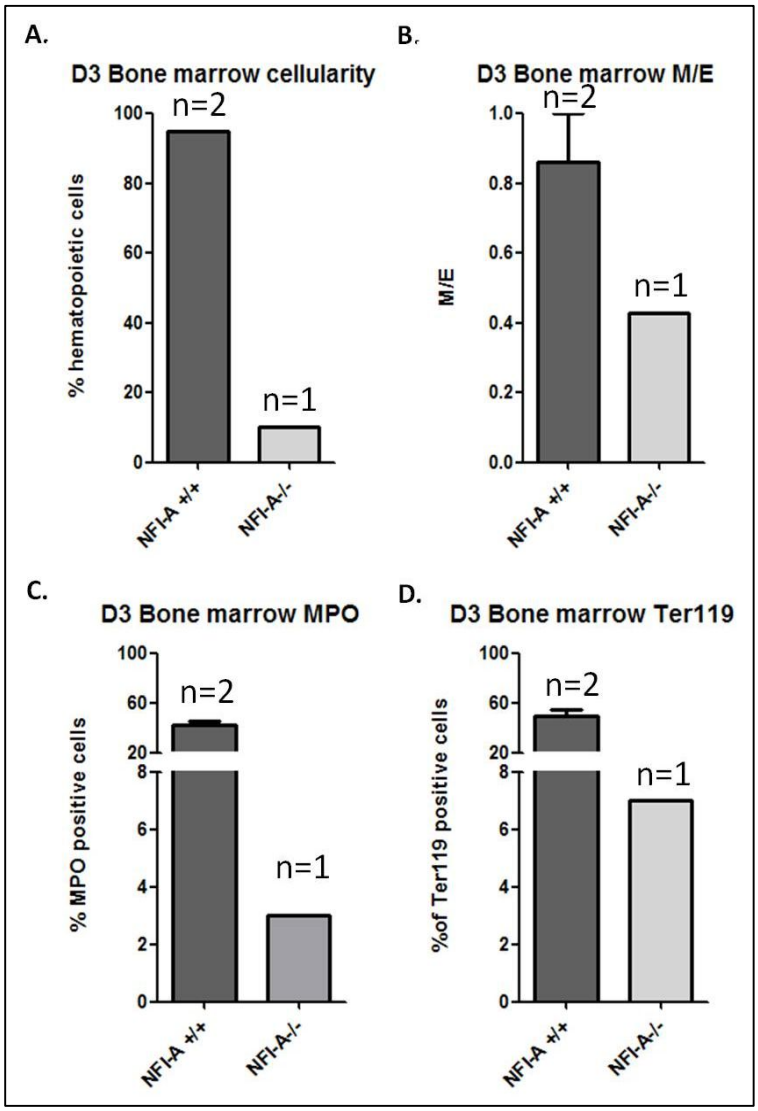

Figure 4.16:

Immunohistochemical analysis of bone marrows of D3 B6N31 mice. (A) Cellularity of hematopoietic compartment of bone marrow of D3 NFI-A +/+ (n=2) and NFI-A -/- (n=1) B6N31 mice. **(B)** M/E of bone marrow of D3 NFI-A +/+ and NFI-A -/- B6N31 mice. **(C)** percentage of MPO positive cells of bone marrow of D3 NFI-A +/+ and NFI-A -/- B6N31 mice. **(D)** Percentage of Ter119 positive cells of bone marrow of D3 NFI-A +/+ and NFI-A -/- B6N31 mice

Moreover D3 NFI-A-/- spleen resulted to be reduced in size respect to D3 NFI-A +/+ spleen (Figure 4.17), confirming the role of NFI-A in spleen's hematopoiesis.

<u>Figure 4.17</u>: Spleens of D3 NFI-A -/- and NFI-A +/+ B6N31 mice.

4.4.5. *B6N31 NFI-A +/- adult mice shows an hematologic dyscrasia characterized by a reduced volume and corpuscular hemoglobin content of erythrocytes*

To further investigate the effect of NFI-A absence on definitive hematopoiesis, in lack of NFI-A -/- adult mice due to the high rate of perinatal mortality, we decided to perform complete blood counts of adult NFI-A +/+ and NFI-A +/- B6N31 mice peripheral blood.

As seen in figure 4.18 there aren't difference either in leucocytic (figure 4.18 A) and platelets-related (figure 4.18 B, C, D) parameters, suggesting a selective role of NFI-A in the maturation of erythroid lineage.

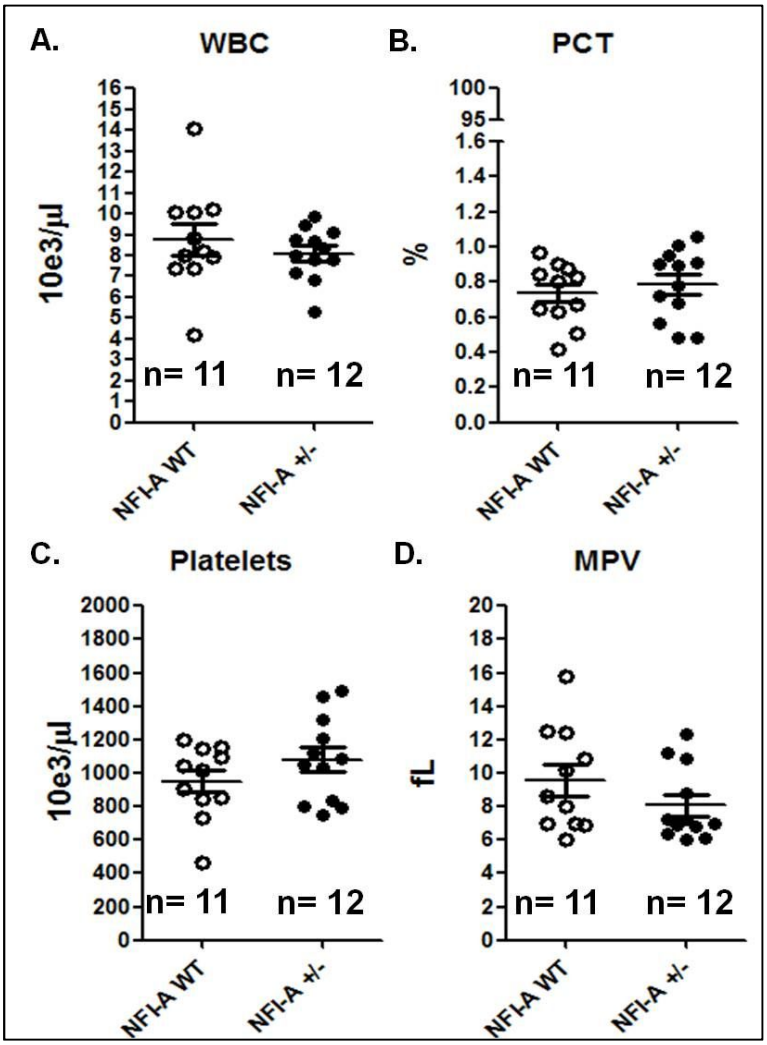

<u>Figure 4.18</u>: Complete blood counts analysis of adult NFI-A +/+ and NFI-A -/- B6N31 mice. Leucocitic and platelet related parameters. (A) WBC of adult NFI-A +/+ and NFI-A -/- B6N31 mice. **(B)** Piastrinocrit (PCT) of adult NFI-A +/+ and NFI-A -/- B6N31 mice. **(C)** Platelets count of adult NFI-A +/+ and NFI-A -/- B6N31 mice. **(D)** Mean Platelets Volume (MPV) of adult NFI-A +/+ and NFI-A -/- B6N31 mice.

Between peripheral blood of NFI-A +/+ and NFI-A +/- mice there are no significant differences in hematocrit (HCT) (figure 4.19A), Hemoglobin content (HGB, figure 4.19B), Mean Corpuscolar Hemoglobin Concentration (MCHC, Figure 4.19C) and number of reticolocytes (figure 4.19D). These parameters were analyzed also distinguishing males from females, without obtaining differences between these groups (data not shown).

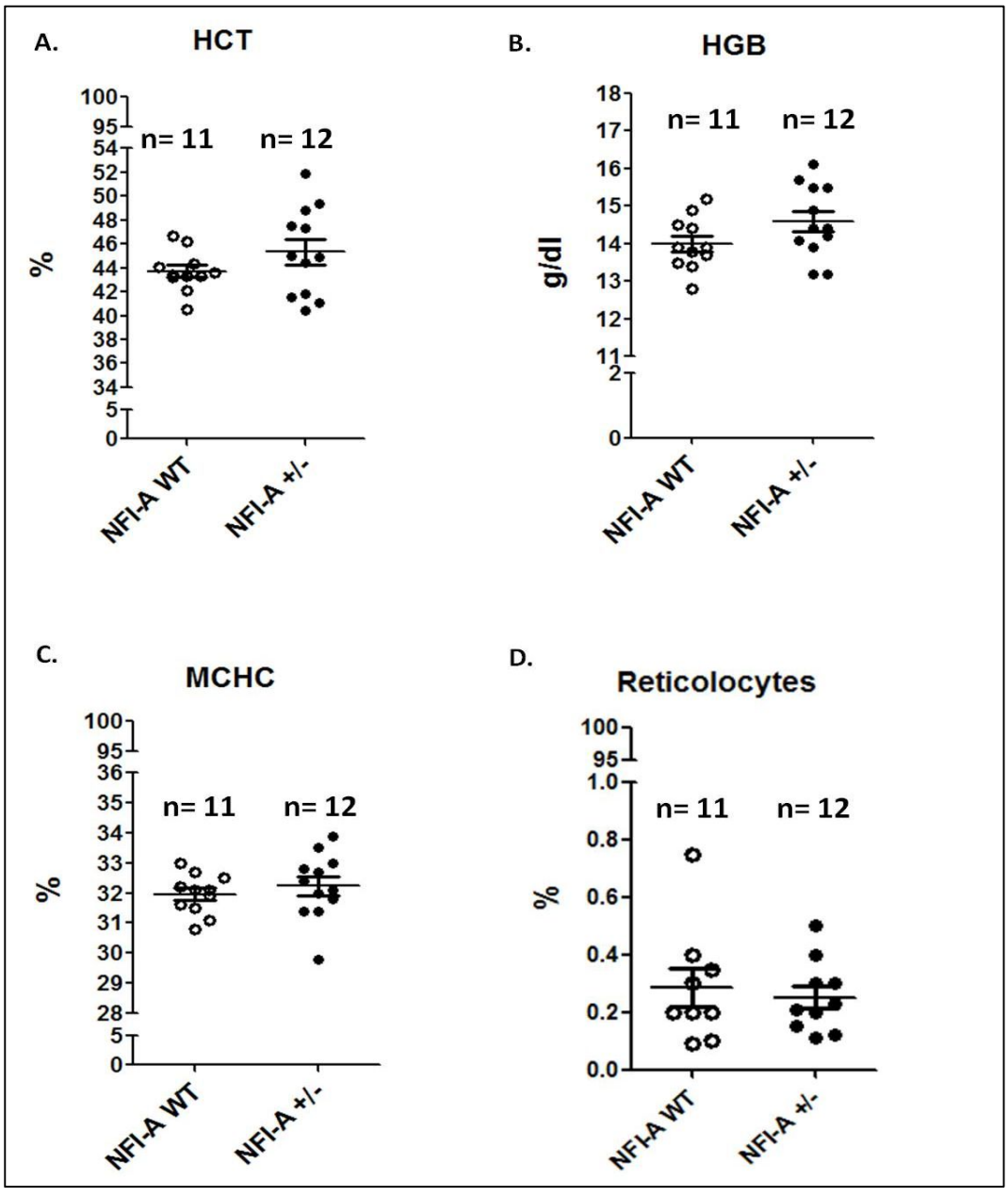

Figure 4.19: Complete blood counts analysis of adult NFI-A +/+ and NFI-A +/- B6N31 mice. (A) HCT, **(B)** HGB, **(C)** MCHC and (D) Reticulocytes count of adult NFI-A +/+ and NFI-A +/- B6N31 mice.

Intriguingly, peripheral blood of NFI-A +/- mice presents a higher erythrocyte number (RBC) compared to peripheral blood of NFI-A +/+ mice, difference more significant considering only the male NFI-A +/+ and NFI-A +/- populations (figure 4.20A). Moreover Mean Corpuscolar Hemoglobin (MCH) of NFI-A +/- peripheral blood is decreased in respect to NFI-A +/+ MCH (figure 4.20B), and this feature is accompanied by a reduced Mean Corpuscolar Volume (MCV) (figure 4.20C) and an increased Red cell Distribution Width (RDW), showing an hematologic dyscrasia with symptoms in common with anemia related to defects of hemoglobin synthesis.

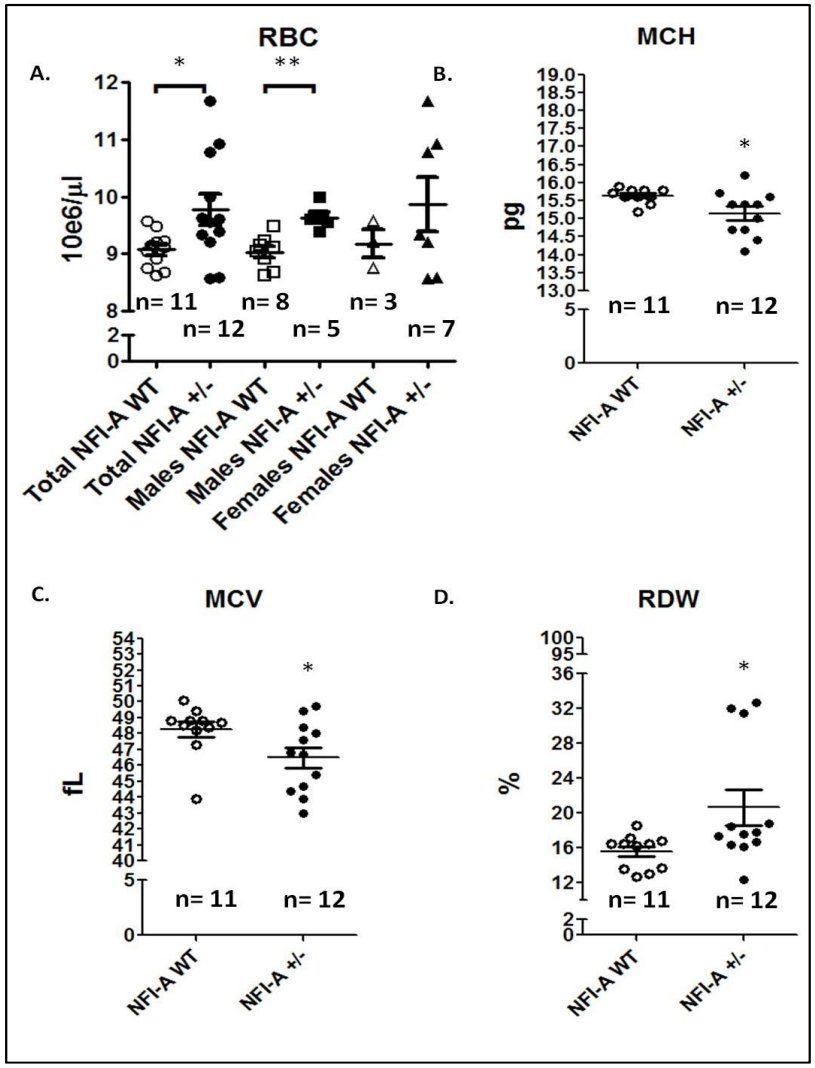

Figure 4.20: Complete blood counts analysis of adult NFI-A +/+ and NFI-A +/- B6N31 mice. **(A)** RBC of adult total NFI-A +/+ and NFI-A +/- B6N31 mice, males NFI-A +/+ and NFI-A +/- B6N31 mice and females NFI-A +/+ and NFI-A +/- B6N31 mice. **(B)** MCH, **(C)** MCV and **(D)** RDW of adult total NFI-A +/+ and NFI-A +/- B6N31 mice.

4.5. B6hyb129 NFI-A -/- mice

We studied the role of NFI-A on hematopoiesis after birth on a NFI-A -/- mouse model different from B6N31: the B6hyb129 strain. B6hyb129 NFI-A -/- mice survive after birth, suggesting a milder phenotype respect to B6N31 NFI-A -/- mice. We received from Dr. Richard Gronostajski spleens and posterior leg's bone marrows of B6hyb129 NFI-A +/+, NFI-A +/- and NFI-A -/- mice, that we analyzed histologically.

4.5.1. *B6hyb129 NFI-A -/- mice present a decreased size and cellularity of spleen respect to wild types*

As already observed in our D3 NFI-A -/- B6N31 pup, spleens from D9 B6hyb129 NFI-A -/- mice resulted smaller in size and less red in color compared to their littermate controls, thus showing a hypocellularity in the erythroid red pulp component (figure 4.21A). The red pulp is composed by a tridimensional meshwork of splenic cords and venous sinuses. Splenic cords are comprised of reticular fibers, reticular cells, and associated macrophages who are highly phagocytic clearing damaged red blood cells. Within the spaces between the cords, there are blood cells including erythrocytes, granulocytes and circulating mononuclear cells (Cesta 2006). To better understand the histological difference between wild type and NFI-A -/- spleens, we embedded spleens in paraffin and sectioned them to do an istochemical study using myeloperoxidase staining (Figure 4.21 B). The myeloperoxidase staining is positive in cells of the granulocyte series and is used to stain cells derived from the myeloid lineage. The NFIA -/- spleens are less stained than the wild type, so also the myeloid lineages are less represented in absence of NFI-A expression. These results suggest an involvement of NFI-A in splenic erythropoiesis and myelopoiesis.

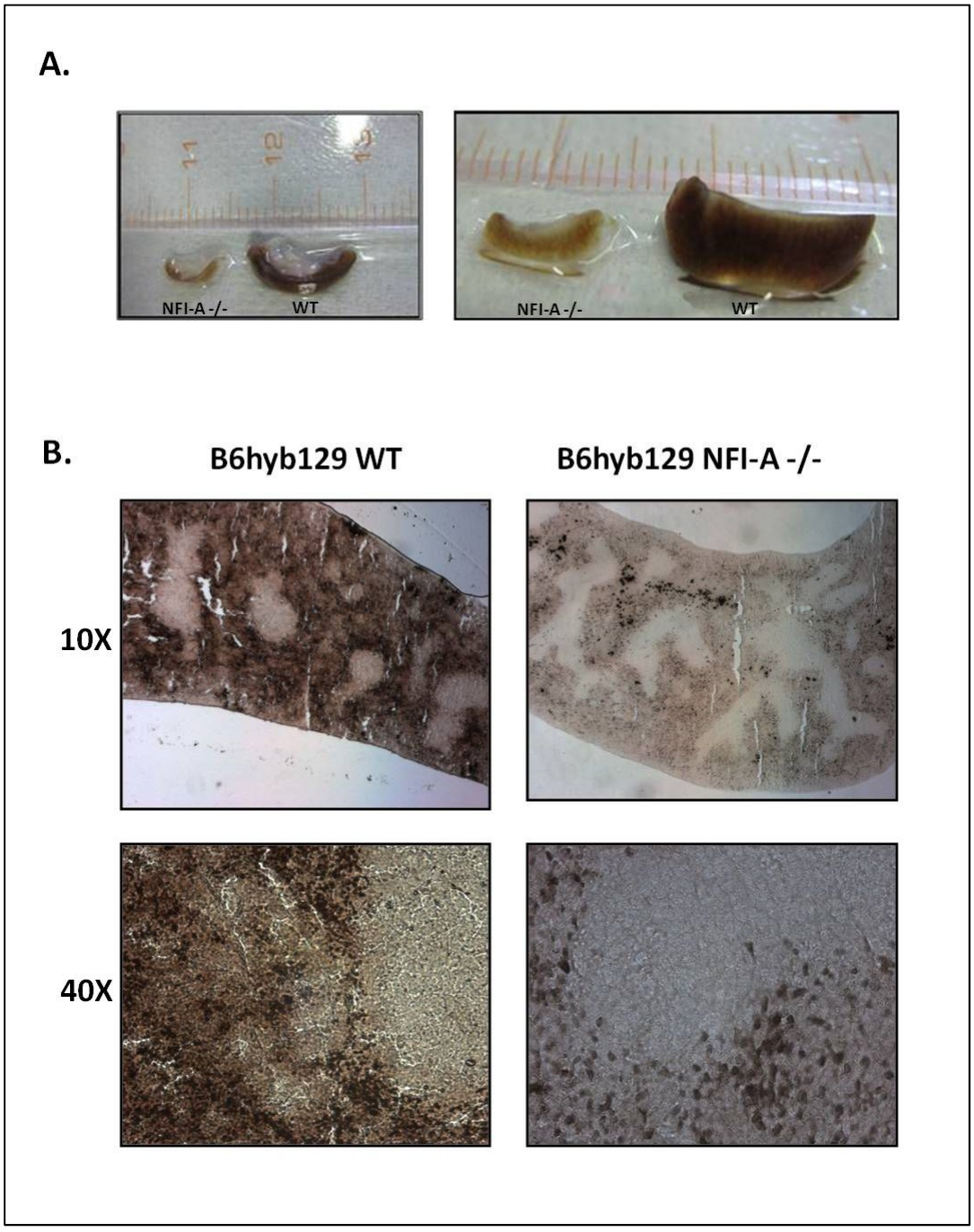

Figure 4.21: NFI-A knockout spleen analysis. (A) Photograph of gross spleen morphology of NFI-A +/+ and NFI-A-/- B6hyb129 mice. Right panel is a higher magnification of the same spleens **(B)** myeloperoxidase staining of NFI-A -\- and NFI-A +/+ spleens at 10x and 40x magnification.

4.5.2. *B6hyb129 NFI-A -/- mice show a decreased bone marrow's myeloid to erythroid ratio*

.

We analyzed by immunohistochemistry bone marrow of 12 days old B6hyb129 mice (Figure 4.22). Bone marrow become fully active as hematopoietic organ between 7 and 10 days after birth (Tada, Widayati et al. 2006). NFI-A -/- mice do not show alteration in the cellularity of hematopoietic component and in erythroid Ter119 positive component (Figure 4.22A,D). Interestingly we have observed a decreased Myeloid to Erythroid ratio (M/E) (Figure 4.22B), due to a decrease of MPO positive component (Figure 4.22C). This is in line with the previous results obtained from E19.0, D1 and D3 B6N31 mice, thus confirming a delayed maturation of bone marrow's hematopoietic compartment with the disruption of *Nfi-A.*

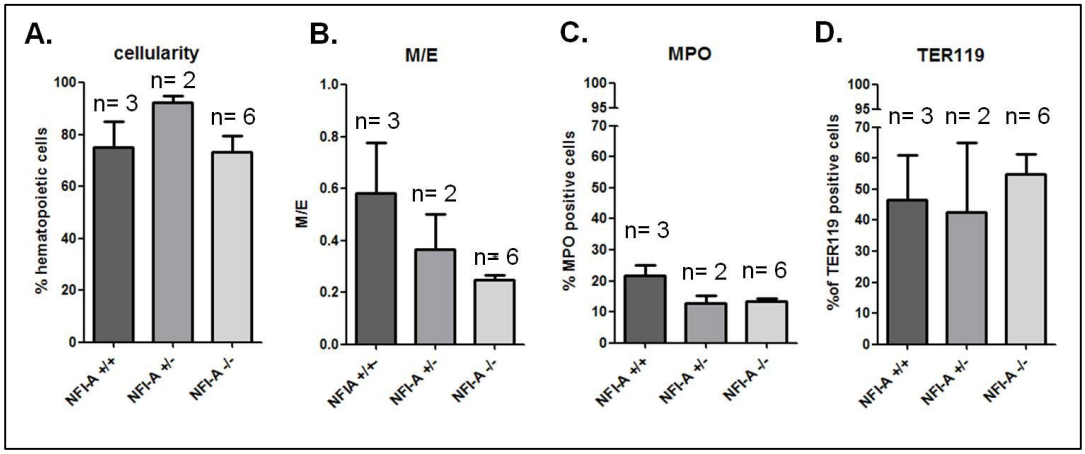

Figure 4.22:Immunohistochemical analysis of D12 bone marrow of B6hyb129. (A) Cellularity of hematopoietic compartment of D12 bone marrow of B6hyb129. **(B)** Myeloid to Erythroid ratio (M/E) of D12 bone marrow of B6hyb129. **(C)** percentage of Myeloperoxidase (MPO) positive cells in D12 bone marrow of B6hyb129. **(D)** percentage of Ter119 positive cells in D12 bone marrow of B6hyb129

5. Discussion

Nuclear Factor I (NFI) transcriptional factors are known for their positive and negative transcriptional regulatory roles in a cell type and promoter specific context. NFI-binding sites have been found in the promoter and enhancer regions of almost every organ system and tissue including promoters of the brain (Bedford, Julius et al. 1998), muscle (Spitz, Salminen et al. 1997), lung (Bachurski, Kelly et al. 1997), liver (Jackson, Rowader et al. 1993) and kidney (Leahy, Crawford et al. 1999), where they act as transcriptional activators or repressors depending on the cell-type and promoter context. NFI genes are differentially expressed during mouse ontogeny and cellular differentiation, which suggests that these proteins could play important roles in gene expression during development. For example knockout of NFI-A causes death in 95% of the mice at post-natal day 1 due to severe neurological defects including hydrocephalus, and agenesis of the corpus callosum (das Neves, Duchala et al. 1999). NFI-B knockout mice die early postnatally and display neurological defects and severe lung hypoplasia (Grunder, Ebel et al. 2002). NFI-C -/- mice show a prominent defect in tooth root development (Steele-Perkins, Butz et al. 2003) and NFI-X-/- mice show neurological defects similar to the NFI-A -/- mice and defects in bone ossification (Driller, Pagenstecher et al. 2007).

The founding member of NFI family, NFI-A, was demonstrated to be a target of miR-223 activity during granulocytopoiesis (Fazi, Rosa et al. 2005). NFI-A compete with C/EBPα for the binding to the miR-223 promoter. The activation of C/EBPα, displace NFI-A from this binding site on miR-223 promoter, allowing miR-223 upregulation. Then, miR-223 repress NFI-A, and the granulocytic differentiation occurs. NFI-A is involved also in monocytic-macrophage differentiation, in which hematopoietic progenitors up-regulate the lineage-specific transcription factor PU.1 inducing the expression of miR-424, which together with PU.1 leads to the activation of terminal differentiation genes through the repression of NFI-A (Rosa, Ballarino et al. 2007).

Further studies indicated that NFI-A is able to control the erythroid-granulocytic lineage decision at the level of HPCs. NFI-A is accumulated during initial erythroid

differentiation and promotes the activation of β-globin gene transcription, while repress the expression of G-CSFR, leading to the erythroid differentiation, shutting off the granulocytic potential (Starnes, Sorrentino et al. 2009). In addiction a study of gene expression profiling and chromatin immunoprecipitation on CD34+ HPCs and leukemic K562 cells revealed that NFI-A is able to induce an erythroid transcriptional program (Starnes, Sorrentino et al. 2010).

In the past several years much has been learned about the developmental origins of hematopoietic stem cells and many considerable progress in the identification and characterization of genes involved in programs of hematopoietic development has been done. In this work we have further investigated the expression and the role of NFIs transcription factors and in particular of NFI-A in controlling primitive and definitive hematopoiesis using mouse models. Our knowledge has benefited from the use of the mouse as a genetic system in which to explore the relationship between specific gene products and in vivo function. Both transgenesis and gene targeting strategies have been used to dissect the hematopoietic system. Inherited mutant or transgenic mouse models offered insights into the physiology and the pathogenesis of diseases, that cell culture experiments or in vitro biochemical assays typically cannot provide.

The study of the expression of NFIs factors, analyzed in CD1 mice, highlighted in particular the correlation between NFI-A expression and the progression of hematopoietic development in CD1 mice, suggesting a role of NFI-A in these processes. Intriguingly the primitive erythroid progenitors EryP-CFC arise and expands in number in the yolk sac between E7.5 and E9.0 and NFI-A resulted to be up-regulated in a time dependent manner in the yolk sac, at both mRNA and protein levels, during this period. These data suggest a role for NFI-A in primitive hematopoiesis, further supported by the high expression of this transcription factor in the EryP-CFC, demonstrated by primitive colony assays. Moreover, the finding that NFI-A expression pattern during embryo development of hematopoietic tissues could be overlapped to AML1 and Hbb-b expression patterns, suggest a role for NFI-A as regulator of the passage between primitive and definitive hematopoiesis. Hbb-b encodes for murine adult β-globin and it has already been demonstrated in our lab that NFI-A affects the expression of human adult β-globin in vitro (Starnes, Sorrentino et al. 2009), so our analysis confirm these previous result in an *in vivo*

model. AML1 is a transcription factor that plays a role in the emergence of HSCs from the AGM region, at early stages of hematopoietic fate determination (Durand and Dzierzak 2005). The existence of a linkage between NFI-A function and the emergence of adult definitive HSCs from AGM is further supported by its higher expression in the hematopoietic cells derived from the second wave of liver colonization by definitive HSCs.

The use of NFI-A -/- mouse models allowed us to better understand the roles of NFI-A on hematopoietic development. Interestingly, definitive hematopoietic embryonic and perinatal tissues react to the absence of NFI-A in different ways. In E13.0 B6N31 NFI-A -/- livers we observed an increase of myeloid compartment compared to erythroid compartment that resulted in a slightly increased M/E ratio. At E12.0 the liver is the main hematopoietic organ. With the progression of hematopoiesis in the subsequent hematopoietic tissues, such as spleen and bone marrow, *Nfi-A* disruption results in hypocellularity of hematopoietic compartment together with a decrease of M/E ratio, due above all to a reduced myeloid compartment. These data, collected from two different strains of NFI-A -/- mice, suggest that the absence of NFI-A could be responsible for the initial impairment of definitive erythropoiesis which followed by the erythroid compartment increase, negatively affecting myelopoiesis. In other words, after the initial expansion of the myeloid compartment, the lack of NFI-A activity pushes myeloid progenitors toward definitive erythropoiesis and this generates an imbalance in the whole myeloid population. This hypothesis is partially supported by the delayed maturation observed in the bone marrow obtained from the unique D3 NFI-A -/- B6N31 pup, which presents also a marked decrease of spleen's dimensions observed also in B6hyb129 NFI-A -/- mice. In D1 NFI-A -/- spleens we observed an increased NFI-B expression and a decreased NFI-C and NFI-X mRNA expression, during the stage of maximum hematopoietic activity of the spleen. NFI-B seems to act as compensator of NFI-A and to be responsible of the reduced levels of NFI-C and NFI-X. Also in D1 bone marrows of NFI-A -/- mice there is a slightly increased NFI-B expression and a decreased expression of NFI-C and NFI-X, a milder phenotype compatible to the fact that bone marrow is still not fully active as hematopoietic organ, so the milder alterations of NFIs expression in the bone marrow of NFI-A -/- mice could be an indication of the development of hematopoiesis in this tissue. Intriguingly, as we demonstrated in CD1 mice and in accord with other not

published data obtained in our lab in human cell lines and in unilineage colonies from human $CD34^+$, NFI-B is not expressed physiologically in adult peripheral blood and hematopoietic tissues. In addiction in recent studies NFI-B has been demonstrated to be upregulated in an high percentage of patients affected from polycythemia vera (PV) with JAK2V617F (Berkofsky-Fessler, Buzzai et al. 2010; Rice, Lin et al. 2012). PV is a clonal hematopoietic disorder characterized by the overproduction of erythroid lineage cells, that belongs to the class of Ph-negative myeloproliferative neoplasms (MPNs). This group of diseases is characterized by a recurrent mutation, JAK2V617F, which is present in $\approx$ 95% of patients with PV. A significant amount of gene deregulation in PV and other myeloproliferative neoplasm can be attributed to the activity of JAK2, but there is a set of genes deregulated in PV that appears independent of JAK2 action. Intriguingly NFI-B belongs to this second group of JAK2 independent deregulated genes (Berkofsky-Fessler, Buzzai et al. 2010). Moreover it has been reported that about 2% of a series of chronic myeloid diseases, including PV, presents structural alterations of the NFI-A gene. These alterations should lead to an inactivation of the protein, probably affecting the capacity of NFI-A to bind DNA and/or to dimerize (Bernard, Gelsi-Boyer et al. 2009). These observations suggest a role for NFI-A as tumor suppressor and for NFI-B as promoter of oncogenesis. We observed in NFI-A -/- definitive hematopoietic tissues a first phase in which there is an increase of the myeloid to erythroid ratio, followed by a second phase in which the up regulation of NFI-B is coupled to an inversion of the myeloid to erythroid ratio with an increase of the erythroid component of the tissue. These observations contribute to support the hypothesis that the up regulation of NFI-B expression could participate to the mechanisms that cause the increase of the erythroid population in NFI-A -/- definitive hematopoietic tissues and in PV patients.

To go more insight the molecular mechanisms in which NFI-A is involved during hematopoiesis, we analyzed mRNA expression of embryonic and adult globins in definitive hematopoietic tissues of B6N31 mice by qRT-PCR. The mammalian β-globin locus is a multigene locus containing several globin genes and a number of regulatory elements. During development, the expression of the genes changes in a process called “switching”. The most important regulatory element in the locus is the locus control region (LCR) upstream of the globin genes that is essential for high-level expression of these genes. The LCR and activate globin genes are in physical

contact, forming a chromatin structure named the Active Chromatin Hub (ACH). Many proteins, both ubiquitously expressed and erythroid specific, are known to be involved in β-globin gene regulation and chromatin looping. Most of these factors bind the promoters of the globin genes and/or the HSs of the LCR and often are present in protein-complexes at these sites. (Noordermeer and de Laat 2008; Sankaran, Xu et al. 2010). The results obtained from qRT-PCR analysis of expression of NFIs and globins performed on B6N31 hematopoietic tissues indicates that NFI-A -/- mice have a delay in the repression of embryonic β-globins and a perinatal decrease in adult globins expression, suggesting an involvement for NFI-A in the control of β-globins switching. Previous results obtained in our lab on K562 cells support this hypothesis: K562 cells that normally doesn't express adult β-globin starts to produce it at high levels under ectopical expression of NFI-A (Starnes, Sorrentino et al. 2009). The ability of NFI-A to bind the promoter of human adult β-globin was also demonstrated by experiments of luciferase and ChIP (Starnes, Sorrentino et al. 2009). It will be interesting to further investigate about this action of NFI-A, looking at a putative direct binding to the LCR of the β-globin locus or at an interaction with factors already known to belong to the protein complexes that bind to the ACH.

The high perinatal mortality rate of B6N31 NFI-A -/- mice, prevent us to analyze their adult definitive hematopoiesis. However complete blood counts of peripheral blood from adults B6N31 NFI-A +/- revealed an hematologic dyscrasia carachterized by a decreased MCV, an increased RDW and a decreased MCH. These features are symptomes of microcytic anemia, a group of disorders correlated to alterated haemoglobin synthesis, demonstrating an haploinsufficiency of NFI-A factor. It's probable that a more strong phenotype of disease, with the development of anemia in NFI-A -/- mice could be related to their high mortality rate.

Recently, NFI-A has been demonstrated to be able to induce the transcription of SLC4A1 and ALAS2 (Starnes, Sorrentino et al. 2010). SLC4A1, also known as band 3 protein, is the major membrane anion exchanger of red cells and is essential for maintaining erythrocytes mechanical stability. Mutations in this protein cause alterations in the structure of the red blood cells membrane, leading to hereditary spherocytosis, a common hemolytic anemia characterized by a spheroidal shape of erythrocytes, presenting a reduced ratio of cell surface area on cell volume (Jarolim,

Rubin et al. 1995). ALAS2, the erythroid specific form of the ALAS enzyme, that catalyze the first step in the heme biosynthetic pathway, is mutated in the most frequent form of inherited sideroblastic anemia: the X-linked sideroblastic anemia (XLSA). XLSA belongs to the group of iron-overloading anemias and hemizigous males presents mycrocitic anemia with iron overload. Knock out of *Alas2* gene in mice results in arrest of erythroid differentiation, and in the emergence of an abnormal cell fraction with large amount of iron accumulated diffusely in the cytoplasm; embryonic death occurs by E11.5, before that definitive hematopoiesis starts (Fleming, Feng et al. 2011). These data suggests that haemoglobin synthesis in NFI-A-/- mice could be affected not only by the alteration of globins expression, but also to defects in heme synthesis and that NFI-A alterations could affect also the stability of the structure of erythroid cells.

The study of the ontogeny of hematopoietic system allowed the identification of regulators of hematopoietic development, a large number of which can cause diseases in later life when dysregulated or mutated. For the first time our study highlights NFI-A as a novel regulator of hematopoiesis during ontogeny, involved in the correct development of primitive and definitive hematopoietic tissues and in the maturation of definitive erythroid and myeloid lineages. Alterations of the correct functioning of NFI-A are probably involved in the development of disease linked to alteration in hemoglobin synthesis, an aspect that will be interesting to better analyze in the future, in order to understand which could be the targets and the mechanisms of NFI-A action in this process.

6. References

Abate, C., L. Patel, et al. (1990). "Redox regulation of fos and jun DNA-binding activity in vitro." Science **249**(4973): 1157-61.

Adamo, L., O. Naveiras, et al. (2009). "Biomechanical forces promote embryonic haematopoiesis." Nature **459**(7250): 1131-5.

Adams, A. D., D. M. Choate, et al. (1995). "NF1-L is the DNA-binding component of the protein complex at the peripherin negative regulatory element." J Biol Chem **270**(12): 6975-83.

Armentero, M. T., M. Horwitz, et al. (1994). "Targeting of DNA polymerase to the adenovirus origin of DNA replication by interaction with nuclear factor I." Proc Natl Acad Sci U S A **91**(24): 11537-41.

Bachurski, C. J., S. E. Kelly, et al. (1997). "Nuclear factor I family members regulate the transcription of surfactant protein-C." J Biol Chem **272**(52): 32759-66.

Bandyopadhyay, S. and R. M. Gronostajski (1994). "Identification of a conserved oxidation-sensitive cysteine residue in the NFI family of DNA-binding proteins." J Biol Chem **269**(47): 29949-55.

Bandyopadhyay, S., D. W. Starke, et al. (1998). "Thioltransferase (glutaredoxin) reactivates the DNA-binding activity of oxidation-inactivated nuclear factor I." J Biol Chem **273**(1): 392-7.

Baron, M. H., J. Isern, et al. (2012). "The embryonic origins of erythropoiesis in mammals." Blood **119**(21): 4828-37.

Bedford, F. K., D. Julius, et al. (1998). "Neuronal expression of the 5HT3 serotonin receptor gene requires nuclear factor 1 complexes." J Neurosci **18**(16): 6186-94.

Berkofsky-Fessler, W., M. Buzzai, et al. (2010). "Transcriptional profiling of polycythemia vera identifies gene expression patterns both dependent and independent from the action of JAK2V617F." Clin Cancer Res **16**(17): 4339-52.

Bernard, F., V. Gelsi-Boyer, et al. (2009). "Alterations of NFIA in chronic malignant myeloid diseases." Leukemia **23**(3): 583-5.

Bethlenfalvay, N. C. and M. Block (1970). "Fetal erythropoiesis. Maturation in megaloblastic (yolk sac) erythropoiesis in the C 57 B1-6J mouse." Acta Haematol **44**(4): 240-5.

Boisset, J. C. and C. Robin (2012). "On the origin of hematopoietic stem cells: progress and controversy." Stem Cell Res **8**(1): 1-13.

Bosher, J., E. C. Robinson, et al. (1990). "Interactions between the adenovirus type 2 DNA polymerase and the DNA binding domain of nuclear factor I." New Biol **2**(12): 1083-90.

Cantor, A. B. and S. H. Orkin (2001). "Hematopoietic development: a balancing act." Curr Opin Genet Dev **11**(5): 513-9.

Cesta, M. F. (2006). "Normal structure, function, and histology of the spleen." Toxicol Pathol **34**(5): 455-65.

Chasis, J. and N. Mohandas (2008). "Erythroblastic islands: niches for erythropoiesis." Blood **112**: 470-478.

Chaudhry, A. Z., G. E. Lyons, et al. (1997). "Expression patterns of the four nuclear factor I genes during mouse embryogenesis indicate a potential role in development." Dev Dyn **208**(3): 313-25.

Chen, M., N. Mermod, et al. (1990). "Protein-protein interactions between adenovirus DNA polymerase and nuclear factor I mediate formation of the DNA replication preinitiation complex." J Biol Chem **265**(30): 18634-42.

Colucci, F., C. Soudais, et al. (1999). "Dissecting NK cell development using a novel alymphoid mouse model: investigating the role of the c-abl proto-oncogene in murine NK cell differentiation." J Immunol **162**(5): 2761-5.

Cooke, D. W. and M. D. Lane (1999). "The transcription factor nuclear factor I mediates repression of the GLUT4 promoter by insulin." J Biol Chem **274**(18): 12917-24.

Corbel, C., J. Salaun, et al. (2007). "Hematopoietic potential of the pre-fusion allantois." Dev Biol **301**(2): 478-88.

Costa, G., V. Kouskoff, et al. (2012). "Origin of blood cells and HSC production in the embryo." Trends Immunol.

Costa, G., V. Kouskoff, et al. (2012). "Origin of blood cells and HSC production in the embryo." Trends Immunol **33**(5): 215-23.

Crawford, D. R., P. Leahy, et al. (1998). "Nuclear factor I regulates expression of the gene for phosphoenolpyruvate carboxykinase (GTP)." J Biol Chem **273**(22): 13387-90.

Cumano, A., J. C. Ferraz, et al. (2001). "Intraembryonic, but not yolk sac hematopoietic precursors, isolated before circulation, provide long-term multilineage reconstitution." Immunity **15**(3): 477-85.

Cumano, A. and I. Godin (2007). "Ontogeny of the hematopoietic system." Annu Rev Immunol **25**: 745-85.

das Neves, L., C. S. Duchala, et al. (1999). "Disruption of the murine nuclear factor I-A gene (Nfia) results in perinatal lethality, hydrocephalus, and agenesis of the corpus callosum." Proc Natl Acad Sci U S A **96**(21): 11946-51.

de Bruijn, M. F., N. A. Speck, et al. (2000). "Definitive hematopoietic stem cells first develop within the major arterial regions of the mouse embryo." Embo J **19**(11): 2465-74.

De la Chapelle, A., A. Fantoni, et al. (1969). "Differentiation of mammalian somatic cells: DNA and hemoglobin synthesis in fetal mouse yolk sac erythroid cells." Proc Natl Acad Sci U S A **63**(3): 812-9.

De Maria, R., A. Zeuner, et al. (1999). "Negative regulation of erythropoiesis by caspase-mediated cleavage of GATA-1." Nature **401**(6752): 489-93.

Dieterlen-Lievre, F. (1975). "On the origin of haemopoietic stem cells in the avian embryo: an experimental approach." J Embryol Exp Morphol **33**(3): 607-19.

Dillon, N., T. Trimborn, et al. (1997). "The effect of distance on long-range chromatin interactions." Mol Cell **1**(1): 131-9.

Downs, K. M. and T. Davies (1993). "Staging of gastrulating mouse embryos by morphological landmarks in the dissecting microscope." Development **118**(4): 1255-66.

Driller, K., A. Pagenstecher, et al. (2007). "Nuclear factor I X deficiency causes brain malformation and severe skeletal defects." Mol Cell Biol **27**(10): 3855-3867.

Durand, C. and E. Dzierzak (2005). "Embryonic beginnings of adult hematopoietic stem cells." Haematologica **90**(1): 100-8.

Fantoni, A., A. De la Chapelle, et al. (1969). "Synthesis of embryonic hemoglobins during erythroid cell development in fetal mice." J Biol Chem **244**(4): 675-81.

Fazi, F., A. Rosa, et al. (2005). "A minicircuitry comprised of microRNA-223 and transcription factors NFI-A and C/EBPalpha regulates human granulopoiesis." Cell **123**(5): 819-31.

Ferkowicz, M. J. and M. C. Yoder (2005). "Blood island formation: longstanding observations and modern interpretations." Exp Hematol **33**(9): 1041-7.

Fleming, R. E., Q. Feng, et al. (2011). "Knockout mouse models of iron homeostasis." Annu Rev Nutr **31**: 117-37.

Fraser, S. T., J. Isern, et al. (2007). "Maturation and enucleation of primitive erythroblasts during mouse embryogenesis is accompanied by changes in cell-surface antigen expression." Blood **109**(1): 343-52.

Gao, B., L. Jiang, et al. (1996). "Transcriptional regulation of alpha(1b) adrenergic receptors (alpha(1b)AR) by nuclear factor 1 (NF1): a decline in the concentration of NF1 correlates with the downregulation of alpha(1b)AR gene expression in regenerating liver." Mol Cell Biol **16**(11): 5997-6008.

Garcia-Porrero, J. A., I. E. Godin, et al. (1995). "Potential intraembryonic hemogenic sites at pre-liver stages in the mouse." Anat Embryol (Berl) **192**(5): 425-35.

Gilbert, S. F. (2005). Biologia dello sviluppo.

Gounari, F., R. De Francesco, et al. (1990). "Amino-terminal domain of NF1 binds to DNA as a dimer and activates adenovirus DNA replication." Embo J **9**(2): 559-66.

Greer, J. P., J. Foerster, et al. (2008). Wintrobe's Clinical Hematology, 12th edition

Gronostajski, R. M. (1986). "Analysis of nuclear factor I binding to DNA using degenerate oligonucleotides." Nucleic Acids Res **14**(22): 9117-32.

Gronostajski, R. M. (1987). "Site-specific DNA binding of nuclear factor I: effect of the spacer region." Nucleic Acids Res **15**(14): 5545-59.

Gronostajski, R. M. (2000). "Roles of the NFI/CTF gene family in transcription and development." Gene **249**(1-2): 31-45.

Gronostajski, R. M., S. Adhya, et al. (1985). "Site-specific DNA binding of nuclear factor I: analyses of cellular binding sites." Mol Cell Biol **5**(5): 964-71.

Grosveld, F., N. Dillon, et al. (1993). "The regulation of human globin gene expression." Baillieres Clin Haematol **6**(1): 31-55.

Grunder, A., T. T. Ebel, et al. (2002). "Nuclear factor I-B (Nfib) deficient mice have severe lung hypoplasia." Mech Dev **112**(1-2): 69-77.

Guehmann, S., G. Vorbrueggen, et al. (1992). "Reduction of a conserved Cys is essential for Myb DNA-binding." Nucleic Acids Res **20**(9): 2279-86.

Hodge, D., E. Coghill, et al. (2006). "A global role for EKLF in definitive and primitive erythropoiesis." Blood **107**(8): 3359-70.

Iavarone, A., E. R. King, et al. (2004). "Retinoblastoma promotes definitive erythropoiesis by repressing Id2 in fetal liver macrophages." Nature **432**(7020): 1040-5.

Jackson, D. A., K. E. Rowader, et al. (1993). "Modulation of liver-specific transcription by interactions between hepatocyte nuclear factor 3 and nuclear factor 1 binding DNA in close apposition." Mol Cell Biol **13**(4): 2401-10.

Jarolim, P., H. L. Rubin, et al. (1995). "Mutations of conserved arginines in the membrane domain of erythroid band 3 lead to a decrease in membrane-associated band 3 and to the phenotype of hereditary spherocytosis." Blood **85**(3): 634-40.

Ji, R. P., C. K. Phoon, et al. (2003). "Onset of cardiac function during early mouse embryogenesis coincides with entry of primitive erythroblasts into the embryo proper." Circ Res **92**(2): 133-5.

Jones, K. A., J. T. Kadonaga, et al. (1987). "A cellular DNA-binding protein that activates eukaryotic transcription and DNA replication." Cell **48**(1): 79-89.

Keller, G., G. Lacaud, et al. (1999). "Development of the hematopoietic system in the mouse." Exp Hematol **27**(5): 777-87.

Kingsley, P. D., J. Malik, et al. (2006). ""Maturational" globin switching in primary primitive erythroid cells." Blood **107**(4): 1665-72.

Kingsley, P. D., J. Malik, et al. (2004). "Yolk sac-derived primitive erythroblasts enucleate during mammalian embryogenesis." Blood **104**(1): 19-25.

Klimchenko, O., M. Mori, et al. (2009). "A common bipotent progenitor generates the erythroid and megakaryocyte lineages in embryonic stem cell-derived primitive hematopoiesis." Blood **114**(8): 1506-17.

Kruse, U., F. Qian, et al. (1991). "Identification of a fourth nuclear factor I gene in chicken by cDNA cloning: NFI-X." Nucleic Acids Res **19**(23): 6641.

Kruse, U. and A. E. Sippel (1994). "The genes for transcription factor nuclear factor I give rise to corresponding splice variants between vertebrate species." J Mol Biol **238**(5): 860-5.

Leahy, P., D. R. Crawford, et al. (1999). "CREB binding protein coordinates the function of multiple transcription factors including nuclear factor I to regulate phosphoenolpyruvate carboxykinase (GTP) gene transcription." J Biol Chem **274**(13): 8813-22.

Leder, A., C. Daugherty, et al. (1997). "Mouse zeta- and alpha-globin genes: embryonic survival, alpha-thalassemia, and genetic background effects." Blood **90**(3): 1275-82.

Leder, A., D. Swan, et al. (1981). "Dispersion of alpha-like globin genes of the mouse to three different chromosomes." Nature **293**(5829): 196-200.

Liu, X. S., X. H. Li, et al. (2007). "Disruption of palladin leads to defects in definitive erythropoiesis by interfering with erythroblastic island formation in mouse fetal liver." Blood **110**(3): 870-6.

Liu, Y., H. U. Bernard, et al. (1997). "NFI-B3, a novel transcriptional repressor of the nuclear factor I family, is generated by alternative RNA processing." J Biol Chem **272**(16): 10739-45.

Livy, D. J. and D. Wahlsten (1997). "Retarded formation of the hippocampal commissure in embryos from mouse strains lacking a corpus callosum." Hippocampus **7**(1): 2-14.

Lowry, O. H., N. J. Rosebrough, et al. (1951). "Protein measurement with the Folin phenol reagent." J Biol Chem **193**(1): 265-75.

Lux, C. T., M. Yoshimoto, et al. (2008). "All primitive and definitive hematopoietic progenitor cells emerging before E10 in the mouse embryo are products of the yolk sac." Blood **111**(7): 3435-8.

Macleod, K. and M. Plumb (1991). "Derepression of mouse beta-major-globin gene transcription during erythroid differentiation." Mol Cell Biol **11**(9): 4324-32.

Magara, F., U. Muller, et al. (1999). "Genetic background changes the pattern of forebrain commissure defects in transgenic mice underexpressing the beta-amyloid-precursor protein." Proc Natl Acad Sci U S A **96**(8): 4656-61.

Matsuoka, S., K. Tsuji, et al. (2001). "Generation of definitive hematopoietic stem cells from murine early yolk sac and paraaortic splanchnopleures by aorta-gonad-mesonephros region-derived stromal cells." Blood **98**(1): 6-12.

Matthews, J. R., N. Wakasugi, et al. (1992). "Thioredoxin regulates the DNA binding activity of NF-kappa B by reduction of a disulphide bond involving cysteine 62." Nucleic Acids Res **20**(15): 3821-30.

McGrath, K. and J. Palis (2008). "Ontogeny of erythropoiesis in the mammalian embryo." Curr Top Dev Biol **82**: 1-22.

McGrath, K. E., P. D. Kingsley, et al. (2008). "Enucleation of primitive erythroid cells generates a transient population of "pyrenocytes" in the mammalian fetus." Blood **111**(4): 2409-17.

McGrath, K. E., A. D. Koniski, et al. (2003). "Circulation is established in a stepwise pattern in the mammalian embryo." Blood **101**(5): 1669-76.

McGrath, K. E. and J. Palis (2005). "Hematopoiesis in the yolk sac: more than meets the eye." Exp Hematol **33**(9): 1021-8.

Medvinsky, A. and E. Dzierzak (1996). "Definitive hematopoiesis is autonomously initiated by the AGM region." Cell **86**(6): 897-906.

Medvinsky, A., S. Rybtsov, et al. (2011). "Embryonic origin of the adult hematopoietic system: advances and questions." Development **138**(6): 1017-31.

Medvinsky, A. L., N. L. Samoylina, et al. (1993). "An early pre-liver intraembryonic source of CFU-S in the developing mouse." Nature **364**(6432): 64-7.

Meisterernst, M., I. Gander, et al. (1988). "A quantitative analysis of nuclear factor I/DNA interactions." Nucleic Acids Res **16**(10): 4419-35.

Meisterernst, M., L. Rogge, et al. (1989). "Structural and functional organization of a porcine gene coding for nuclear factor I." Biochemistry **28**(20): 8191-200.

Mermod, N., E. A. O'Neill, et al. (1989). "The proline-rich transcriptional activator of CTF/NF-I is distinct from the replication and DNA binding domain." Cell **58**(4): 741-53.

Messina, G., S. Biressi, et al. (2010). "Nfix regulates fetal-specific transcription in developing skeletal muscle." Cell **140**(4): 554-66.

Mikkola, H. K. and S. H. Orkin (2006). "The journey of developing hematopoietic stem cells." Development **133**(19): 3733-44.

Moore, M. A. and J. J. Owen (1965). "Chromosome marker studies on the development of the haemopoietic system in the chick embryo." Nature **208**(5014): 956 passim.

Moore, M. A. and J. J. Owen (1967). "Experimental studies on the development of the thymus." J Exp Med **126**(4): 715-26.

Morita, Y., A. Iseki, et al. (2011). "Functional characterization of hematopoietic stem cells in the spleen." Exp Hematol **39**(3): 351-359 e3.

Mul, Y. M., C. P. Verrijzer, et al. (1990). "Transcription factors NFI and NFIII/oct-1 function independently, employing different mechanisms to enhance adenovirus DNA replication." J Virol **64**(11): 5510-8.

Muller, A. M., A. Medvinsky, et al. (1994). "Development of hematopoietic stem cell activity in the mouse embryo." Immunity **1**(4): 291-301.

Noordermeer, D. and W. de Laat (2008). "Joining the loops: beta-globin gene regulation." IUBMB Life **60**(12): 824-33.

North, T., T. L. Gu, et al. (1999). "Cbfa2 is required for the formation of intra-aortic hematopoietic clusters." Development **126**(11): 2563-75.

North, T. E., W. Goessling, et al. (2009). "Hematopoietic stem cell development is dependent on blood flow." Cell **137**(4): 736-48.

Orkin, S. H. and L. I. Zon (2008). "Hematopoiesis: an evolving paradigm for stem cell biology." Cell **132**(4): 631-44.

Osada, S., S. Daimon, et al. (1997). "Nuclear factor 1 family proteins bind to the silencer element in the rat glutathione transferase P gene." J Biochem **121**(2): 355-63.

Ottersbach, K., A. Smith, et al. (2009). "Ontogeny of haematopoiesis: recent advances and open questions." Br J Haematol **148**(3): 343-55.

Ozaki, H. S. and D. Wahlsten (1992). "Prenatal formation of the normal mouse corpus callosum: a quantitative study with carbocyanine dyes." J Comp Neurol **323**(1): 81-90.

Palis, J. (2008). "Ontogeny of erythropoiesis." Curr Opin Hematol **15**(3): 155-61.

Palis, J., J. Malik, et al. "Primitive erythropoiesis in the mammalian embryo." Int J Dev Biol **54**(6-7): 1011-8.

Palis, J., J. Malik, et al. (2010). "Primitive erythropoiesis in the mammalian embryo." Int J Dev Biol **54**(6-7): 1011-8.

Palis, J., S. Robertson, et al. (1999). "Development of erythroid and myeloid progenitors in the yolk sac and embryo proper of the mouse." Development **126**(22): 5073-84.

Palis, J. and G. B. Segel (1998). "Developmental biology of erythropoiesis." Blood Rev **12**(2): 106-14.

Palis, J. and M. C. Yoder (2001). "Yolk-sac hematopoiesis: the first blood cells of mouse and man." Exp Hematol **29**(8): 927-36.

Pazin, M. J. and J. T. Kadonaga (1997). "What's up and down with histone deacetylation and transcription?" Cell **89**(3): 325-8.

Peschle, C., F. Mavilio, et al. (1985). "Haemoglobin switching in human embryos: asynchrony of zeta----alpha and epsilon----gamma-globin switches in primitive and definite erythropoietic lineage." Nature **313**(5999): 235-8.

Putz, G., A. Rosner, et al. (2006). "AML1 deletion in adult mice causes splenomegaly and lymphomas." Oncogene **25**(6): 929-39.

Rabbitts, T. H. (1994). "Chromosomal translocations in human cancer." Nature **372**(6502): 143-9.

Rajas, F., M. Delhase, et al. (1998). "Nuclear factor 1 regulates the distal silencer of the human PIT1/GHF1 gene." Biochem J **333 (Pt 1)**: 77-84.

Rice, K. L., X. Lin, et al. (2012). "Analysis of genomic aberrations and gene expression profiling identifies novel lesions and pathways in myeloproliferative neoplasms." Blood Cancer J **1**(11): e40.

Ristiniemi, J. and J. Oikarinen (1989). "Histone H1 binds to the putative nuclear factor I recognition sequence in the mouse alpha 2(I) collagen promoter." J Biol Chem **264**(4): 2164-74.

Rosa, A., M. Ballarino, et al. (2007). "The interplay between the master transcription factor PU.1 and miR-424 regulates human monocyte/macrophage differentiation." Proc Natl Acad Sci U S A **104**(50): 19849-54.

Rosenbauer, F. and D. G. Tenen (2007). "Transcription factors in myeloid development: balancing differentiation with transformation." Nat Rev Immunol **7**(2): 105-17.

Rupp, R. A., U. Kruse, et al. (1990). "Chicken NFI/TGGCA proteins are encoded by at least three independent genes: NFI-A, NFI-B and NFI-C with homologues in mammalian genomes." Nucleic Acids Res **18**(9): 2607-16.

Rybtsov, S., M. Sobiesiak, et al. (2011). "Hierarchical organization and early hematopoietic specification of the developing HSC lineage in the AGM region." J Exp Med **208**(6): 1305-15.

Samokhvalov, I. M., N. I. Samokhvalova, et al. (2007). "Cell tracing shows the contribution of the yolk sac to adult haematopoiesis." Nature **446**(7139): 1056-61.

Sangiorgi, F., C. M. Woods, et al. (1990). "Vimentin downregulation is an inherent feature of murine erythropoiesis and occurs independently of lineage." Development **110**(1): 85-96.

Sankaran, V. G., J. Xu, et al. (2010). "Advances in the understanding of haemoglobin switching." Br J Haematol **149**(2): 181-94.

Silver, L. and J. Palis (1997). "Initiation of murine embryonic erythropoiesis: a spatial analysis." Blood **89**(4): 1154-64.

Spitz, F., M. Salminen, et al. (1997). "A combination of MEF3 and NFI proteins activates transcription in a subset of fast-twitch muscles." Mol Cell Biol **17**(2): 656-66.

Starnes, L. M., A. Sorrentino, et al. (2010). "A transcriptome-wide approach reveals the key contribution of NFI-A in promoting erythroid differentiation of human CD34(+) progenitors and CML cells." Leukemia **24**(6): 1220-3.

Starnes, L. M., A. Sorrentino, et al. (2009). "NFI-A directs the fate of hematopoietic progenitors to the erythroid or granulocytic lineage and controls beta-globin and G-CSF receptor expression." Blood **114**(9): 1753-63.

Steele-Perkins, G., K. G. Butz, et al. (2003). "Essential role for NFI-C/CTF transcription-replication factor in tooth root development." Mol Cell Biol **23**(3): 1075-84.

Szabo, P., J. Moitra, et al. (1995). "Identification of a nuclear factor-I family protein-binding site in the silencer region of the cartilage matrix protein gene." J Biol Chem **270**(17): 10212-21.

Tada, T., D. T. Widayati, et al. (2006). "Morphological study of the transition of haematopoietic sites in the developing mouse during the peri-natal period." Anat Histol Embryol **35**(4): 235-40.

Wolber, F. M., E. Leonard, et al. (2002). "Roles of spleen and liver in development of the murine hematopoietic system." Exp Hematol **30**(9): 1010-9.

Wong, P. M., S. W. Chung, et al. (1986). "Properties of the earliest clonogenic hemopoietic precursors to appear in the developing murine yolk sac." Proc Natl Acad Sci U S A **83**(11): 3851-4.

Yoshimoto, M., E. Montecino-Rodriguez, et al. (2011). "Embryonic day 9 yolk sac and intra-embryonic hemogenic endothelium independently generate a B-1 and marginal zone progenitor lacking B-2 potential." Proc Natl Acad Sci U S A **108**(4): 1468-73.